FR-15978
12 APRIL 1982

ADVANCED TURBINE STUDY

FINAL REPORT

Prepared under Contract NAS8-33821
for
National Aeronautics and Space Administration
George C. Marshall Space Flight Center
Marshall Space Center, Alabama 35812

Prepared by
Pratt & Whitney Aircraft Group
Government Products Division
P.O. Box 2691, West Palm Beach, Florida 33402

UNITED TECHNOLOGIES
PRATT & WHITNEY
AIRCRAFT

Printed in the United States of America

FR-15978
12 APRIL 1982

ADVANCED TURBINE STUDY

FINAL REPORT

Prepared under Contract NAS8-33821
for
National Aeronautics and Space Administration
George C. Marshall Space Flight Center
Marshall Space Center, Alabama 35812

Prepared by
Pratt & Whitney Aircraft Group
Government Products Division
P.O. Box 2691, West Palm Beach, Florida 33402

UNITED
TECHNOLOGIES
PRATT&WHITNEY
AIRCRAFT

Printed in the United States of America

TABLE OF CONTENTS

SECTION 1.0 - INTRODUCTION

1.1 GENERAL

From August 1980 through December 1981, Pratt & Whitney Aircraft Group, Government Products Division (GPD), West Palm Beach, Florida, conducted an Advanced Turbine Study for the NASA Marshall Space Flight Center under Contract NAS8-33821.

The purpose of the study was to determine the available increase in turbine horsepower achieved by increasing turbine inlet temperature over a range of 1800° to 2600°R, while applying current gas turbine airfoil cooling technology. Four cases of rocket turbine operating conditions were investigated.

	CASE 1	CASE 1A	CASE 2	CASE 3
Propellants	O_2/H_2	O_2/H_2	O_2/CH_4	O_2/CH_4
Fuel Flowrate, pps	160	80	280	50
Pressure Ratio, T-T	1.6:1	1.6:1	1.6:1	20:1
Inlet Temperature Range, °R	1800-2600	1800-2600	1800-2600	1800-2600
Inlet Pressure, psia	6000	6000	6000	4000
Turbine Speed, rpm	38000	38000	24000	24000

Film cooling was found to be the required scheme for these rocket turbine applications because of the high heat flux environments. Conventional convective or impingement cooling, used in jet engines, is inadequate in a rocket turbine environment because of the resulting high temperature gradients in the airfoil wall, causing high strains and low cyclic life.

The case 1 and 1A hydrogen-rich turbine environment experienced a loss, or no gain, in delivered horsepower as turbine inlet temperature was increased at constant airfoil life. The effects of film cooling with regard to reduced flow available for turbine work, dilution of mainstream gas temperature and cooling re-entry losses, offset the relatively low specific work capability of hydrogen when increasing turbine inlet temperature over the 1800 to 2600°R range. However, the Case 2 and 3 methane-rich environment experienced an increase in delivered horsepower as turbine inlet temperature was increased at

constant airfoil life. This was possible because the large increase in specific work capability of methane over the 1800 to 2600°R temperature range was greater than the horsepower reduction associated with film cooling.

It is realized that additional detailed trade studies, required prior to hardware commitment, could change the turbine configurations and horsepower levels presented in this report. However, sufficient detail has been used to make the case-to-case comparisons valid and they provide a good base for future studies.

Based on the results of this study it is recommended that refractory, RSR and single-crystal materials, along with advanced convective cooling, be investigated for future technology/research programs especially for the hydrogen-rich environment.

1.2 PROGRAM HIGHLIGHTS

The Advanced Turbine Study contract was initiated on 1 August 1980. The contract was signed by GPD on 17 July 1980.

Contract Modification No. 1 was incorporated on 7 May 1981, revising the original scope of work by deleting two oxidizer-rich turbines and adding one fuel-rich turbine.

Contract Modification No. 2 was incorporated on 7 July 1981, revising the distribution of technical reports produced under this contract.

A total of eight bi-monthly status reports were issued during the technical effort period of performance, and a mid-term review was held with NASA on 24 March 1981 via telephone conference call.

SECTION 2.0 - TECHNICAL EFFORT

2.1. MATERIALS SURVEY

The blade and vane material used for all four cases was MAR-M-200 D.S. (directionally solidified). This material was selected in the beginning of the program, as reported in Status Report No. 1, October 10, 1980. One of the reasons for this selection was its excellent low cycle fatigue (LCF) properties in a hydrogen environment. Free hydrogen is present not only in the H_2/O_2 turbine, but also in the disassociated combustion gases of the CH_4/O_2 turbines. The properties of this alloy are fully characterized, making the analysis simple and accurate. Figure 2.1-1 shows the LCF design curve used. This alloy is currently in use in the F100 high pressure turbine; therefore, its manufacturing cost and durability characteristics are known.

A more advanced nickel-base, single-crystal alloy, PWA 1480, has recently been run in experimental F100 engines and has shown an approximately 200 per cent improvement in LCF over the MAR-M-200 material. This material has recently been tested under Contract NAS8-33821 in a hydrogen environment, and it could be used in a future rocket turbine study. If PWA 1480 material were used in this study, the lines of constant life on the horsepower versus turbine inlet temperature (TIT) curve would all move to a higher turbine inlet temperature level. In other words, the improved material would permit the production of more horsepower for a given-life machine, by providing a higher turbine inlet temperature capability. Another material that offers possible promise for future rocket application is Rapid Solidification Rate (RSR) powder, that can be directionally recrystallized. A current DARPA Contract, F33615-80-C, is funding alloy-coating optimization, airfoil design and rig testing. Successful alloys emerging from this program would be considered for future rocket turbine applications.

Use of a refractory material for the blades and vanes would have a large payoff in this application, since the need for cooling would be eliminated, along with the associated aerodynamic and thermodynamic cooling penalties. A small amount of research on refractory airfoils has been done in the past. Any future work with refractory airfoils should begin with a feasibility study which would draw on past experience and current contract work throughout the industry. Refractory materials were not used in this study because it is beyond our current technology for turbine applications.

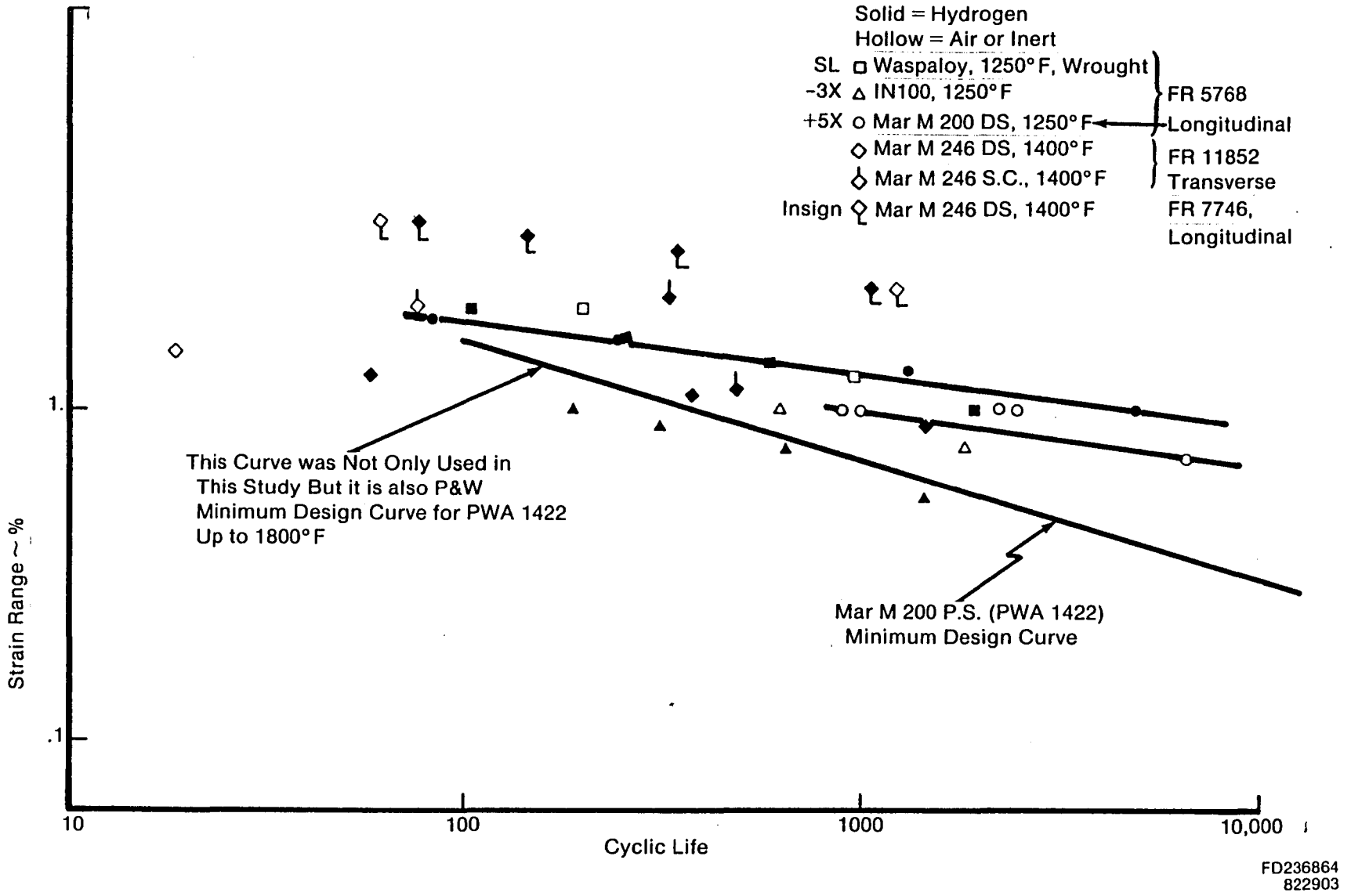

Figure 2.1-1. LCF Data

2.2 COOLING TECHNIQUES

At the beginning of this study, it was envisioned that simple convection cooling would adequately cool the rocket turbine airfoils up to 2600°R turbine inlet temperatures (TIT). These types of schemes are adequate for jet engine turbine airfoils at these TIT levels. These schemes have typical cast wall thicknesses of 0.040 to 0.080 inches, and are cooled from the inside (core) of the airfoil. Several examples are pictured in Figure 2.2-1. Calculations revealed that very large temperature gradients occurred through the thick, cooled airfoil wall. See Figure 2.2-2 for an example. This is due to the high heat fluxes that are encountered when cooling in a high pressure rocket environment. These large thermal gradients through the wall not only cause low cycle fatigue (LCF) problems, but also the hot-side wall operates very close to hot-gas temperature. Thus, simple convective cooling schemes were abandoned.

Transpiration and thermosyphon cooling techniques are considered impractical for turbine airfoils using today's technologies. The strucural integrity of a transpiration scheme in a highly stressed environment is questionable. Also, plugging of the minute coolant passages by carbon deposits in the methane turbine would cause catastophic failure.

Film cooling was selected as the method of cooling the turbine airfoils for this contract. Film cooling has been used in P&WA turbines for over ten years and is successfully used in the F100 turbine. An internal baffle was used to regulate the coolant uniformly to various parts of the airfoil. The film coolant provides a protective layer of cool fluid on the outside of the airfoils, thereby reducing the heat flux from the source. An example of film cooling for the first vane of Case No. 1A is shown in Figure 2.2-3. The hottest location on the outside surface is cooled 700°F below the hot gas temperature. As a comparison, the simple convective cooling schemes provided only 20°F of temperature reduction. A good feature of film cooling is that it can easily be optimized experimentally, by adding or plugging film holes during engine testing until design life is obtained. The unfavorable aspect of film cooling is that large amounts of flow are required to cover the entire outside surface of the airfoil, which causes significant efficiency losses and reduces the horsepower output of the turbine.

The amount of cooling flow can be reduced by using an advanced convective cooling scheme. The large gradient through the wall is reduced by using a very thin wall with high conductivity. The technology needed for this scheme has yet to be developed for turbine airfoils. Further discussion of this idea is presented in the Recommendations Section.

Temperature information is expressed in degrees Fahrenheit for heat transfer analyses and computer-generated output.

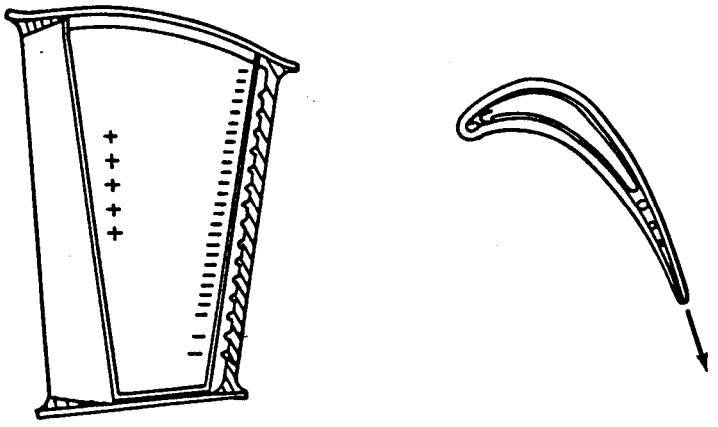

Simple Chordwise Cooling With Trailing Edge Discharge

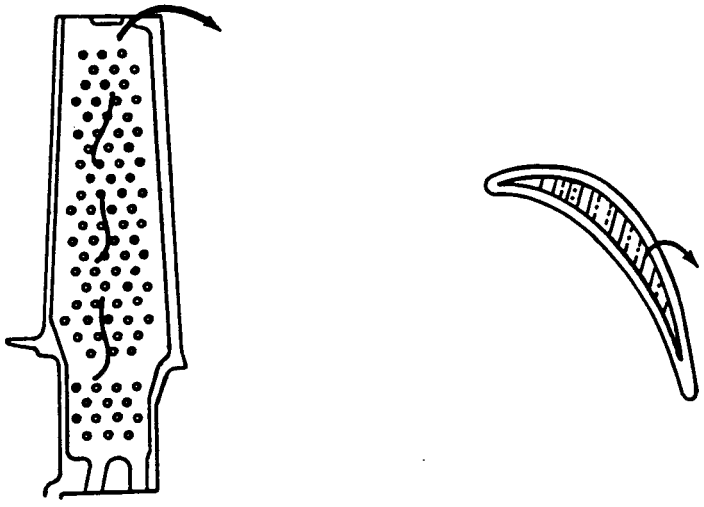

Simple Radial Flow Convective Cooling

FD243408
822903

Figure 2.2-1. Examples of Simple Cooling Schemes

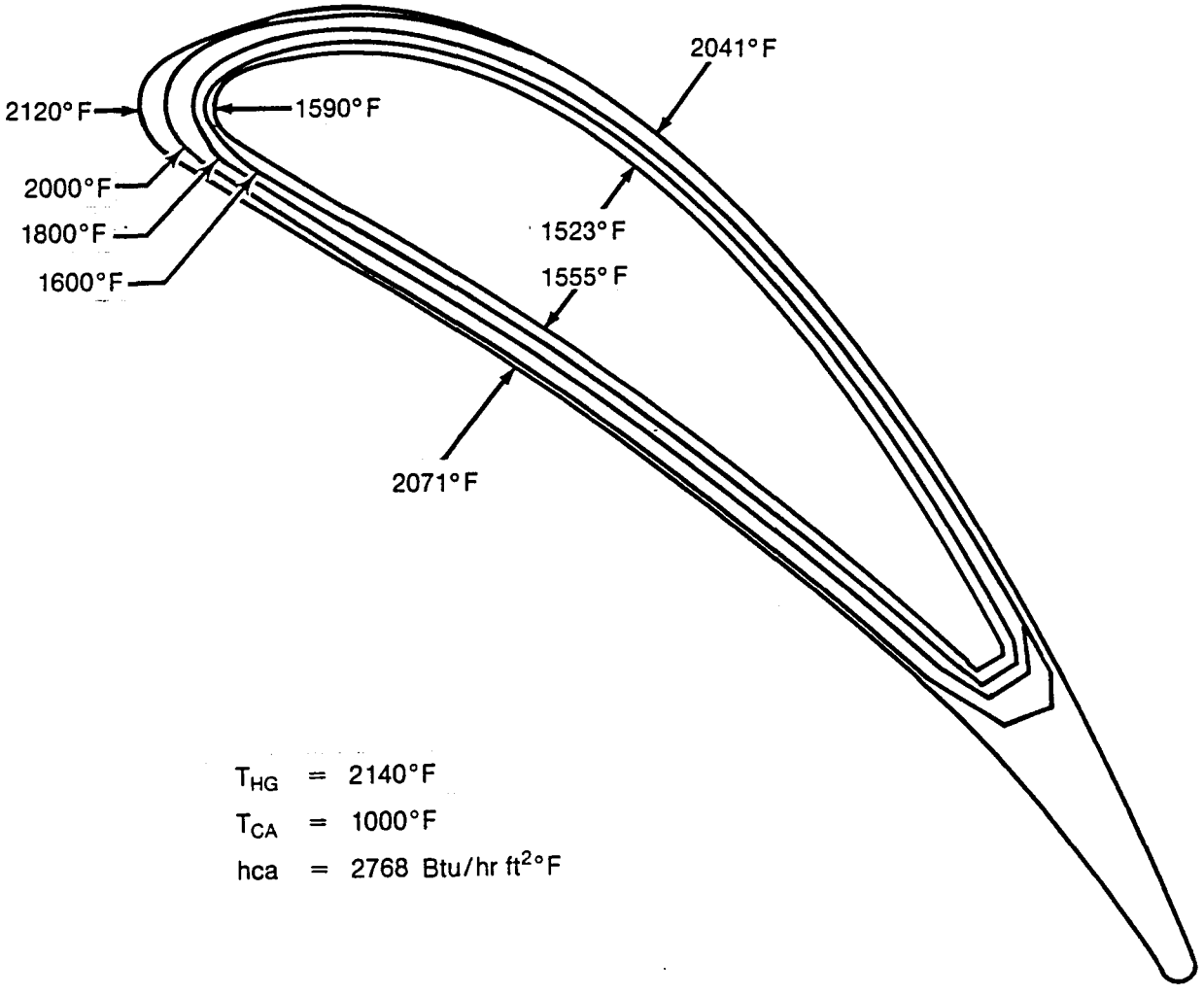

FD236865
822903

Figure 2.2-2. Simple Radial Flow Convective Cooling Isotherms at Full Power

Row	Holes/Row	Diameter	H_2 Flow Lbs/Sec/Foil	Coolant P_t/P_s
1	18	.015	.0233	1.03
2	17	.019	.0354	1.03
3	18	.015	.0233	1.03
4	17	.015	.0268	1.04
5	18	.015	.0344	1.06
6	26	.015	.0286	1.025
7	26	.015	.0303	1.03
8	26	.015	.0280	1.03
9	26	.015	.0277	1.03
10	26	.015	.0278	1.03
11	26	.015	.0280	1.03
12	26	.015	.0284	1.03
13	26	.015	.0264	1.025
14	26	.015	.0277	1.025
15	26	.015	.0238	1.02
16	26	.015	.0241	1.02
17	26	.015	.0243	1.02
18	26	.015	.0337	1.03
19	26	.015	.0337	1.03
20	26	.015	.0337	1.03

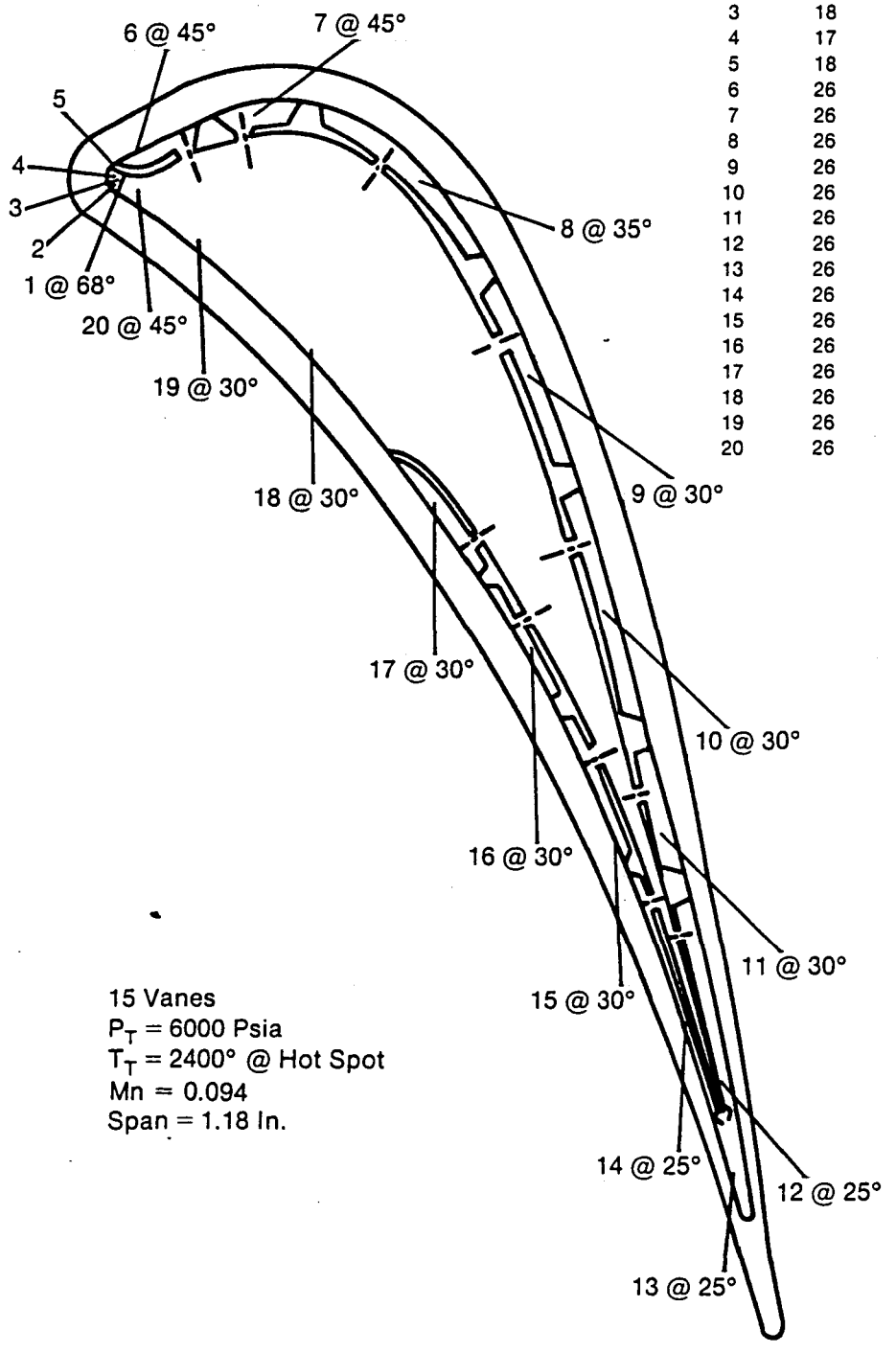

FD236866
822903

Figure 2.2-3. Case 1A First Vane Filmhole Design

2.3 HEAT TRANSFER AND DURABILITY ANALYSIS

A detailed coolant flow and heat transfer analysis was performed for the first vanes of all four cases and for the first blades of Cases 1 and 2. The isotherms for these six airfoils at full power are shown in Figures 2.3-1 through 2.3-4. Transient heat transfer and strain analysis resulted in the strain range that the airfoil undergoes during a start-to-full-power excursion. This analysis was performed several times, using different full-power TIT levels. The resultant strain range versus TIT is shown for all cases in Figures 2.3-5 to 2.3-8. Using the strain range versus cyclic life curve for PWA 1422, the curves of cyclic life versus TIT were generated, and are shown in Figures 2.3-9 to 2.3-12. From these curves, the lines of constant life on the horsepower curve were generated.

The thermal analysis of the vanes and blades included gas temperature additions to account for preburner exit temperature variations. Since the vanes are stationary, they experience the worst circumferential variation, which was estimated to be 260°, 200°, and 155° for turbine inlet temperatures (TIT) of 2600°R, 2200°R, and 1800°R, respectively. For example, at 2600°R TIT the first vanes were analyzed at 2600° minus 460° plus 260°, equalling 2400°F as shown in Figures 2.3-1 through 2.3-4. Since the blades rotate, they experience only the average of the circumferential variations at any radial location. The radial peaks were estimated to be 200°, 150°, and 100° at TIT's of 2600°, 2200°, and 1800°R, respectively. These radial peaks were added to the blade total relative temperature, which is different for each case.

Coolant inlet conditions were assumed to be 450°F and 1.05 times turbine inlet total pressure. This pressure is required to insure coolant outflow of the first vane leading edge film holes. Coolant temperature was similar to the measured coolant temperature in the disk region of the XLR 129-P-1 rocket engine reported in AFRPL-TR-71-1, Volume II, Figure 587.

Case 3 showed the largest payoff in horsepower gain by going from uncooled to cooled, while holding life constant. One of the reasons for this is that the Case 3 bending stress was very low, due to its short span height. The effect of adding cooling was thus magnified, since the only major component of stress was the thermal stress, which the coolant reduced. A study was undertaken to see if the poor horsepower payoff for Case 1 would change if the Case 1 first bending stresses were reduced. Figure 2.3-13 shows the results of that study. By reducing the bending stresses to zero, the minimum cooled vane TIT capability increased about 200°F. This still did not show a horsepower gain, as shown in the figure.

The cooling-scheme geometries for all the airfoils analyzed are presented in Appendix A. They all use small (.015-inch) film holes at shallow angles to the surface. The internal baffle meters the flow to various sections of the airfoil. This baffle compensates for the lower static dump pressure in the mainstream over the high Mach number regions of the airfoil.

A study was done to determine how much the coolant could be reduced if smaller (less than .015-inch) film holes were used. The groundrules were that the maximum film temperature would remain constant by varying the number of holes per row, such that the hole spacing-to-diameter ratio remained constant. As the hole diameter was reduced, the number of rows of holes was increased, in order to maintain the maximum film temperature. The results showed that by reducing the diameter from .015 to .010 inches, the coolant could be reduced 17 percent. The hole diameter of .015 inches was used for the entire study because it was felt to be a practical manufacturing limit, with less susceptibility to plugging.

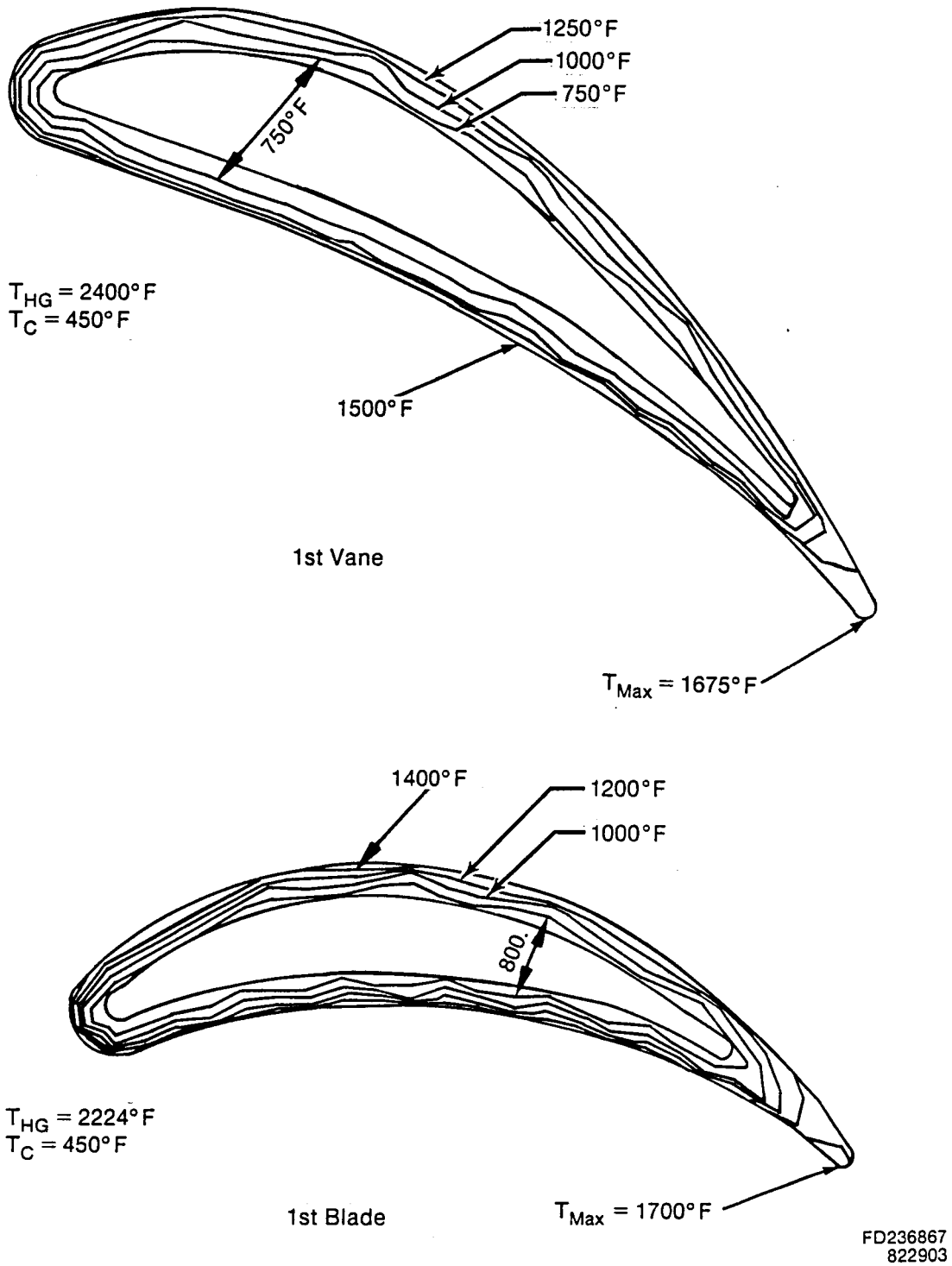

Figure 2.3-1. Isotherms at Full Power, Case 1, 2600°R Turbine Inlet Temperature

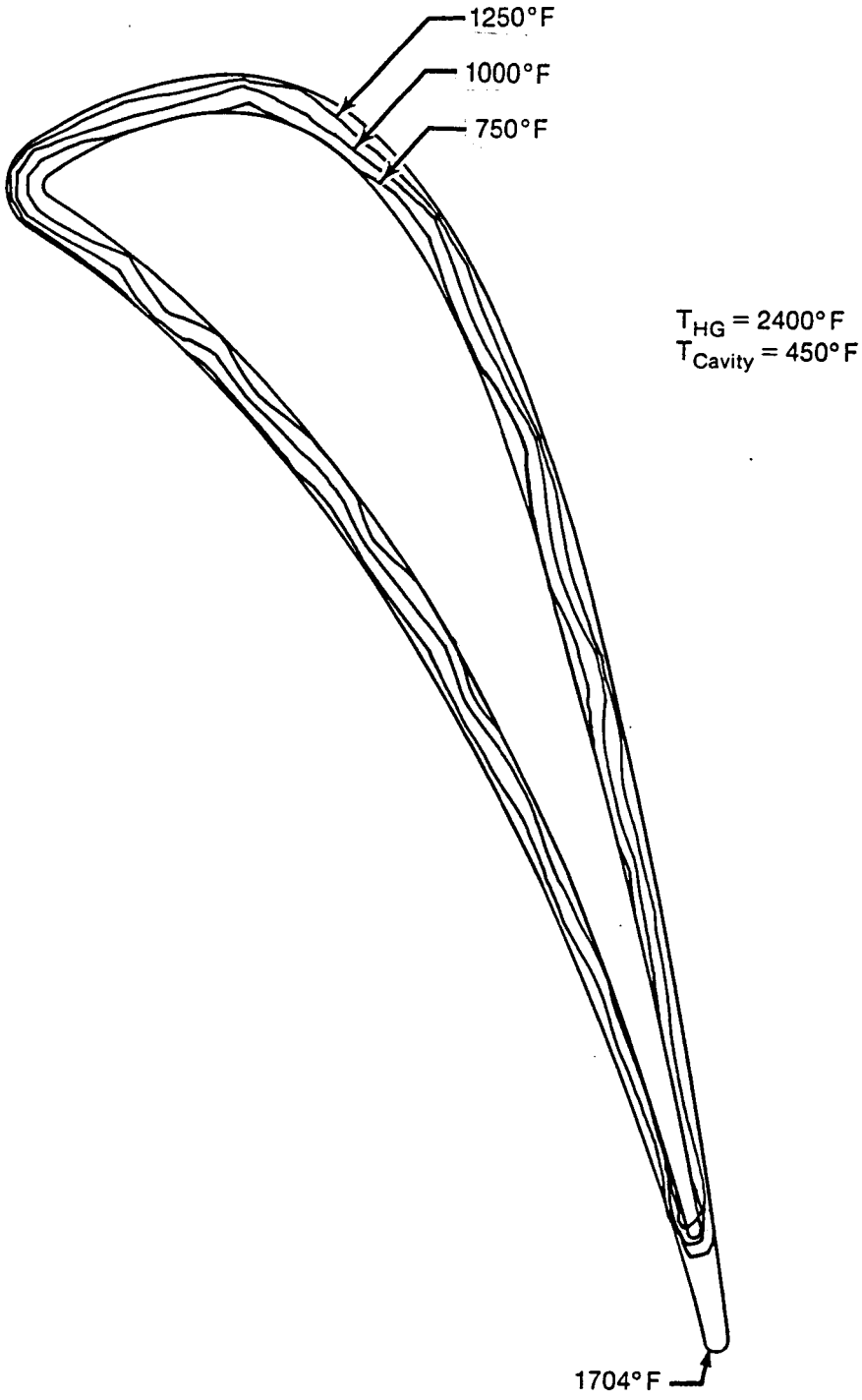

Figure 2.3-2. Case 1A First Vane
2600°R Turbine Inlet Temperature

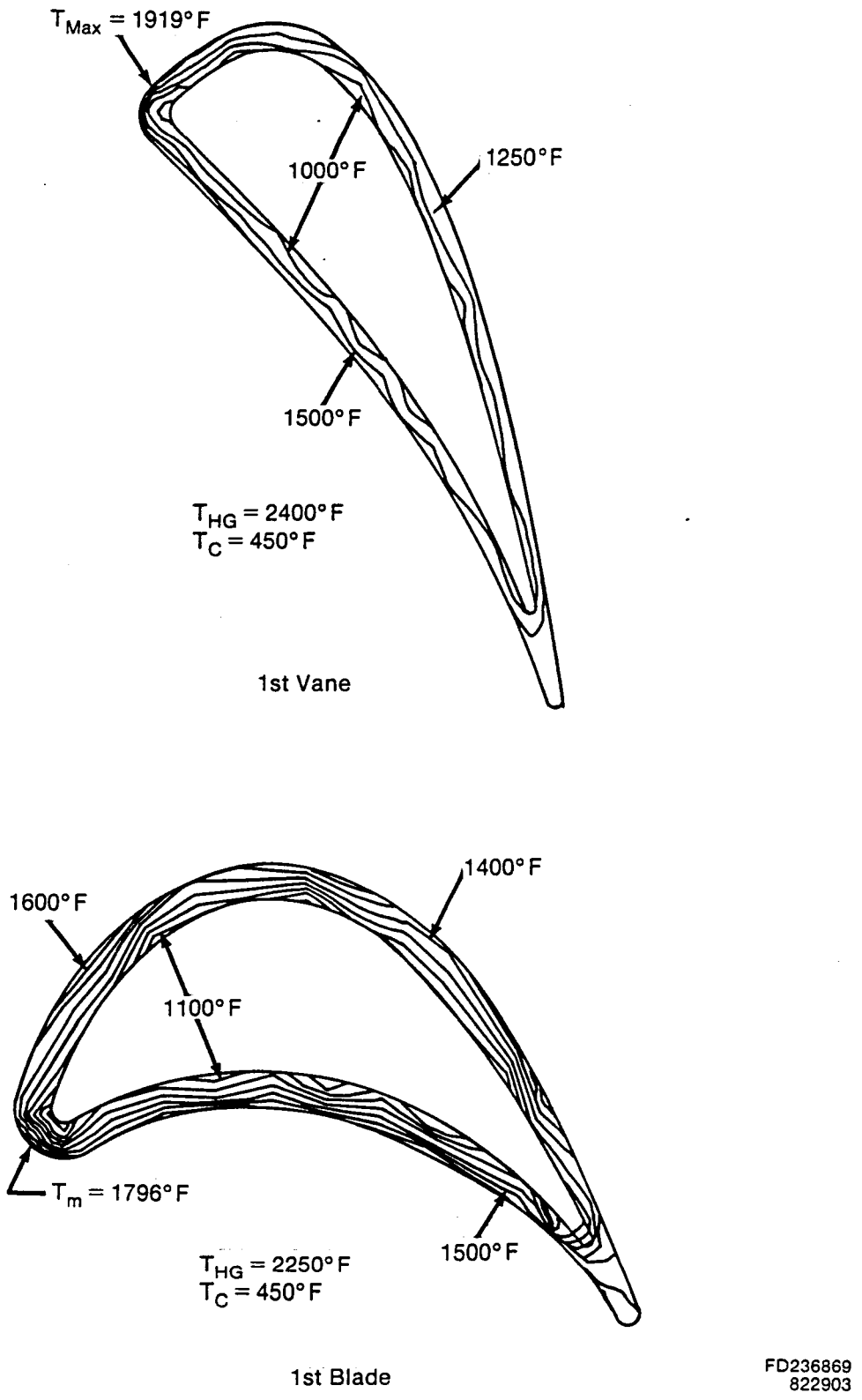

Figure 2.3-3. Case 2 Isotherms at Full Power 2600°R TIT

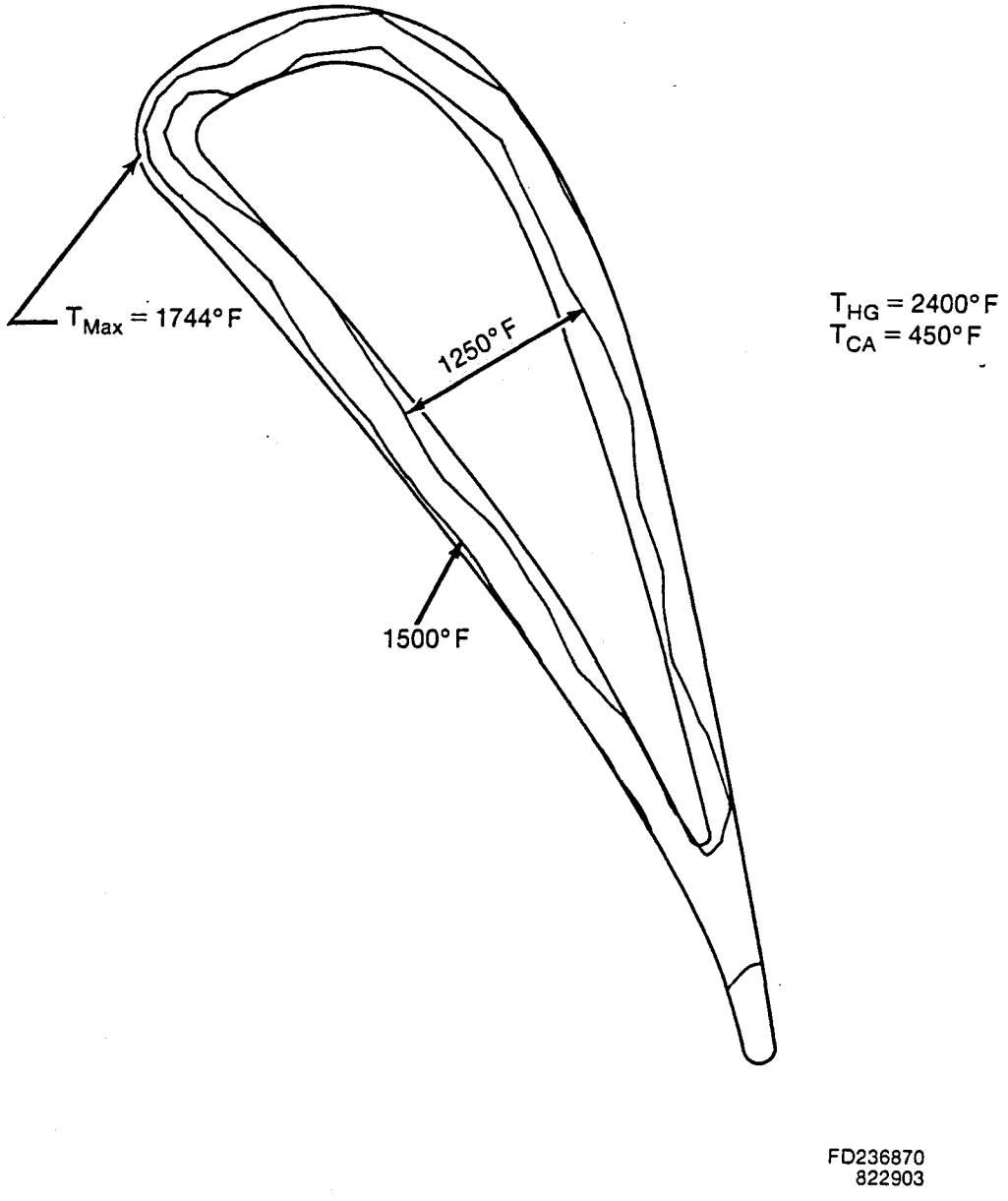

Figure 2.3-4. Case 3 First Vane Isotherms at Full Power 2600°R Turbine Inlet Temperature

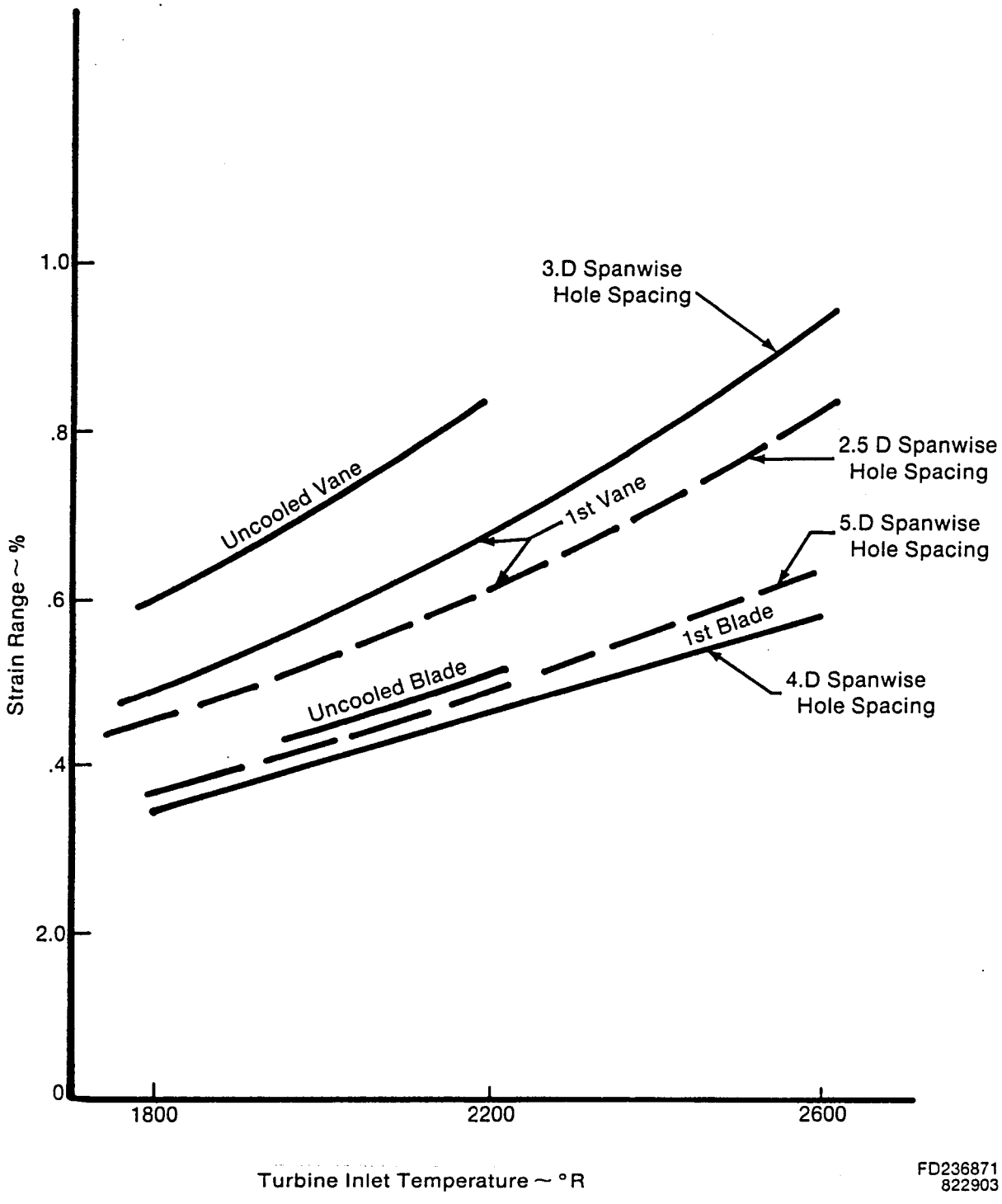

Figure 2.3-5. Case 1 Airfoil Strain Range vs. Turbine Inlet Temperature at Full Power

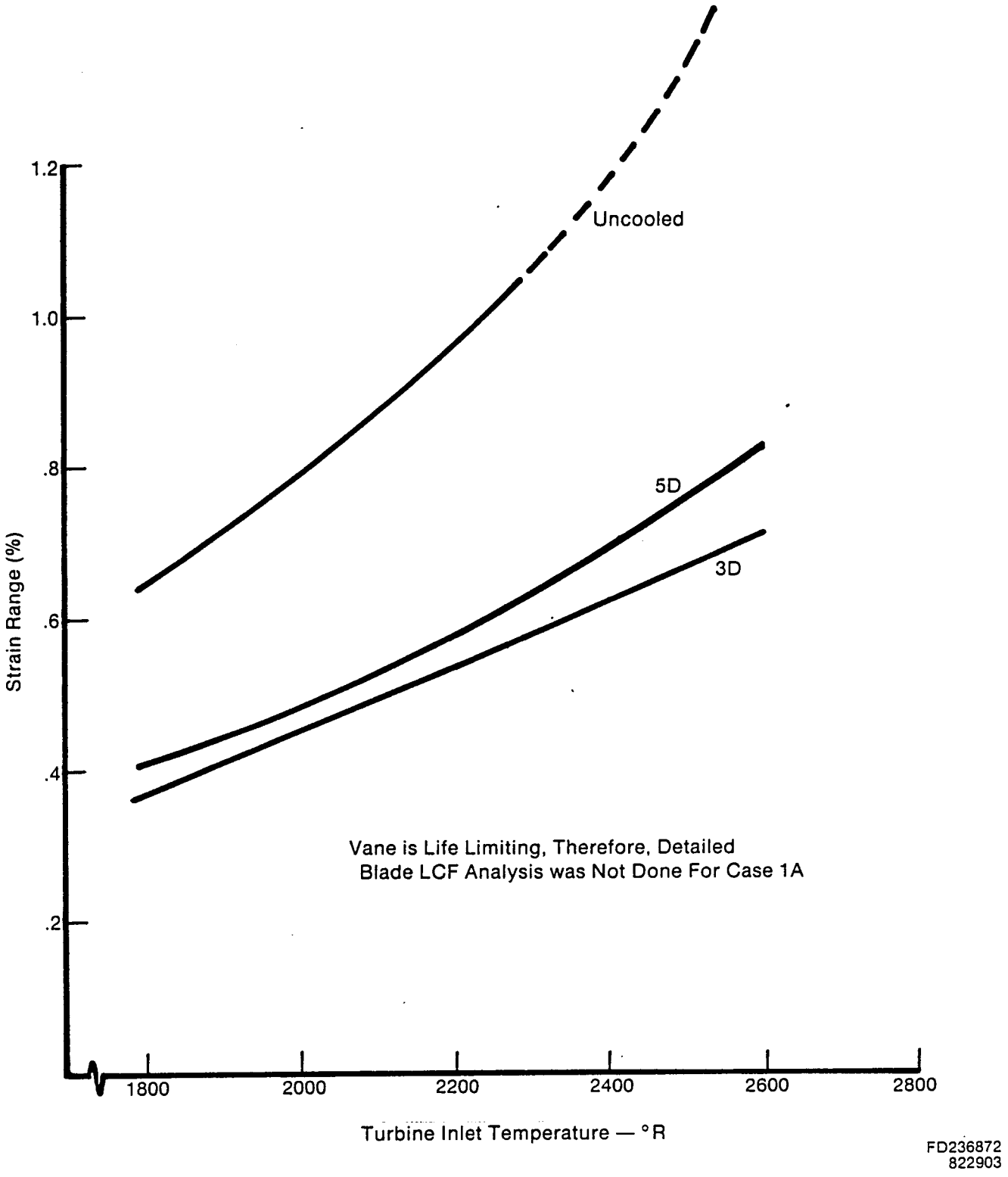

Figure 2.3-6. Case 1A First Vane Strain Range vs. Turbine Inlet Temperature

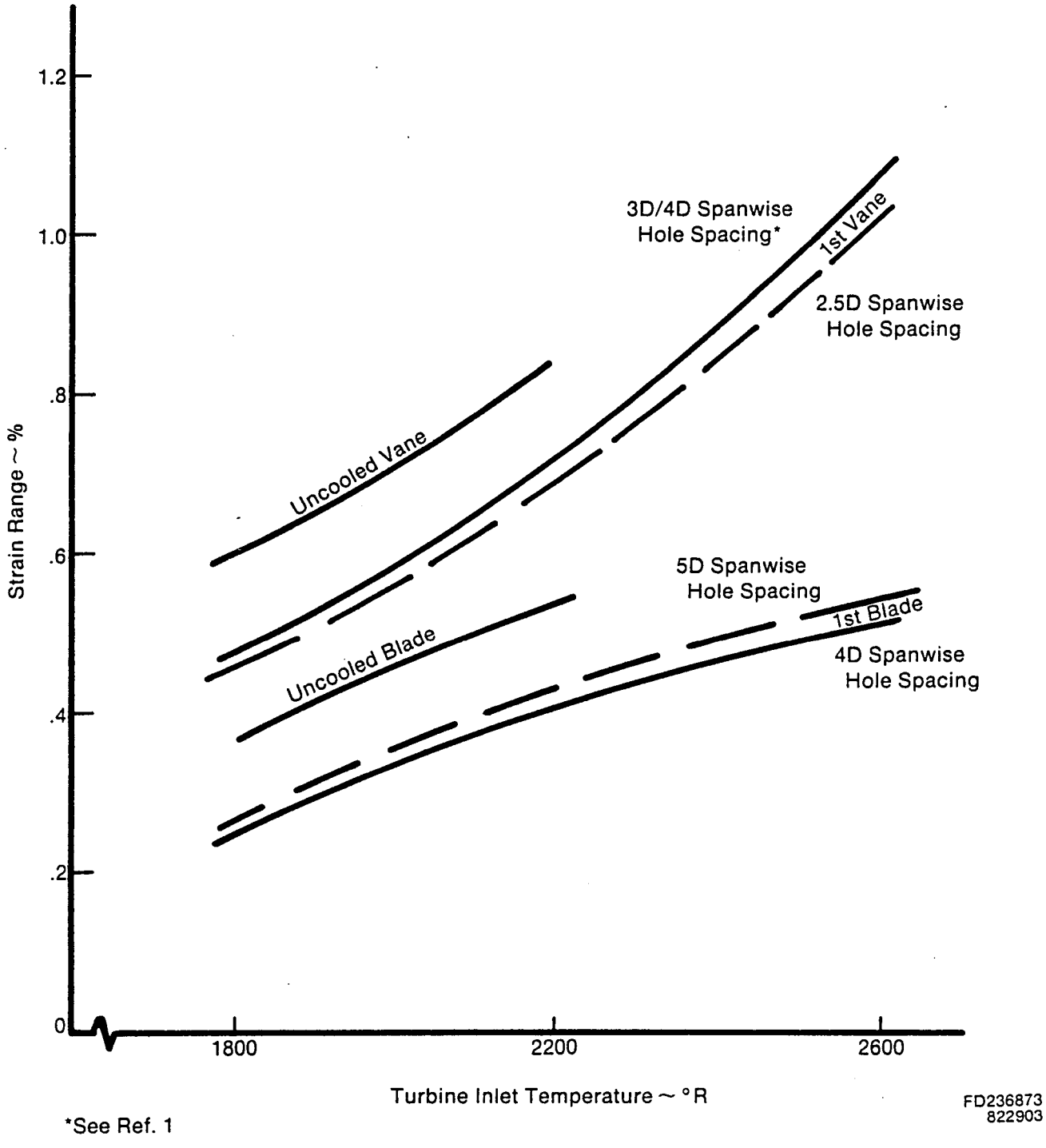

*See Ref. 1

Figure 2.3-7. Case 2 Turbine Strain Range vs. Turbine Inlet Temperature

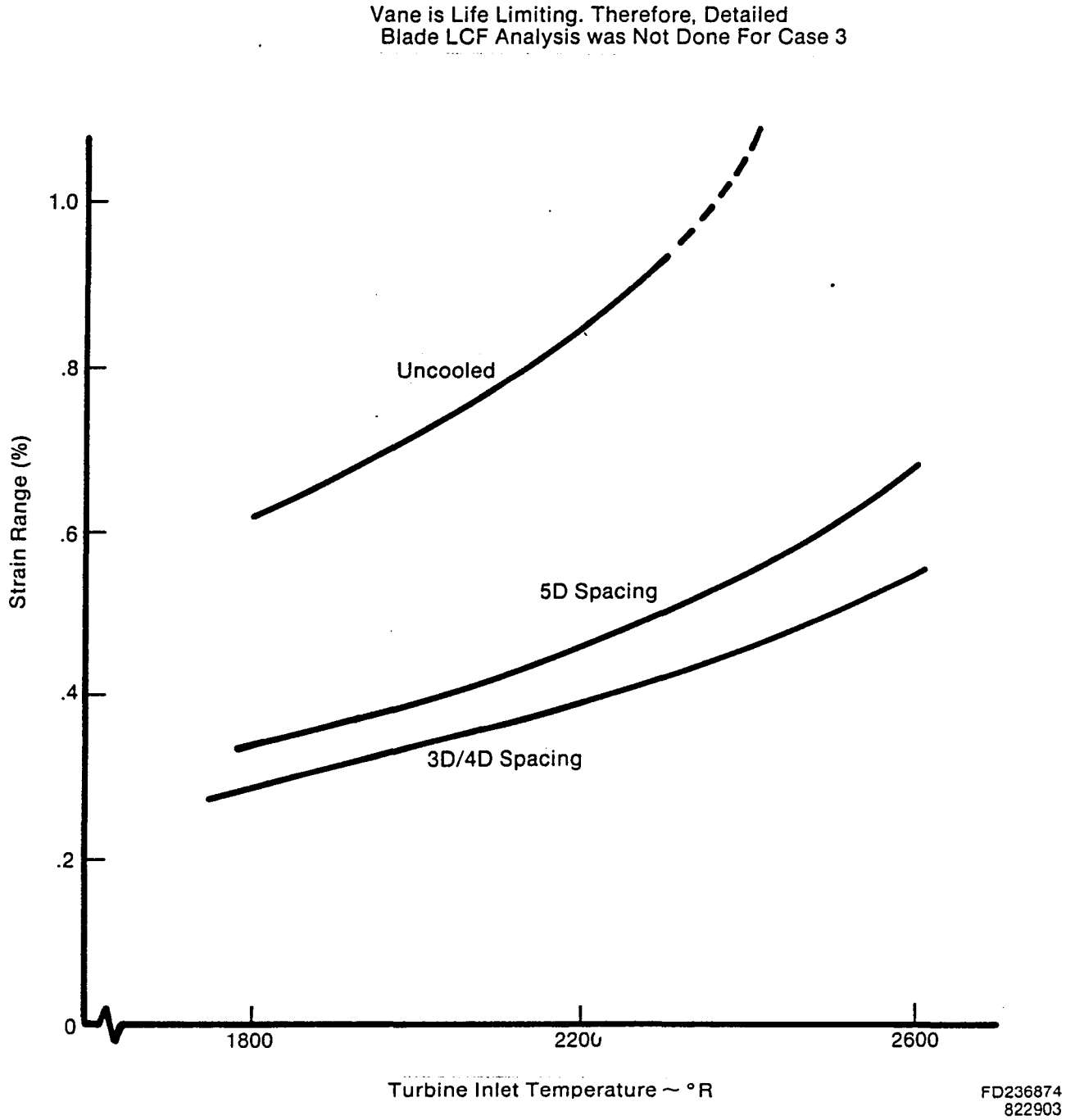

Figure 2.3-8. Case 3 Turbine Vane Strain Range vs. Turbine Inlet Temperature

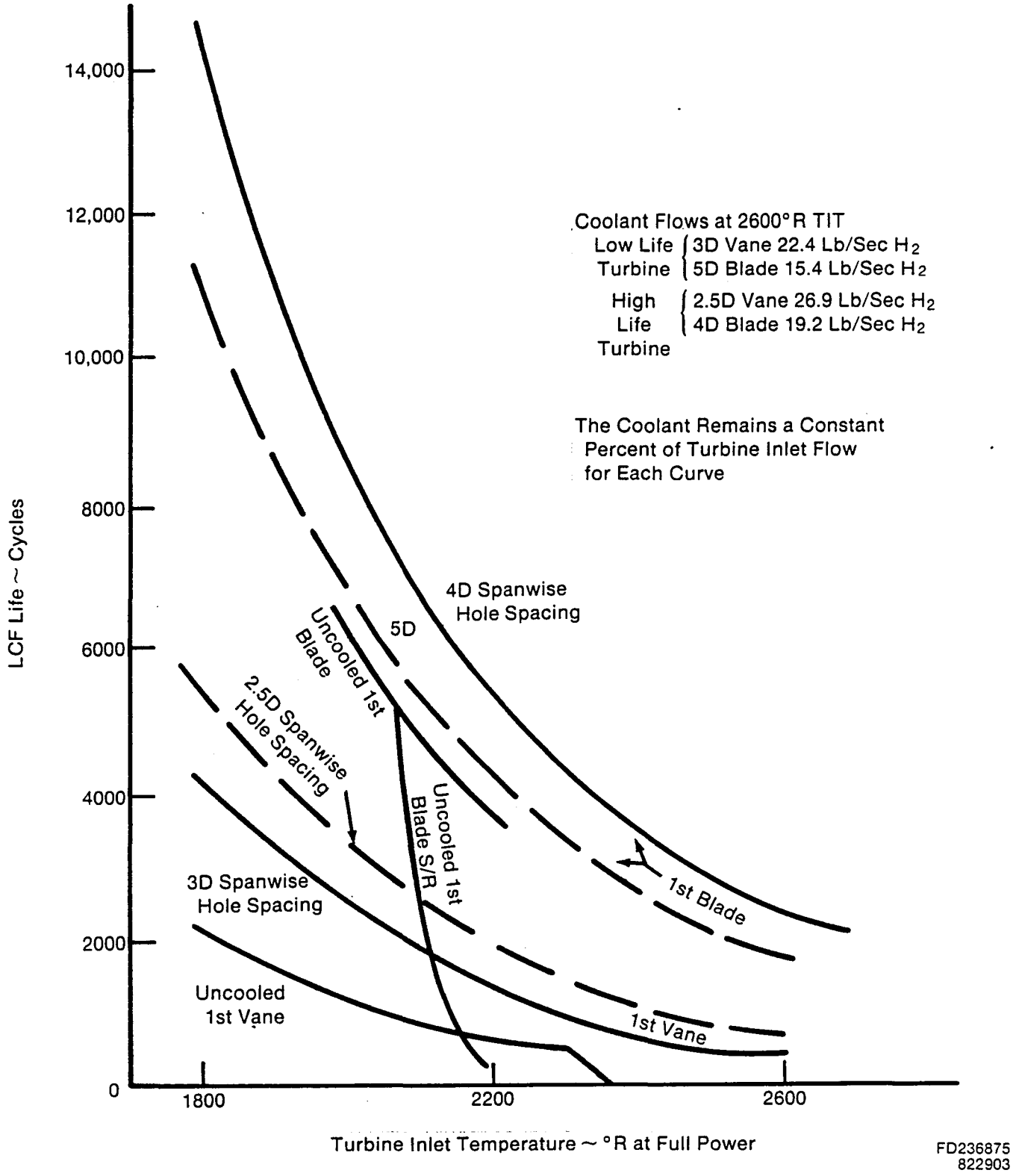

Figure 2.3-9. Case 1 Airfoil Cyclic Life vs. Turbine Inlet Temperature

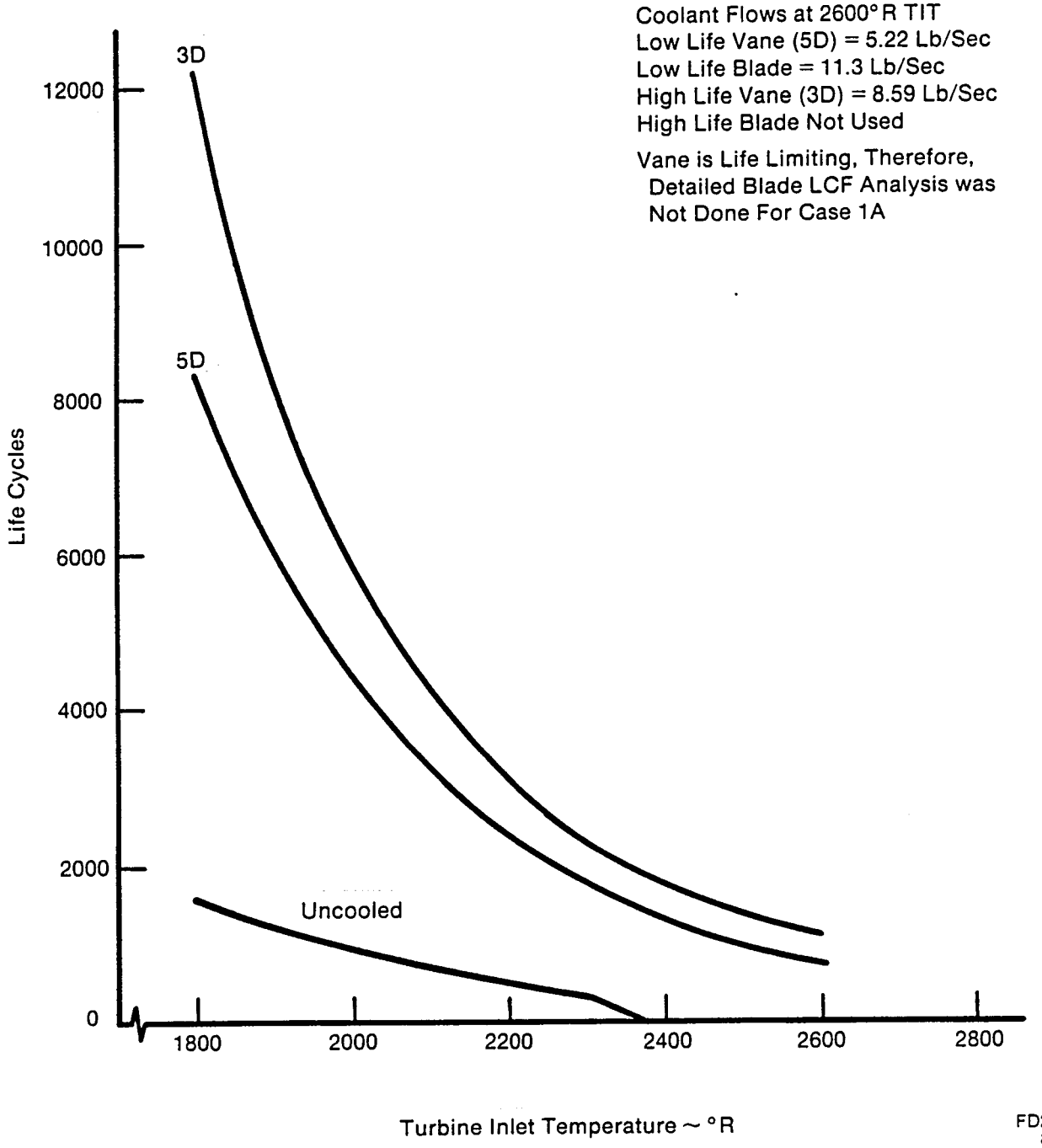

Figure 2.3-10. Case 1A First Vane Life Cycles vs. Turbine Inlet Temperature

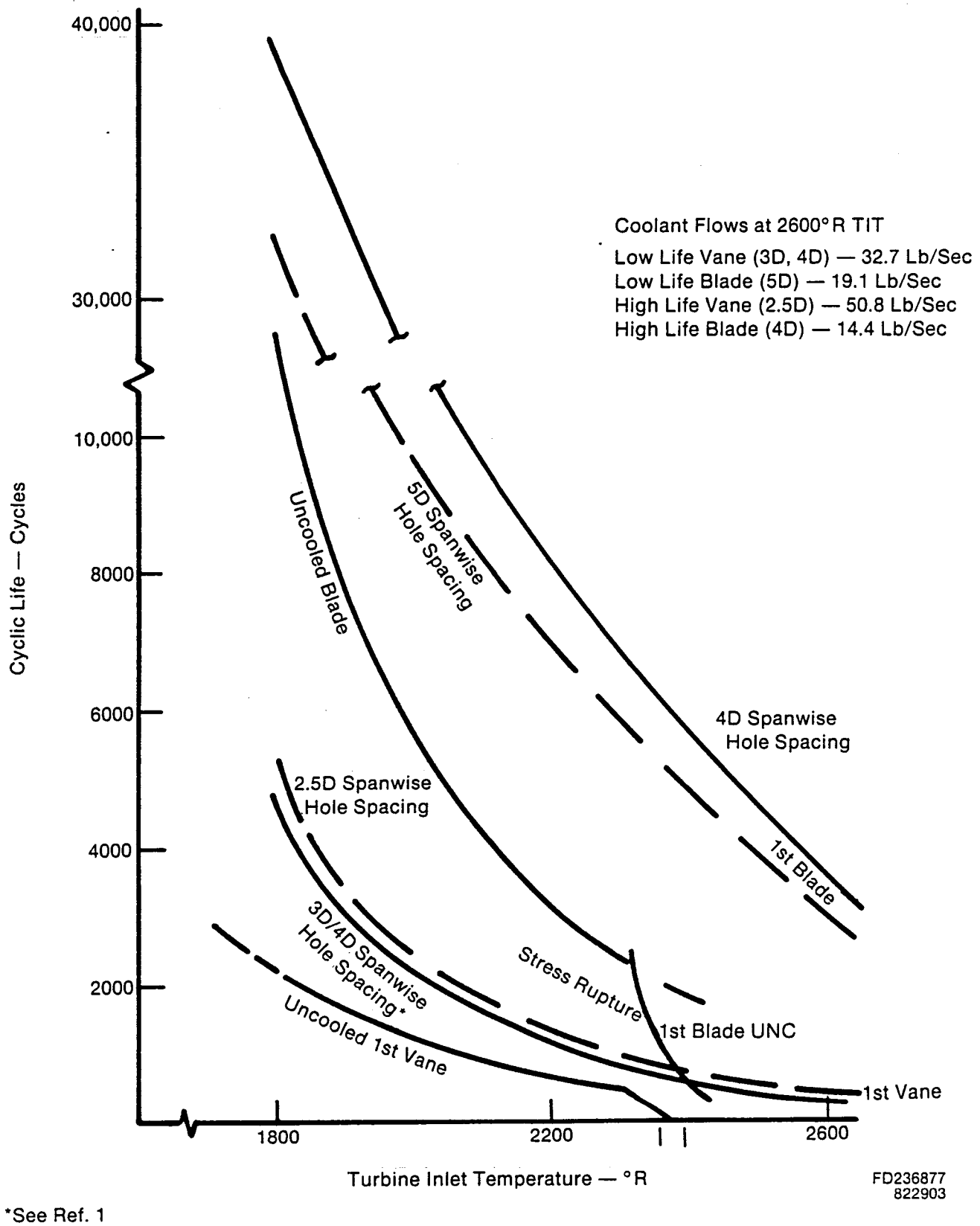

*See Ref. 1

Figure 2.3-11. Case 2 Turbine Cyclic Life vs. Turbine Inlet Temperature

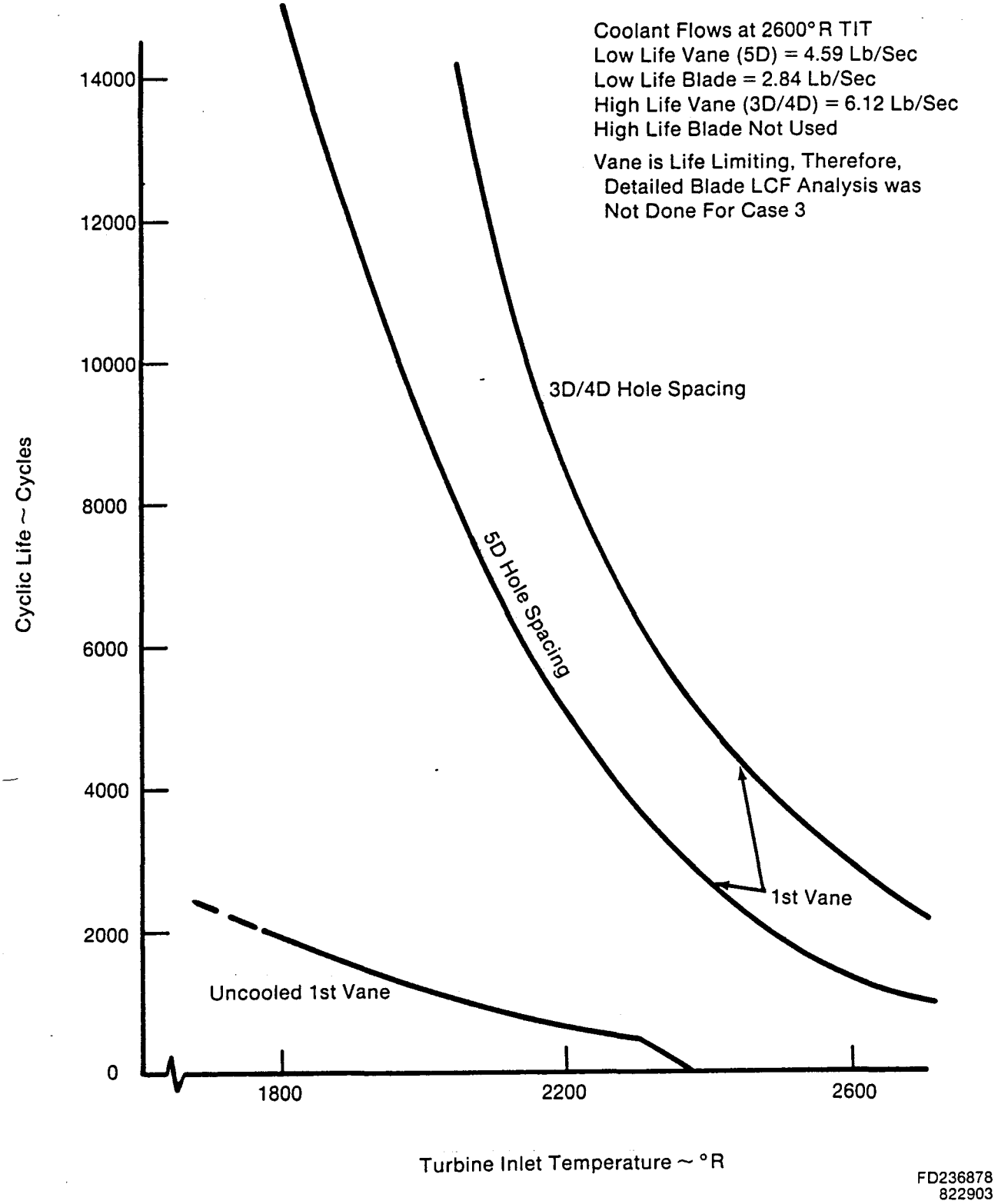

Figure 2.3-12. Case 3 Turbine Cyclic Life vs. Turbine Inlet Temperature

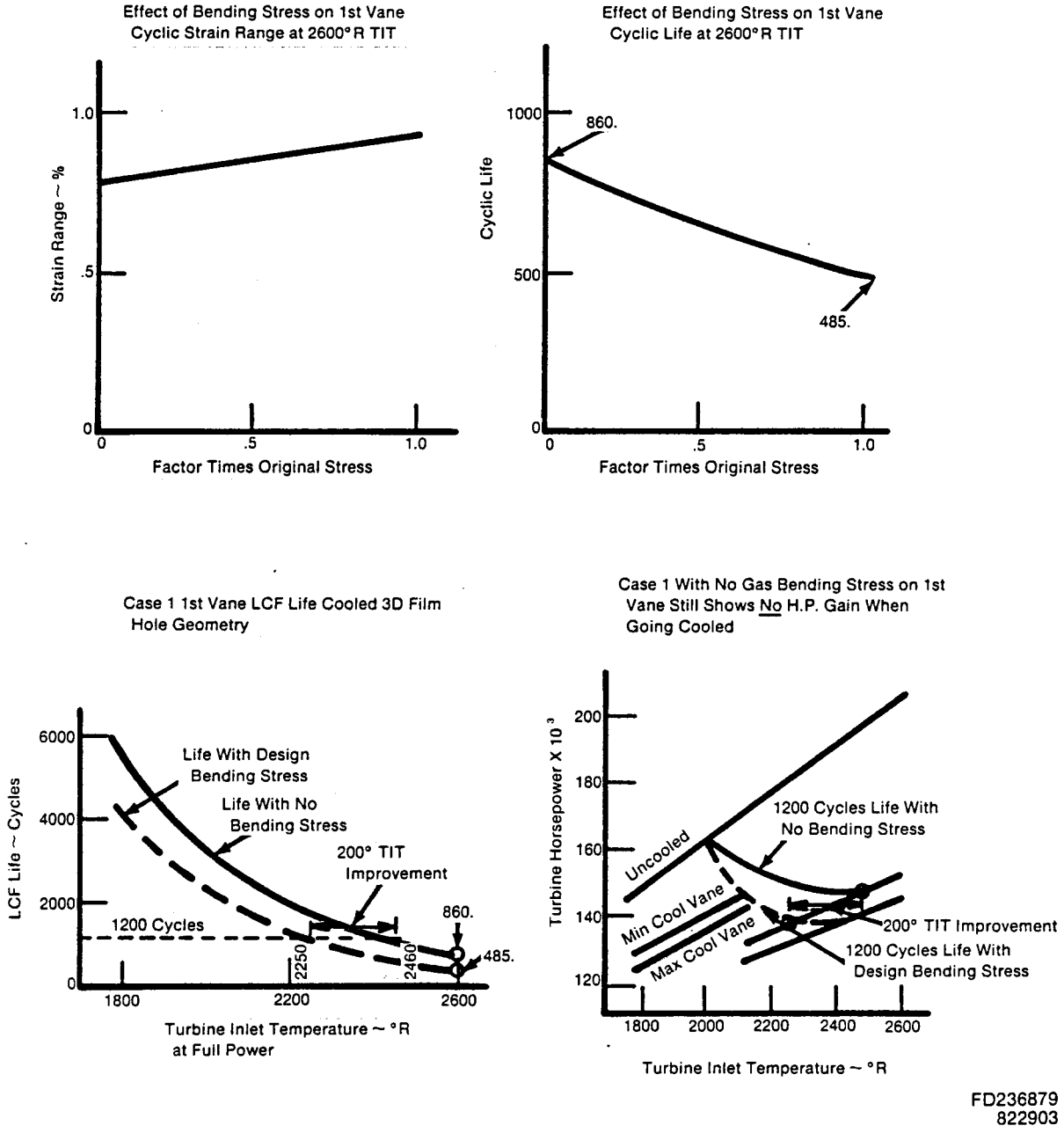

Figure 2.3-13. Case 1 with Reduced First Vane Bending Stresses

2.4 TURBINE EFFICIENCY AND AERODYNAMICS

Efficiency Definition

The definition of turbine effficiency quoted in this study is listed below:

$$\eta = \frac{\Sigma W_1 \text{ Blade } (\Delta H_1 \text{ Stage}) \ldots + W_N \text{ Blade } (\Delta H_N \text{ Stage})}{WEX\ (\Delta H \text{ Ideal})}$$

W_1 Blade = Blade flowrate available for work (lbm/sec)

ΔH_1 Stage = Stage actual specific work (Btu/lbm)

WEX = Turbine exit flowrate (lbm/sec)

ΔH_{Ideal} = Turbine ideal specific work (Btu/lbm)

$\Delta H_{Ideal} = Cp\ TOO\ (1 - p/p)^{\frac{\gamma-1}{\gamma}}$ where TOO is a mixed temperature based on all coolant and leakage flow entering upstream of the first vane throat.

A more detailed explanation has been included in Appendix B.

Aerodynamic Parameters

Turbine sizing studies have been completed for all four cases of the advanced turbine study. All cases have been optimized for peak turbine efficiency, while staying within proven structural limitations and aerodynamic criteria to insure low risk designs.

The optimization studies included wheel speed (diameter), annulus area (airfoil height), and airfoil aspect ratio (axial chord). These studies were made on our meanline design system which evaluates each airfoil row for profile, secondary and trailing edge losses as the geometry is varied. This design system quickly evaluates where the optimum or peak turbine efficiency will occur for a given set of operating requirements. All of the turbine configurations for this study are at or near their maximum efficiencies for the operating conditions and structural limitations used. Additional detailed studies are recommended to fine-tune the final designs prior to hardware commitment.

Groundrules and aerodynamic design criteria used in this study which influence turbine sizing or performance are listed below:

1. Fuel flow (different for each case) was held constant over the temperature range investigated.

2. Structural limitations
   - o 1300 ft/sec maximum rim speed
   - o 500×10^8 in.^{2} rpm^2 maximum blade AN^2 (annulus area times rpm^2

3. Low reaction blades (10% root static pressure reaction)

4. Equal stage work split

5. Vane and blade mean load coefficients . 0.7 and 0.9, respectively

6. Blade hot running radial tip clearance = .015 inches

The detailed aerodynamic results of this study can be found in Appendix B.

The following is a case-by-case summary of the turbine aerodynamic characteristics for the four cases investigated.

Case No. 1

Operating Conditions

Propellants	O_2/H_2
Fuel flowrate	160 pps
Pressure ratio (T-T)	1.6:1
Inlet temperature	1800-2600°R
Inlet pressure	6000 psia
Rotative speed	38,000 rpm

Two-stage, axial flow turbine configurations were selected for Case 1 requirements. Originally, a single-stage design was being investigated, but this was rejected because of excessive exit losses due to high exit swirl and high Mach numbers.

The relatively high flow of Case No. 1, combined with the structural limitations, results in high flow coefficients (Cx/U) over the entire temperature range investigated. For example, at a TIT of 1800°R, Cx/U = 0.8 and at a TIT of 2600°R, Cx/U = 1.5.

Our analysis indicates that a Cx/U of 0.5 to 0.7 is optimum for the level of velocity ratio (U/C = 0.5) of Case No. 1. Cx/U is normally reduced by opening up the annulus area and/or increasing wheel speed. However, Case No. 1 is already at the limit for both of these parameters.

A reduction in speed from 38,000 to 30,000 rpm and an increase in diameter, to maintain a rim speed of 1300 ft per sec, will allow a 60 percent increase in area for lower Cx/U and an approximately 5 percent higher turbine efficiency. However, additional losses such as increased airfoil cooling, higher exit swirl, and disk windage losses would work against the 5 percent efficiency gain.

Because of the high flow coefficients of Case No. 1, additional trade studies to include rotative speed are recommended prior to final configuration selection. This, of course, would have to include the speed effects on the pump as well as on the turbine, to insure an overall cycle benefit. Even with a speed optimization study, the results shown on the power curve in Section 5 at the high temperature locations are not expected to change appreciably (2 to 3%).

The two-stage turbine configurations used for this study require an exit guide vane to take out approx 20 deg of exit swirl. A three-stage turbine could possibly eliminate the need for an exit guide vane. However, the available pressure ratio (1.6) is considered marginal for providing healthy blade root designs in three stages.

Case No. 1A

Operating Conditions

Propellants	O_2/H_2
Fuel flowrate	80 pps
Pressure ratio (T-T)	1.6:1
Inlet temperature	1800-2600°R
Inlet pressure	6000 psia
Rotative speed	38,000 rpm

Case 1A has similar operating conditions to Case 1, except that the fuel flow has been reduced by 50 percent. Once again, two-stage, axial flow turbine configurations have been selected for Case 1A, for the same reasons given in Case 1.

Because of the lower flowrate, the flow coefficients (Cx/U) are near optimum over the temperature range investigated for Case 1A at a TIT of 1800°R, Cx/U = 0.42 and at a TIT of 2600°R, Cx/U = 0.67. Even with the lower flow, all the turbine configurations still required the maximum rim speed and AN^2 to obtain their peak efficiency.

The reduced flow also resulted in lower airfoil gas angles, causing the exit swirl to reach approx 40 deg. This may require two sets of turning vanes to redirect the flow axially. This decision would be made in the final hardware phase.

Case No. 2

Operating Conditions

Propellants	O_2/CH_4
Fuel flowrate	280 pps
Pressure ratio (T-T)	1.6:1
Inlet temperature	1800-2600°R
Inlet pressure	6000 psia
Rotative speed	24,000 rpm

Single-stage, axial flow turbine configurations were selected for Case No. 2 requirements. All of the turbine configurations are fully optimized for flow coeffficent (Cx/U) and velocity ratio (U/C) over the temperature range investigated.

A single-stage design could be used for Case 2, for two basic reasons. First, the sonic velocity of a methane-rich environment is approximately one-half that of a hydrogen-rich environment. Therefore, for a given Mach number the methane turbine will have much lower gas velocities than a hydrogen turbine. This allows optimum

work coefficients and velocity ratios to be achieved at low wheel speeds. The second reason is that the low rotative speed of 24,000 rpm allows an annulus area of 2.5 times larger than that at 38,000 rpm, for an AN^2 of 500×10^8. Thus the low wheel speed required, along with the annulus area capability of the Case 2 turbine allowed fully optimized configurations to be obtained with a single stage.

These turbine configurations have essentially zero exit-swirl, therefore, an exit guide vane will not be required.

Case No. 3

Operating Conditions

Propellants	O_2/CH_4
Fuel flowrate	50 pps
Pressure ratio (T-T)	20:1
Inlet temperature	1800-2600°R
Inlet pressure	4000 psia
Rotative speed	24,000 rpm

Four-stage, axial flow turbine configurations were selected for Case No. 3 requirements. Near-optimum flow coefficients and velocity ratios over the temperature range investigated have been achieved using a common flowpath. These configurations required maximum rim speeds and AN^2 values to obtain peak efficiency.

Case No. 3 has the largest variation in velocity ratio, from U/C of 0.66 at 1800°R to U/C of 0.50 at 2600°R, of the four cases investigated. Two primary reasons for this variation are the large change in specific work capability of methane as temperature is increased and the fact that all the turbine configurations were optimized at the maximum diameter, thus, constant rim speed.

Case 1 and 1A turbines were also at constant diameters but, because the specific work variation between 1800°R and 2600°R is small (13%) for hydrogen properties, the velocity ratio range is also small.

Case No. 2, like Case No. 3, has a wide range in specific work (60%); however, the turbine configurations could be optimized at each temperature level without exceeding the maximum rim speed or AN^2 limitations. Thus, Case 2 has essentially a constant velocity ratio at all operating conditions.

Case No. 3 with low flow requirements was restricted at the 1800°R region from going to a lower diameter, because of its already very low vane aspect ratio. If a smaller diameter were used, the vane height would also have to be reduced to maintain a reasonable exit angle. This was considered to be a risk, since the aspect ratio was already very low at 0.39.

Because of the large variation in velocity ratio for Case No. 3 turbines, there is also a large variation in exit swirl over the temperature range investigated. At 2200°R and 2600°R the exit swirl is -10 deg and -15 deg, respectively. At 1800°R the swirl is -50 deg. At the higher temperatures where the swirl is 10 to 15 deg, additional trade studies with work split and/or diameter should be able to eliminate the need for an exit guide vane. At the 1800°R region a double cascade of exit vanes will be required. Another possibility is a three-stage design, since the exit angle is greater than 90 deg leaving the four-stage configuration.

2.5 TURBINE POWER

Available turbine horsepower for all four cases is presented in Figures 2.5-1 to 2.5-4, as a function of TIT and airfoil cyclic life for varying amounts of airfoil cooling.

Film cooling was used in this study because earlier results showed conventional convective cooling is insufficient in the high heat flux environment of rocket turbines. Two levels of cooling, maximum and minimum, were used to generate the power maps as a function of airfoil cooling. Maximum and minimum cooling flows are achieved by varying the radial spacing of the airfoil film holes.

The fuel flow was held constant over the range of turbine inlet temperatures investigated. Therefore, the total inlet flow was reduced for the cooled turbine, with respect to both fuel and oxidizer, for a given O/F ratio. The coolant for disks, airfoils and platforms has been accounted for in terms of available flow for work and in mixing losses for the coolant re-entry into the mainstream. Blade coolant pumping has been included where applicable.

The limiting cyclic life shown is the expected life of the airfoil, using PWA 1422 minimum material properties. The vane life analysis is for the hot spot vane. The blade life analysis was done using the peak radial gas temperature. See page 9 for a detailed explanation of gas temperature additions. No safety factors were used in the predicted airfoil lives.

The following is a case-by-case summary of the power maps generated for this study.

Case No. 1

The results of Case No. 1, shown in Figure 2.5-1, indicate a loss in turbine horsepower as TIT is increased at constant airfoil life. This horsepower loss is due primarily to the effect that airfoil cooling has on total flow available for work, dilution of mainstream gas temperature, and coolant re-entry losses. The following illustrates these effects for a TIT of 2200°R on an uncooled and a minimum-cooled vane and blade.

	Uncooled	Min. Cooled Vane & Blade	% Change
Horsepower	178,000	136,000	24
W_{blade} (pps)	305	263	14
T_{mixed} (°R)*	2200	2060	6
Efficiency (%)	82.4	77.8	4.6

* Total absolute into blade

The biggest loss in horsepower for Case 1 is due to the reduction in blade flow available for work. Even though the blade coolant re-enters the mainstream flowpath upstream of the first blade, the total flow has been reduced because of the loss in oxidizer. The second largest effect is the mixing of the vane coolant with mainstream gases, causing a dilution of temperature upstream of the blade. The third major effect is the turbine efficiency change due to cooling re-entry losses, blade pumping, and geometry changes associated with the lower flow requirements.

The amount of cooling used for this study is 12 and 15 percent for the minimum and maximum vane, respectively, and 9 per cent for the minimum blade. The percentage of cooling is based on total inlet flow (fuel plus oxidizer), and includes both airfoil and platform cooling.

The results of this study clearly show that improved cooling, such as an advanced convective cooling scheme, will be required before an increase in turbine horsepower can be realized at higher inlet temperatures without sacrificing airfoil life.

Case No. 1A

The results of Case No. 1A, shown in Figure 2.5-2, indicate very little change in delivered turbine horsepower when increasing TIT at constant airfoil life. The percentage loss in turbine horsepower associated with airfoil cooling is similar to Case 1, as illustrated below for a TIT of 2200°R.

	Uncooled	Min. Cooled Vane & Blade	% Change
Horsepower	88,200	70,000	21
W_{blade} (pps)	150	134	11
T_{mixed} (°R)	2200	2140	3
Efficiency (%)	82.5	75.3	7.2

The primary reason that Case 1A did not show a loss in horsepower when temperature is increased, as Case 1 did, is due to the reduced first vane gas bending stresses associated with the lower flow requirements. Since the major contributor to airfoil strain is now thermal stress, not gas bending stress, film cooling provides a great improvement in TIT capability.

The amount of cooling used in this study is 5 and 9 percent for the minimum and maximum vane, respectively, and 10 percent for the minimum blade. The percentage of cooling is based on total inlet flow (fuel plus oxidizer), and includes both airfoil and platform cooling. Because of the lower vane stresses and total surface area of Case 1A, compared to Case 1, a lower percentage of coolant was used. The percentage of blade coolant is similar for Case 1 and 1A, due to similar centrifugal stress levels.

The results of Case 1A also show the need for improved cooling, such as an advanced convective cooling scheme, will be required before an increase in turbine horsepower can be realized at higher inlet temperatures without sacrificing airfoil life.

Case No. 2

The results of Case No. 2, shown in Figure 2.5-3, indicate that approximately 10 percent higher turbine horsepower can be achieved when increasing TIT at constant airfoil life. The loss in horsepower due to airfoil cooling is lower for Case 2 than in Cases 1 and 1A, as illustrated below.

	Uncooled	Min. Cooled Vane & Blade	% Change
Horsepower	62,000	53,100	14
W_{blade} (pps)	400	379	5
T_{mixed} (°R)	2200	2090	5
Efficiency (%)	84.5	80.0	4.5

This lower horsepower loss is due primarily to the 5 percent loss in available flow for work, compared to the 14 percent loss in Case No. 1. There are two reasons for this. First, the lower O/F ratio of methane (0.46), compared to hydrogen (0.93), at 2200°R results in a lower percentage of oxidizer lost for a given percentage of coolant. Second, the percentage of coolant required for Case 2 is less than for Case 1.

Another important difference is the change in specific work capability of hydrogen and methane over the temperature range investigated. Hydrogen properties show a 13 percent increase in ideal specific work capability, when going from 1800°R to 2600°R. Methane shows a 60 percent increase in ideal specific work capability over the same temperature change. Therefore, the combination of low horsepower loss for airfoil cooling, plus the higher specific work increase at elevated temperatures, contributed to an increase in turbine horsepower as TIT is increased for Case No. 2.

The amount of cooling used in this study is 10 and 17 percent for the minimum and maximum vane, respectively. The minimum blade cooling is 5 percent. The percentage of cooling is based on total inlet flow (fuel plus oxidizer), and includes airfoil and platform cooling.

Case No. 3

The results of Case No. 3, shown in Figure 2.5-4, indicate that a substantial gain in turbine horsepower can be realized by increasing TIT, without sacrificing airfoil life. Airfoil cooling effects on turbine horsepower are illustrated below for a turbine inlet temperature of 2200°R.

	Uncooled	Min. Cooled Vane & Blade	% Change
Horsepower	56,900	50,500	13
W_{blade} (pps)	69.0	65.0	6
T_{mixed} (°R)	2200	2110	4
Efficiency (%)	78.6	72.3	6.4

Similar to Case No. 2, the combination of a low percentage loss in available flow for work with the cooled airfoils, plus the large increase in specific work capability of methane fuel over the temperature range investigated, results in a gain in horsepower, as TIT is increased.

The amount of airfoil cooling used in this study is 8 and 11 percent for the minimum and maximum vane, respectively. The minimum blade cooling is 6 percent.

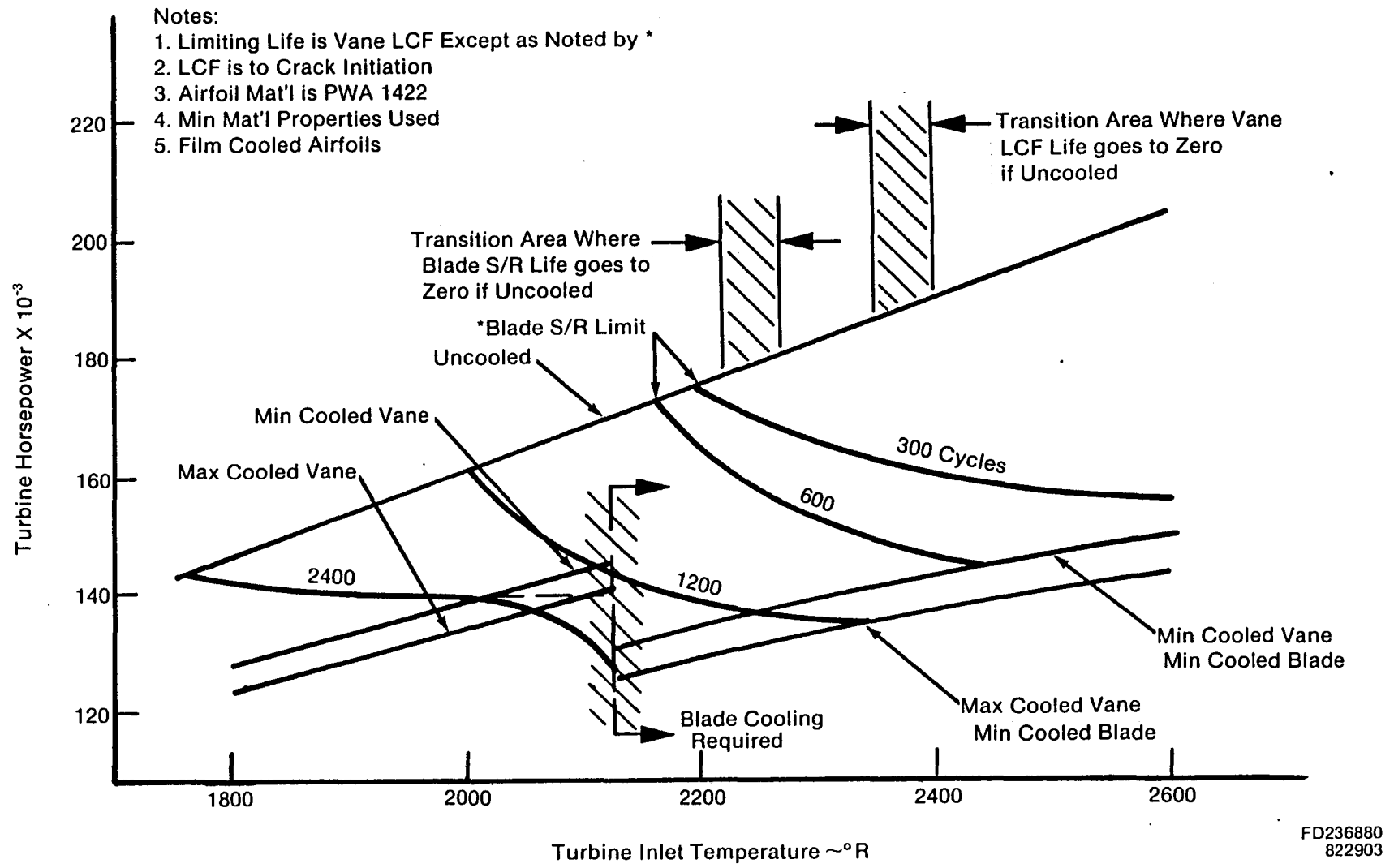

Figure 2.5-1. Case 1 Delivered Turbine HP vs. TIT

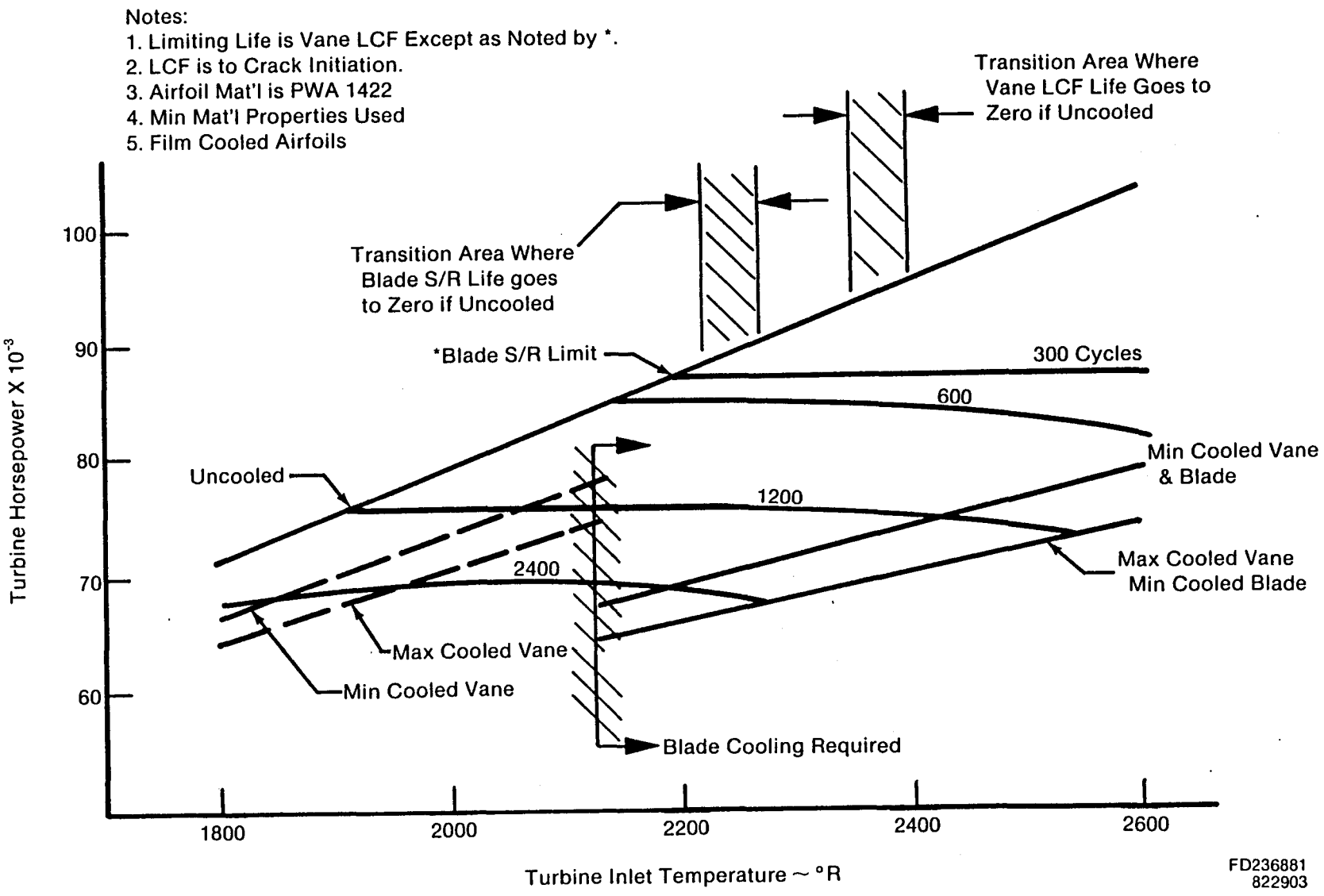

Figure 2.5-2. Case 1A Delivered Turbine HP vs. TIT

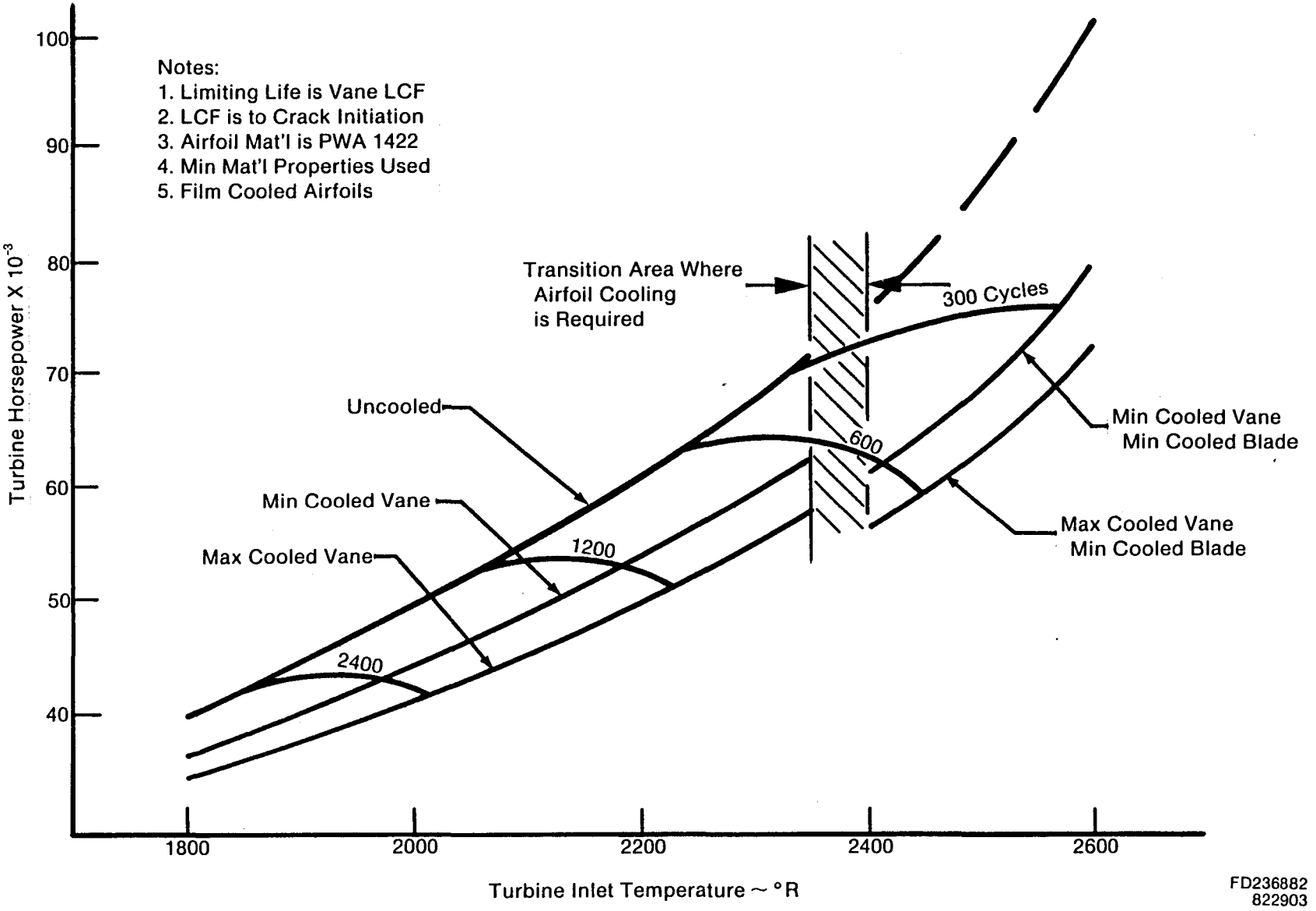

Figure 2.5-3. Case 2 Delivered Turbine HP vs. TIT

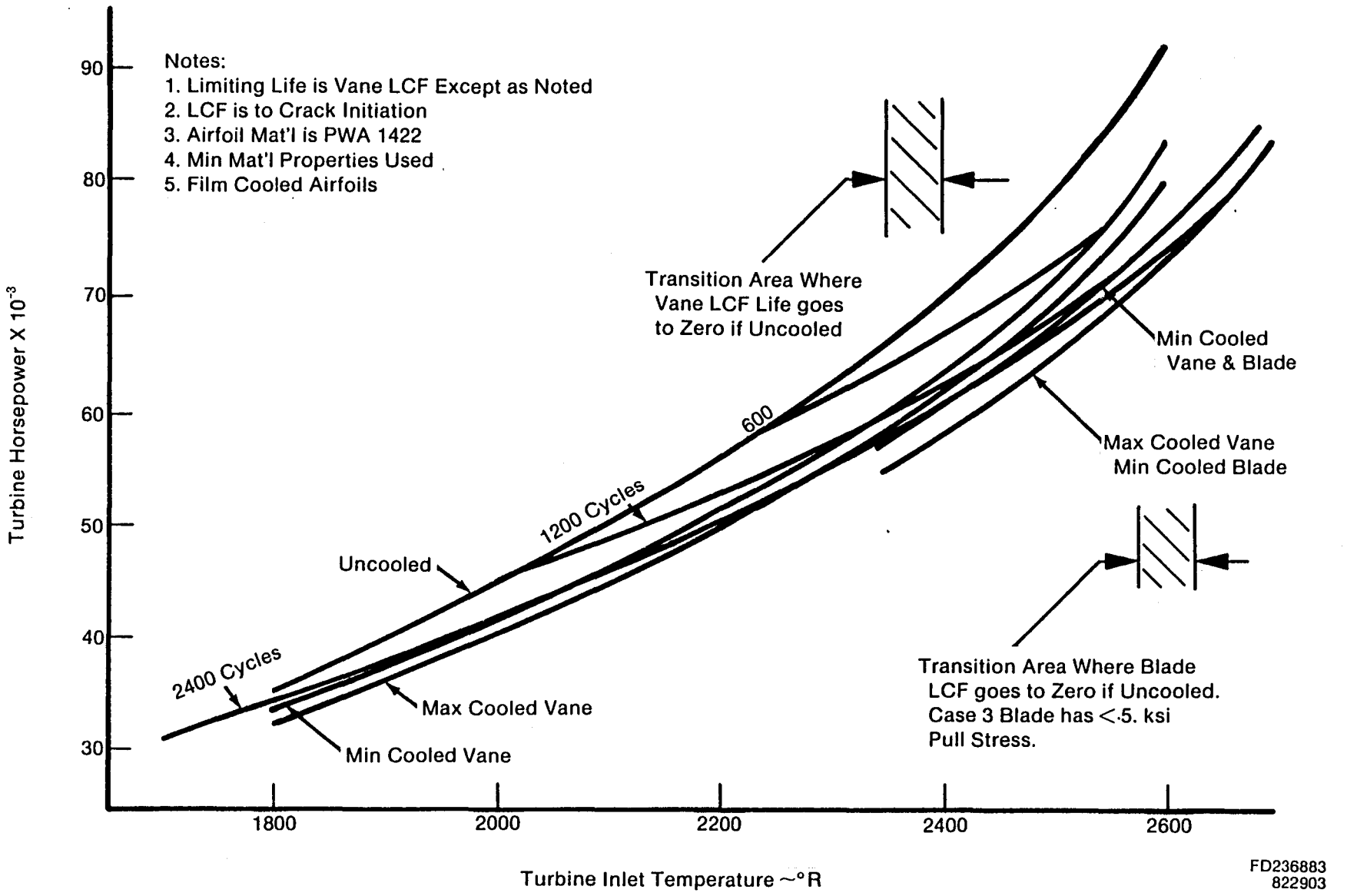

Figure 2.5-4. Case 3 Delivered Turbine HP vs. TIT

2.6 RECOMMENDATIONS

Future projects that might yield large turbine horsepower payoffs by permitting higher turbine inlet temperature operation are listed below:

1. An advanced convective cooling scheme was conceived during this contract and is pictured in Figure 2.6-1. Grooves are either machined or photo-engraved on the outside surface of a cast or forged airfoil. The outside is then covered with an electroformed or sputtered layer of high conductivity material while the grooves are temporarily shielded with a removable filler. The advantage of this scheme is that the temperature gradient through the wall is greatly reduced over simple convective cooling systems, because the coolant passage is close to the outside wall. A technology program that develops this concept for turbine airfoils would yield a turbine horsepower increase by minimizing coolant quantities and associated losses.

2. Use of a refractory material for turbine airfoils would permit higher turbine inlet temperature operation than conventional alloys. Higher TIT capability would translate directly into greater horsepower output. A feasibility study could investigate the alloy selection, manufacturing method and analytical considerations. If the refractory material proved feasible, a development program would follow.

3. The material used in this study was directionally solidified MAR-M-200. More advanced single-crystal alloys are available, but they have not been screened for hydrogen embrittlement problems. The life and horsepower benefits using these alloys should be assessed. Hydrogen embrittlement tests should precede any fuel-rich turbine development work, if the payoff using these alloys is found worthwhile.

Fuel-rich turbines using methane as a fuel have several unique traits which require investigation before significant development work proceeds. The following recommendations address these areas of concern:

1. Free carbon in the combustion products of a methane turbine could cause problems. Solid particle erosion of the airfoils would occur for re-useable turbines. Also, plugging of coolant holes would cause problems. Carbon build-up on the rotor blades would add to the centrifugal stresses, thus reducing life. A study should be performed that would identify operating conditions (O/F ratio, pressure, etc.) that would cause free carbon to be present in the combustion products, so that these operating conditions could be avoided.

2. The combustion properties of CH_4/O_2 vary considerably, depending on whether frozen or equilibrium conditions are assumed. Since turbine characteristics are calculated using these properties, it is essential that their values are known. An investigation should be performed that would identify which assumption (frozen or equilibrium) should be used.

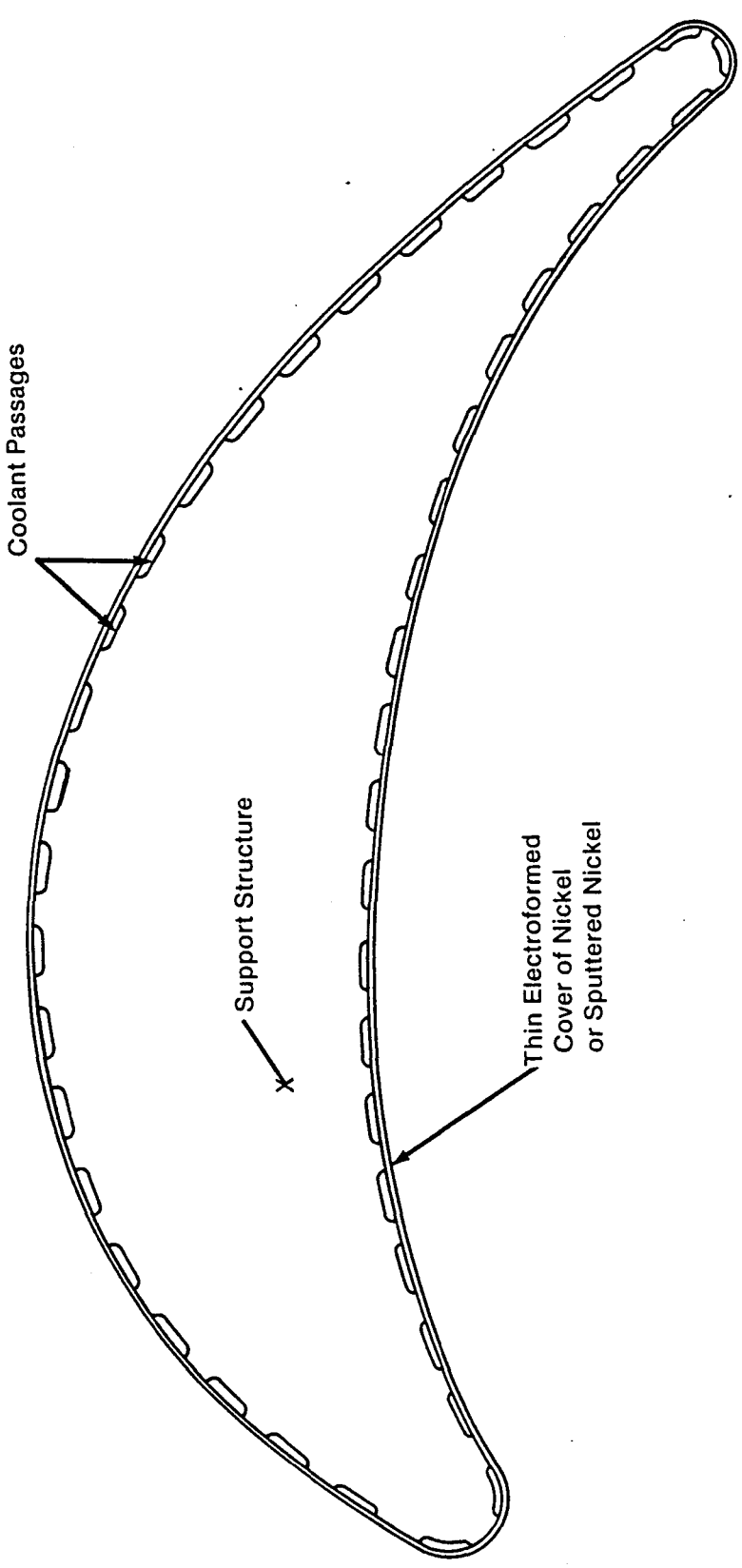

Figure 2.6-1. Advanced Convective Cooling

APPENDIX A

AIRFOIL COOLING SCHEMES

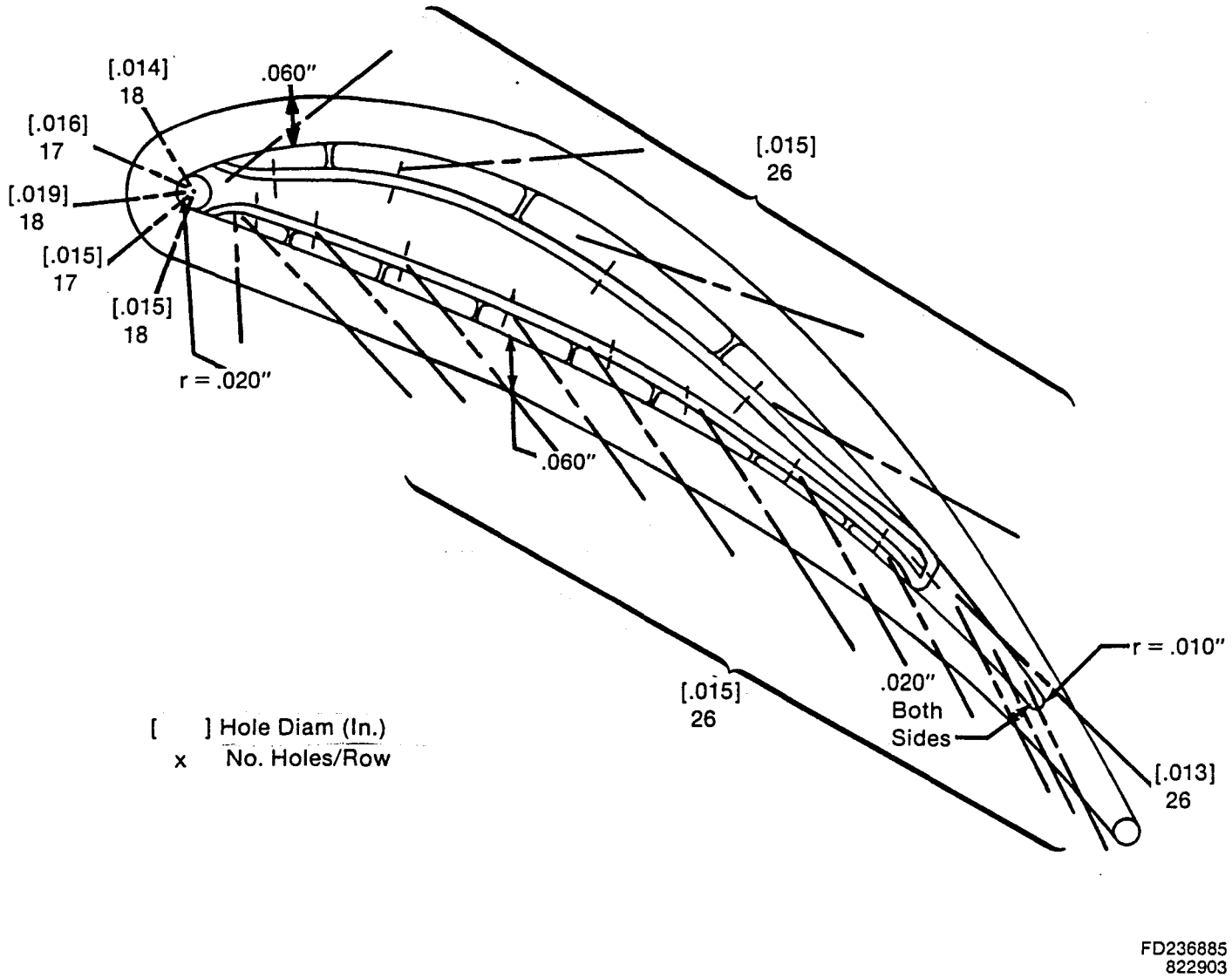

Figure A.1. Case 1 Preliminary Geometry Definition
First Vane, Number of Foils = 30

Row	Number Holes Per Row	Diameter	H_2 Flow Lb/Sec/Airfoil	Coolant PT/PS	Row	Number Holes Per Row	Diameter	H_2 Flow Lb/Sec/Airfoil	Coolant P_T/P_S
1	19	0.013″	.0344	1.15	9	20	0.015″	0.0237	1.05
2	19	0.013″	.0359	1.17	10	20	0.015″	0.0272	1.05
3	19	0.015″	.0163	1.02	11	20	0.015″	0.0274	1.05
4	19	0.013″	.0381	1.20	12	20	0.015″	0.0275	1.05
5	19	0.013″	.0438	1.31	13	20	0.015″	0.0276	1.05
6	20	0.015″	.0237	1.05	14	20	0.015″	0.0277	1.05
7	20	0.015″	.0237	1.05	15	20	0.015″	0.0277	1.05
8	20	0.015″	.0238	1.05	16	20	0.015″	0.0277	1.05

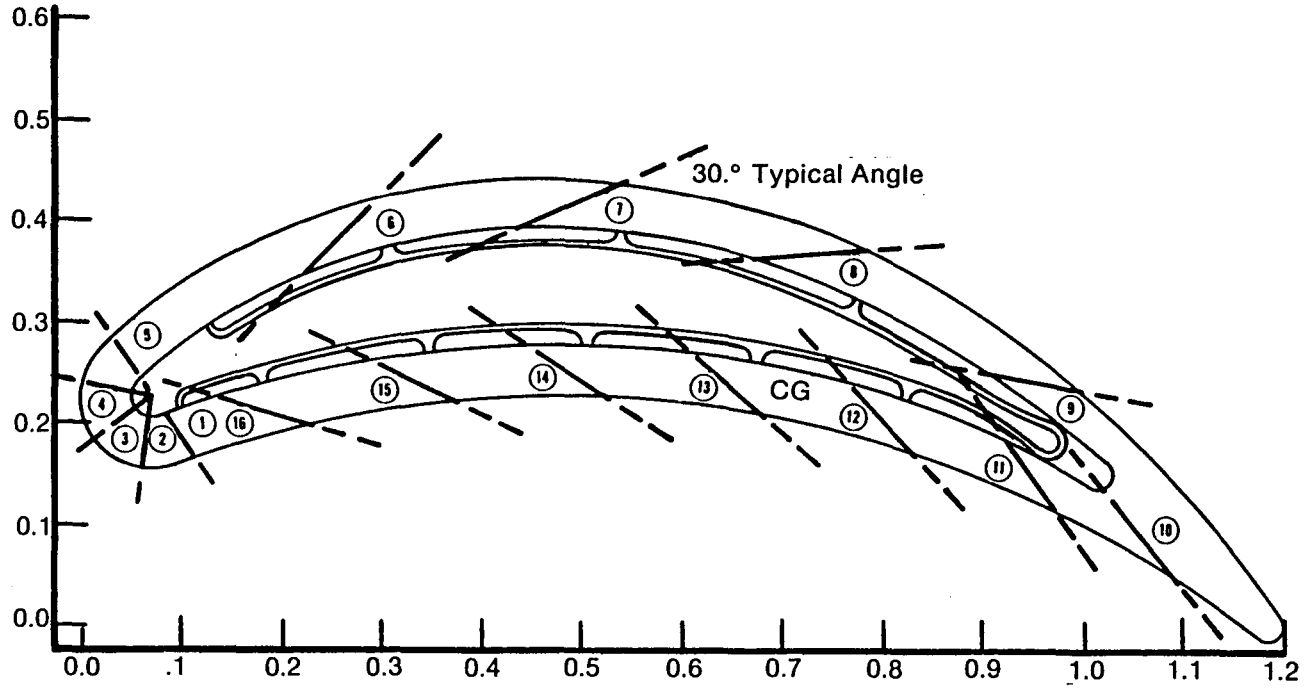

T_{TREL} = 2480°R = 204
= 2684°R
P_{TREL} = 5275. Psia
M_{REL} = 0.364
42 Blades

Span = 1.18 Inch
δ_{Pull} = 27000 Psia

FD236886
822903

Figure A-2. Case 1 2600°R, Two-Stage First Blade Mean

Row	Holes/Row	Diameter	H_2 Flow Lbs/Sec/Foil	Coolant P_T/P_S
1	18	.015	.0233	1.03
2	17	.019	.0354	1.03
3	18	.015	.0233	1.03
4	17	.015	.0268	1.04
5	18	.015	.0344	1.06
6	26	.015	.0286	1.025
7	26	.015	.0303	1.03
8	26	.015	.0280	1.03
9	26	.015	.0277	1.03
10	26	.015	.0278	1.03
11	26	.015	.0280	1.03
12	26	.015	.0284	1.03
13	26	.015	.0264	1.025
14	26	.015	.0277	1.025
15	26	.015	.0238	1.02
16	26	.015	.0241	1.02
17	26	.015	.0243	1.02
18	26	.015	.0337	1.03
19	26	.015	.0337	1.03
20	26	.015	.0337	1.03

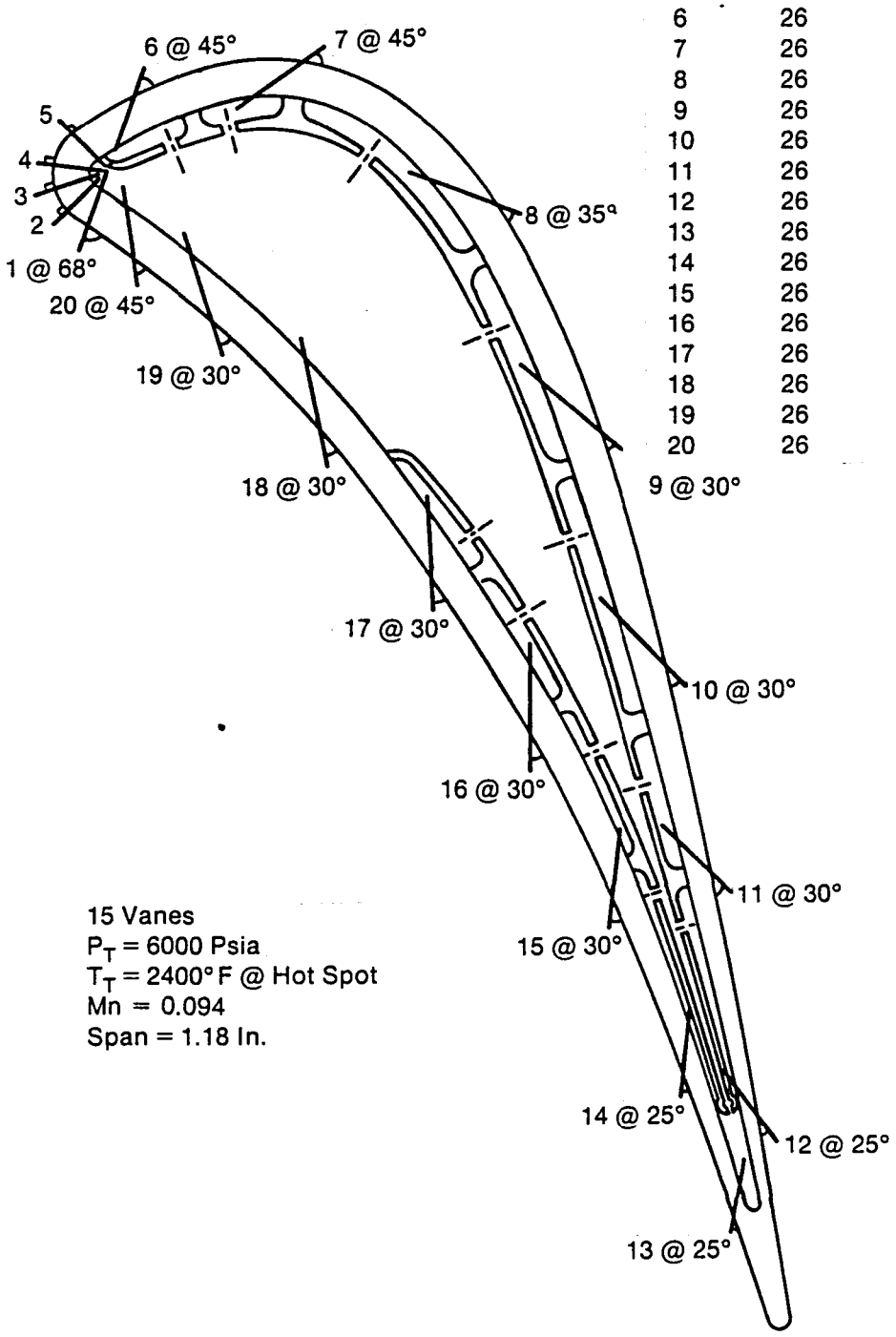

Figure A-3. Case 1A First Vane Filmhole Design

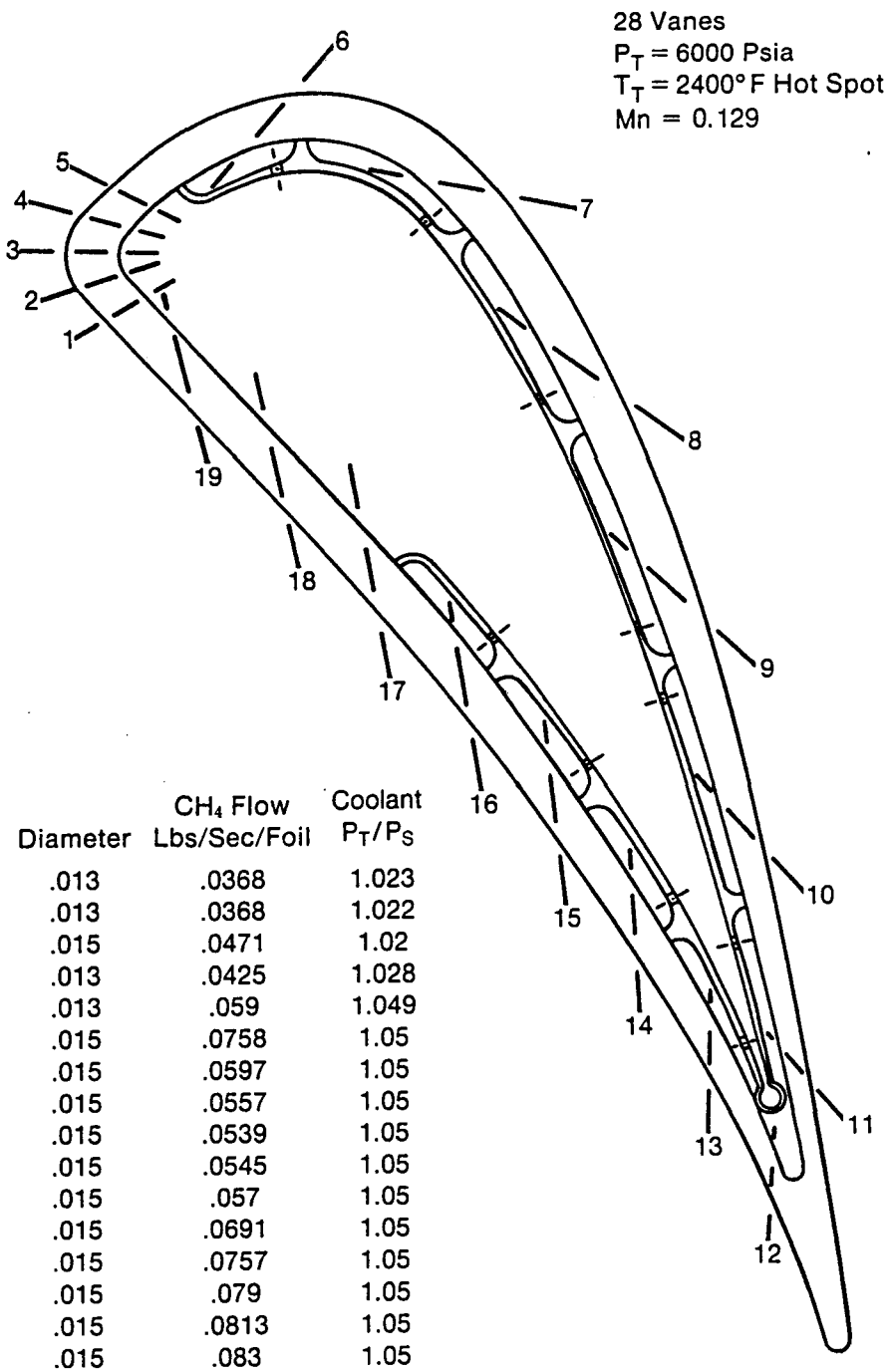

Row	Number Holes Per Row	Diameter	CH_4 Flow Lbs/Sec/Foil	Coolant P_T/P_S
1	18	.013	.0368	1.023
2	18	.013	.0368	1.022
3	18	.015	.0471	1.02
4	18	.013	.0425	1.028
5	18	.013	.059	1.049
6	19	.015	.0758	1.05
7	19	.015	.0597	1.05
8	19	.015	.0557	1.05
9	19	.015	.0539	1.05
10	19	.015	.0545	1.05
11	19	.015	.057	1.05
12	19	.015	.0691	1.05
13	19	.015	.0757	1.05
14	19	.015	.079	1.05
15	19	.015	.0813	1.05
16	19	.015	.083	1.05
17	19	.015	.0763	1.043
18	19	.015	.0657	1.033
19	19	.015	.0597	1.028

Figure A-4. Case 2 First Vane

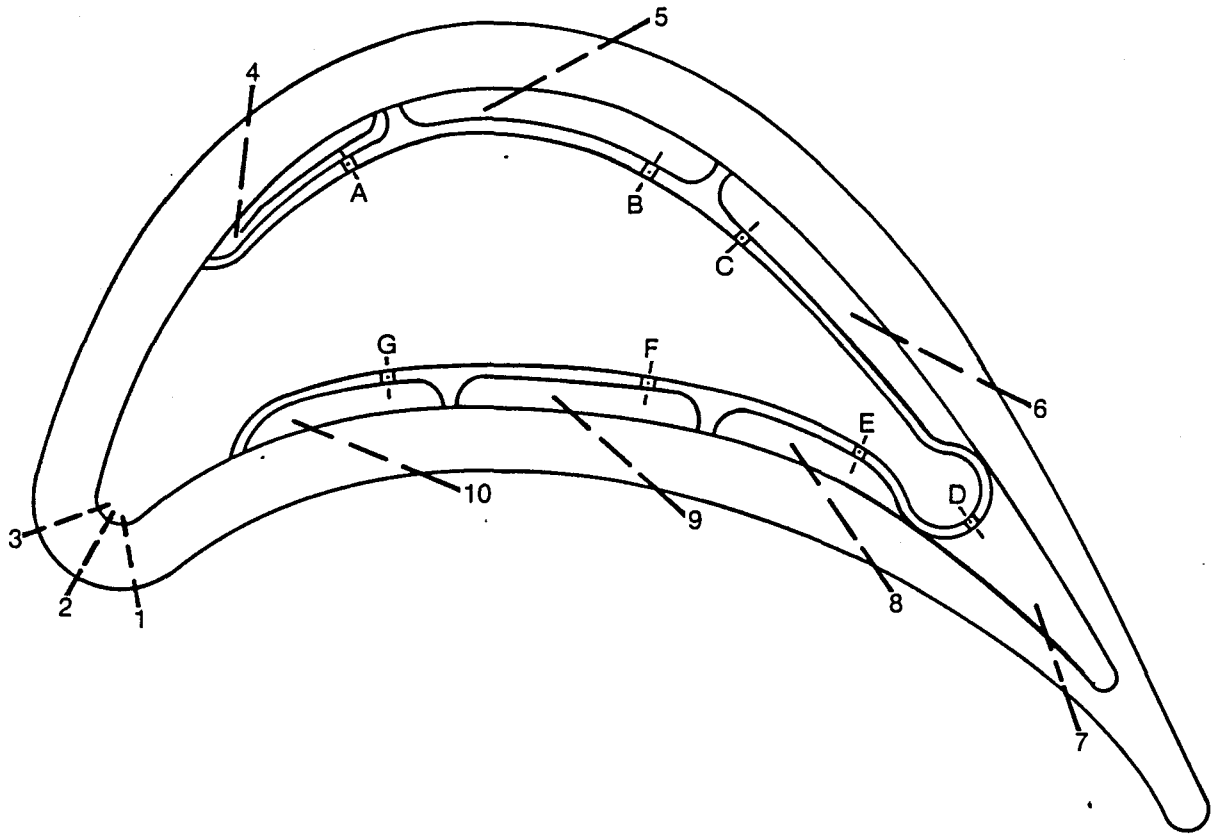

Row	Holes/Row	Hole Dia.	CH_4 Flow Lb/Sec	Coolant P_T/P_S
1	11	.015"	.0455	1.082
2	11	.015"	.0214	1.02
3	11	.015"	.0505	1.106
4	17	.015"	.0274	1.02
5	17	.015"	.0253	1.02
6	17	.015"	.0261	1.02
7	17	.015"	.0296	1.02
8	17	.015"	.0304	1.02
9	17	.015"	.0311	1.02
10	17	.015"	.0316	1.02

FD236889
822903

Figure A-5. Case 2 First Blade

38 Vanes
0.265 Inch Span
P_T = 4000 Psia
T_T = 2400.°F (Hot Spot)
Mn = 0.151

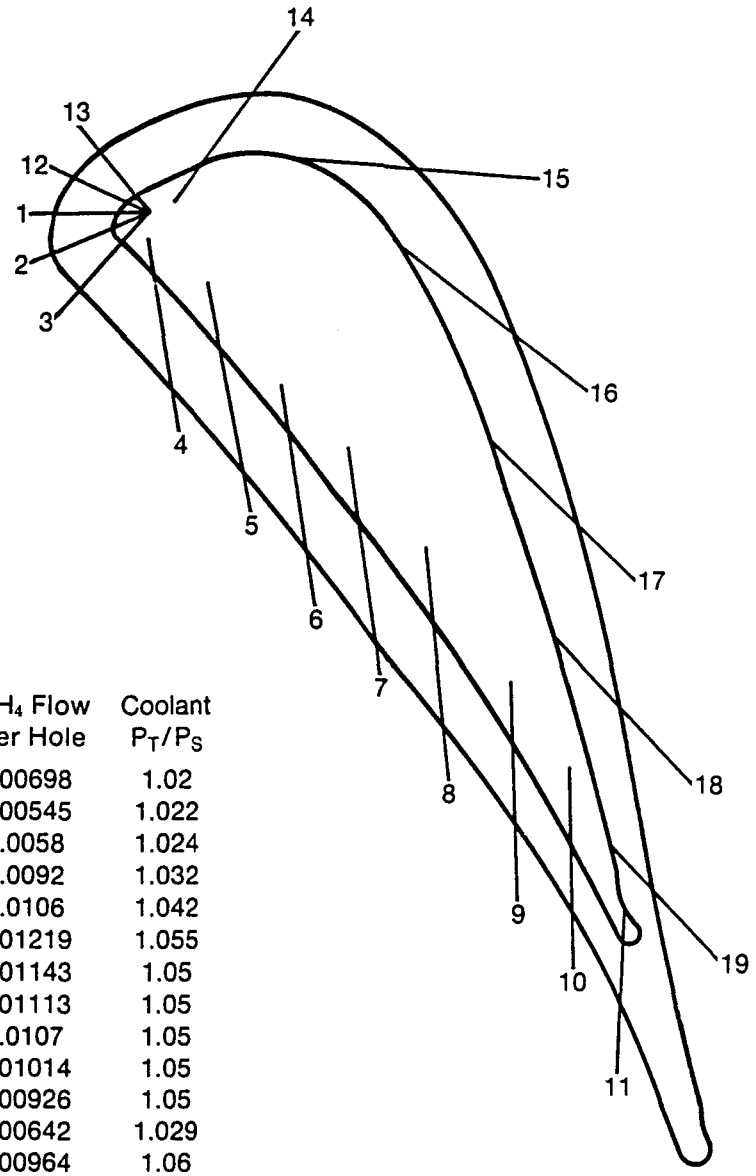

Row	Number Holes	Diameter	CH_4 Flow Per Hole	Coolant P_T/P_S
1	4	.015	.00698	1.02
2	4	.013	.00545	1.022
3	4	.013	.0058	1.024
4	4	.015	.0092	1.032
5	4	.015	.0106	1.042
6	4	.015	.01219	1.055
7	4	.015	.01143	1.05
8	4	.015	.01113	1.05
9	4	.015	.0107	1.05
10	4	.015	.01014	1.05
11	4	.015	.00926	1.05
12	4	.013	.00642	1.029
13	4	.013	.00964	1.06
14	4	.015	.01029	1.05
15	4	.015	.00713	1.05
16	4	.015	.00595	1.05
17	4	.015	.00583	1.05
18	4	.015	.00616	1.05
19	4	.015	.00671	1.05

Figure A-6. Case 3 Vane Film Hole Geometry

APPENDIX B

TURBINE AERODYNAMICS

CASE 1

TURBINE EFFICIENCY DEFINITION

AND AERODYNAMIC PARAMETERS

The definition of turbine efficiency quoted in this study is listed below:

$$\eta = \frac{W1B(\Delta HACT\ 1\ STG) + W2B(\Delta HACT\ 2\ STG)}{WEX(\Delta HIDEAL)}$$

$$= \frac{W1B(Cp(T01-TX1)+W2B(Cp(T02-TX2)}{WEX\ (Cp \times T01\ (1 - PX2/P01^{\frac{\gamma-1}{\gamma}}))}$$

*T01 Turbine inlet total temperature - °R

**T02 2nd Stage inlet total temperature - °R

P01 Turbine inlet total pressure - psia

PX2 Turbine exit total pressure - psia

***TX1 1st stage exit total temperature - °R

***TX2 2nd stage exit total temperature - °R

W1B 1st stage blade flowrate available for work which includes any coolant or leakage entering the mainstream flowpath upstream of the blade gaging (throat) - lbm/sec

W2B 2nd stage blade flowrate available for work which includes any coolant or leakage entering the mainstream flowpath upstream of the 2nd blade gaging (throat) - lbm/sec

WEX Turbine exit flowrate including all coolant or leakage entering the mainstream flowpath - lbm/sec.

γ Ratio of specific heats at inlet conditions.

Cp Specific heat at constant pressure - Btu/lbm°F

* T01 is based on a mixed temperature calculation which includes all coolant and leakage entering the mainstream flowpath stream of the 1st vane gaging (throat).

** T02 is based on the 1st stage inlet mixed temperature (T01) minus the ΔT due to 1st stage work plus a mixed temperature calculation including all coolant and leakage entering the mainstream aft of the 1st vane gaging and upstream of the 2nd vane gaging.

*** TX1 and TX2 are calculated from stage inlet temperatures minus stage work for their respective stages.

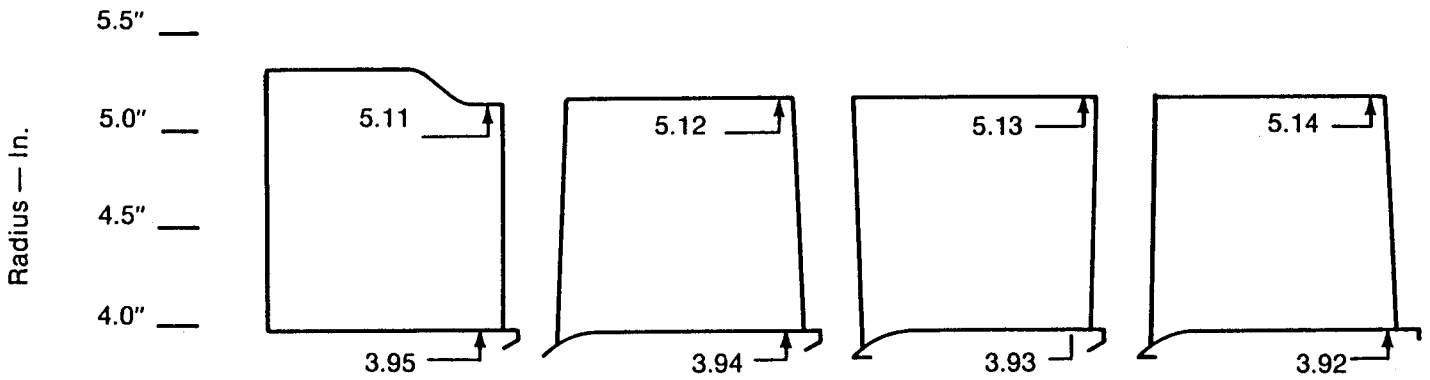

Turbine Data (Overall)	Uncooled	Min Cooled Vane	Max Cooled Vane
$\eta_{T\text{-}T}$ %	83.8	82.8	82.7
$PR_{T\text{-}T}$	1.6	1.6	1.6
U/C_m	.48	.49	.50
$\dot{w}\sqrt{T}/P$ @ Inlet	1.89	1.58	1.51
Speed — RPM	38000	38000	38000
C_x/U_m	.96	.84	.82

First Stage Data	Vane	Blade	Vane	Blade	Vane	Blade
# Foils	26	38	25	36	24	36
Aspect Ratio	.97	.98	.97	.98	.97	.98
Turning — Degrees	65	100	67	105	67	106
Zweifel Coeff.	.7	.9	.7	.9	.7	.9
U_{rim} (Ft/Sec)	—	1300	—	1300	—	1300
AN^2 (IN^2/RPM^2)	—	500 X 10^8	—	500	—	500

FD236891
822903

Figure B.1-1. Case No. 1
Too = 1800°R, H_2/O_2

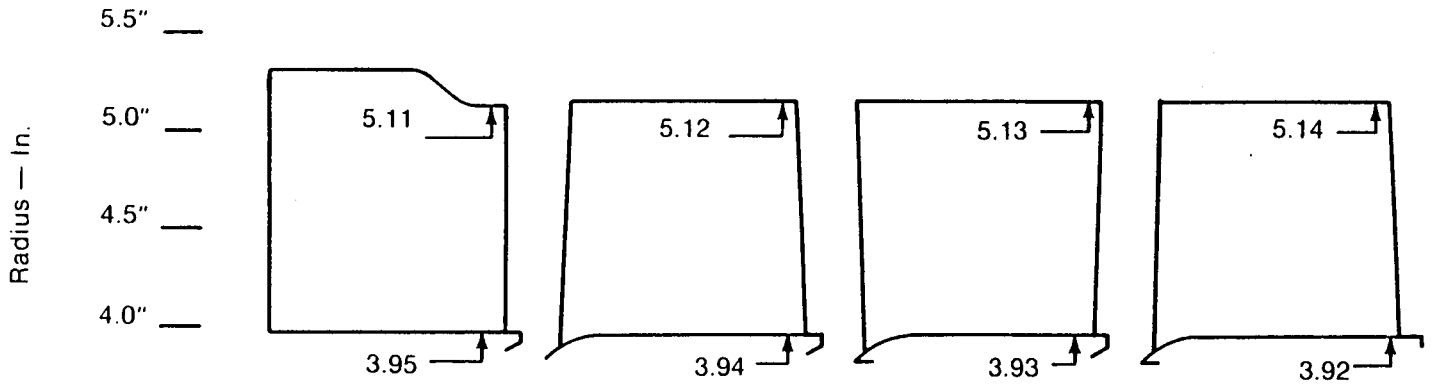

Turbine Data: (Overall)	Uncooled	Min Cooled Vane Min Cooled Blade	Max Cooled Vane Min Cooled Blade
$\eta_{T\text{-}T}$ %	82.4	77.8	77.1
$PR_{T\text{-}T}$	1.6	1.6	1.6
U/C_m	.47	.49	.48
$\dot{w}\sqrt{T}/P$ @ Inlet	2.37	1.69	1.62
Speed — RPM	38000	38000	38000
C_x/U_m	1.2	.93	.91

First Stage Data	Vane	Blade	Vane	Blade	Vane	Blade
# Foils	29	40	25	38	24	38
Aspect Ratio	.97	.98	.97	.98	.97	.98
Turning — Degrees	60	91	67	103	67	105
Zweifel Coeff.	.7	.9	.7	.9	.7	.9
U_{rim} (Ft/Sec)	—	1300	—	1300	—	1300
AN^2 (IN^2/RPM^2)	—	500 X 10^8	—	500	—	500

Figure B.1-2. Case No. 1

FD236892
822903

Too = 2200°R, H_2/O_2

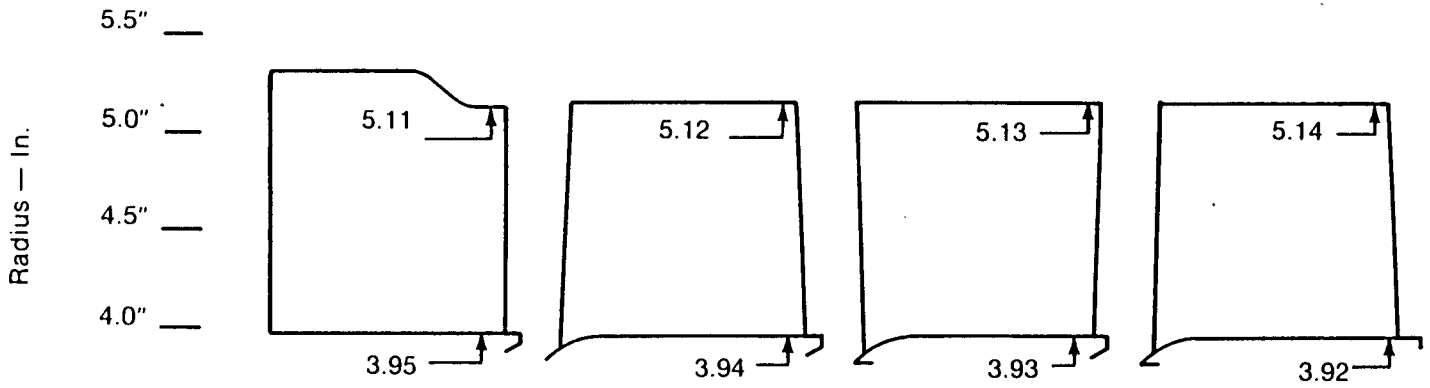

Turbine Data (Overall)	Uncooled	Min Cooled Vane Min Cooled Blade	Max Cooled Vane Min Cooled Blade
η_{T-T} %	80.8	76.6	76.2
PR_{T-T}	1.6	1.6	1.6
U/Cm	.47	.48	.49
$\dot{w}\sqrt{T7}/P'$ @ Inlet	2.92	2.01	1.91
Speed — RPM	38000	38000	38000
Cx/Um	1.5	1.06	.98

First Stage Data	Vane	Blade	Vane	Blade	Vane	Blade
# Foils	31	42	27	40	26	40
Aspect Ratio	.97	.98	.97	.98	.97	.98
Turning — Degrees	56	82	58	96	58	98
Zweifel Coeff.	.7	.9	.7	.9	.7	.9
Urim (Ft/Sec)	—	1300	—	1300	—	1300
AN^2 (IN^2/RPM^2)	—	500 X 10^8	—	500	—	500

Figure B.1-3. Case No. 1

Too = 2600°R, H_2/O_2

FD236893
822903

$\dot{w}_{in.} = 1 + O/F\ (W_{H2} - \Sigma_{4\text{-}7})$

$\dot{w}_{H2} = 160$ PPS

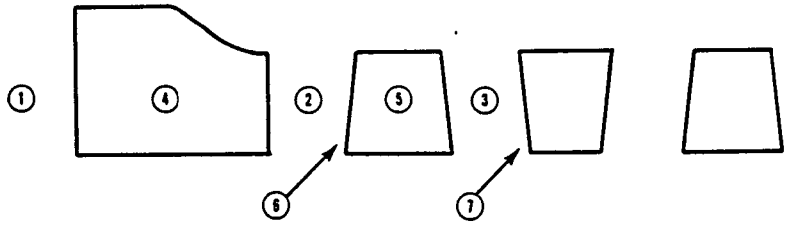

T_{00} = 1800°R O/F = 0.7	Uncooled 1st Stg	Uncooled 2nd Stg	Min Cooled Vane 1st Stg	Min Cooled Vane 2nd Stg	Max Cooled Vane 1st Stg	Max Cooled Vane 2nd Stg
① Turbine Inlet Flow ~ PPS	267.5	268.2	222.9	249.9	213.5	245.9
② Blade Gaging Flow ~ PPS	267.6	269.2	249.3	250.9	245.4	247.0
③ Exit Flow ~ PPS	268.2	270.1	249.9	251.8	245.9	247.9
④ Vane & P/F C/A Flow ~ PPS	—	—	26.2	—	31.8	—
⑤ Blade & P/F C/A Flow ~ PPS	—	—	—	—	—	—
⑥ F Disk C/A, Leakage Flow ~ PPS	.2	1.0	.1	1.0	.1	1.0
⑦ R. Disk C/A, Leakage Flow ~ PPS	.6	.9	.6	.9	.6	.9

T_{00} = 2200°R O/F = 0.93			Min Cooled Vane Min Cooled Blade		Max Cooled Vane Min Cooled Blade	
① Turbine Inlet Flow ~ PPS	303.7	304.4	216.9	262.6	206.7	257.7
② Blade Gaging Flow ~ PPS	303.8	305.4	262.0	263.6	257.1	258.7
③ Exit Flow ~ PPS	304.4	306.3	262.6	264.5	257.7	259.6
④ Vane & P/F C/A Flow ~ PPS	—	—	25.5	—	30.7	—
⑤ Blade & P/F C/A Flow ~ PPS	—	—	19.4	—	19.5	—
⑥ F. Disk, C/A, Leakage Flow ~ PPS	.1	1.0	.1	1.0	.1	1.0
⑦ R. Disk C/A, Leakage Flow ~ PPS	.6	.9	.6	.9	.6	.9

T_{00} = 2600°R O/F = 1.185			Min Cooled Vane Min Cooled Blade		Max Cooled Vane Min Cooled Blade	
① Turbine Inlet Flow ~ PPS	343.8	344.5	236.8	286.5	224.6	279.9
② Blade Gaging Flow ~ PPS	343.9	345.5	285.9	287.5	279.3	280.9
③ Exit Flow ~ PPS	344.5	346.4	286.5	288.4	279.9	281.8
④ Vane & P/F C/A Flow ~ PPS	—	—	27.8	—	33.4	—
⑤ Blade & P/F C/A Flow ~ PPS	—	—	21.2	—	21.2	—
⑥ F. Disk C/A, Leakage Flow ~ PPS	.1	1.0	.1	1.0	.1	1.0
⑦ R. Disk C/A, Leakage Flow ~ PPS	.6	.9	.6	.9	.6	.9

FD236894
822903

Figure B.1-4. Case No. 1 Flow Schematic

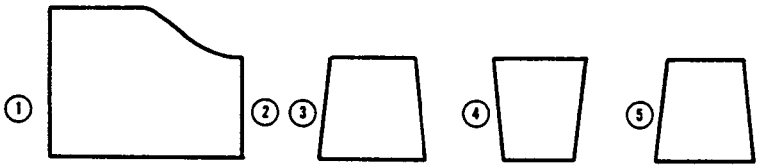

T_{00} = 1800°R	Uncooled	Min Cooled Vane	Max Cooled Vane
① Turbine Inlet ABS ~ °F	1340	1340	1340
② 1st Vane Exit ABS ~ °F	1340	1244	1223
③ 1st Blade Inlet REL ~ °F	1281	1187	1166
④ 2nd Vane Inlet ABS ~ °F	1241	1150	1129
⑤ 2nd Blade Inlet REL ~ °F	1182	1093	1073

T_{00} = 2200°R		Min Vane & Blade	Max Vane Min Blade
① Turbine Inlet ABS ~ °F	1740	1740	1740
② 1st Vane Exit ABS ~ °F	1740	1601	1555
③ 1st Blade Inlet REL ~ °F	1669	1533	1489
④ 2nd Vane Inlet ABS ~ °F	1621	1412	1371
⑤ 2nd Blade Inlet REL ~ °F	1550	1346	1306
T_{00} = 2600°R			
① Turbine Inlet ABS ~ °F	2140	2140	2140
② 1st Vane Exit ABS ~ °F	2140	1960	1918
③ 1st Blade Inlet REL ~ °F	2056	1880	1840
④ 2nd Vane Inlet ABS ~ °F	2002	1727	1688
⑤ 2nd Blade Inlet REL ~ °F	1919	1650	1612

FD236895
822903

Figure B.1-4a. Case No. 1 Gas Path Temperatures

	Uncooled		Min Cooled Vane		Max Cooled Vane	
T_{00} = 1800°R	Stg #1	Stg #2	Stg #1	Stg #2	Stg #1	Stg #2
$\eta_{T\text{-}T}$ Base ~ %	86.6	84.5	86.9	85.3	86.9	85.4
$\Delta\eta$ Disk C/A, Leakage, Windage	.2	.2	.2	.2	.2	.2
$\Delta\eta$ Vane & Platform Cooling	—	—	3.7	—	3.8	—
$\Delta\eta$ Blade & Platform Cooling	—	—	—	—	—	—
$\Delta\eta$ Blade Pumping	—	—	—	—	—	—
$\Delta\eta$ Exit Guide Vane	—	2.3	—	1.9	—	2.1
$\eta_{T\text{-}T}$ Cooled ~ %	86.4	82.0	83.0	83.2	82.9	83.1
$\eta_{T\text{-}T}$ Cooled Overall ~ %	83.8		82.8		82.7	

			Min Cooled Vane Min Cooled Blade		Max Cooled Vane Min Cooled Blade	
T_{00} = 2200°R						
$\eta_{T\text{-}T}$ Base ~ %	85.7	82.6	86.3	84.8	85.6	84.8
$\Delta\eta$ Disk C/A, Leakage, Windage	.2	.2	.2	.2	.2	.2
$\Delta\eta$ Vane & Platform Cooling	—	—	3.7	—	4.4	—
$\Delta\eta$ Blade & Platform Cooling	—	—	3.6	—	3.5	—
$\Delta\eta$ Blade Pumping	—	—	2.2	—	2.2	—
$\Delta\eta$ Exit Guide Vane	—	2.7	—	2.6	—	2.5
$\eta_{T\text{-}T}$ Cooled ~ %	85.5	79.7	76.6	82.0	75.3	82.1
$\eta_{T\text{-}T}$ Cooled Overall ~ %	82.4		77.8		77.1	

FD236840
822903

Figure B.1-5. Case No. 1 Turbine Efficiency

T_{00} = 2600°R	Uncooled		Min Cooled Vane Min Cooled Blade		Max Cooled Vane Min Cooled Blade	
	Stg #1	Stg #2	Stg #1	Stg #2	Stg #1	Stg #2
η_{T-T} Base ~ %	84.4	80.1	85.1	84.2	85.3	84.4
$\Delta\eta$ Disk C/A, Leakage, Windage	.2	.2	.2	.2	.2	.2
$\Delta\eta$ Vane & Platform C/A	—	3.6	.3.6	—	4.4	
$\Delta\eta$ Blade & Platform C/A	—	—	3.9	—	3.8	—
$\Delta\eta$ Blade Pumping	—	—	2.2	—	2.2	—
$\Delta\eta$ Exit Guide Vane	—	2.1	—	2.4	—	2.4
η_{T-T} Cooled ~ %	84.2	77.8	75.2	81.6	74.7	81.8
η_{T-T} Cooled Overall ~ %	80.8		76.6		76.2	

FD236841
822903

Figure B.1-6. Case No. 1 Turbine Efficiency

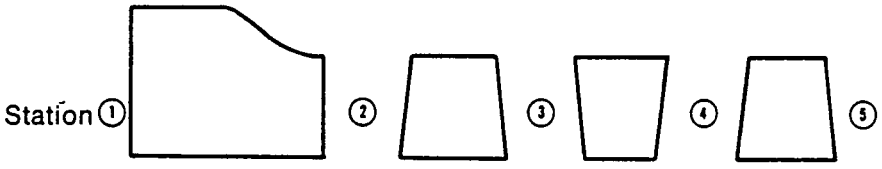

T_{00} = 2200°R, P_{00} = 6000 Psia, Min Cooled Vane & Blade

Station ① Static Pressure	5873. Psia
Station ② Static Pressure	4975. Psia
Station ③ Static Pressure	4624. Psia
Station ④ Static Pressure	3851. Psia
Station ⑤ Static Pressure	3547. Psia

1. Static Pressures are Mid-Span Values.
2. Although the Quoted Pressures are for a Specific Configuration the Level is Typical Over the Horsepower Map.

FD236896
822903

Figure B.1-7. Case No. 1 Gas Path Static Pressures

CASE 1A

TURBINE EFFICIENCY DEFINITION

AND AERODYNAMIC PARAMETERS

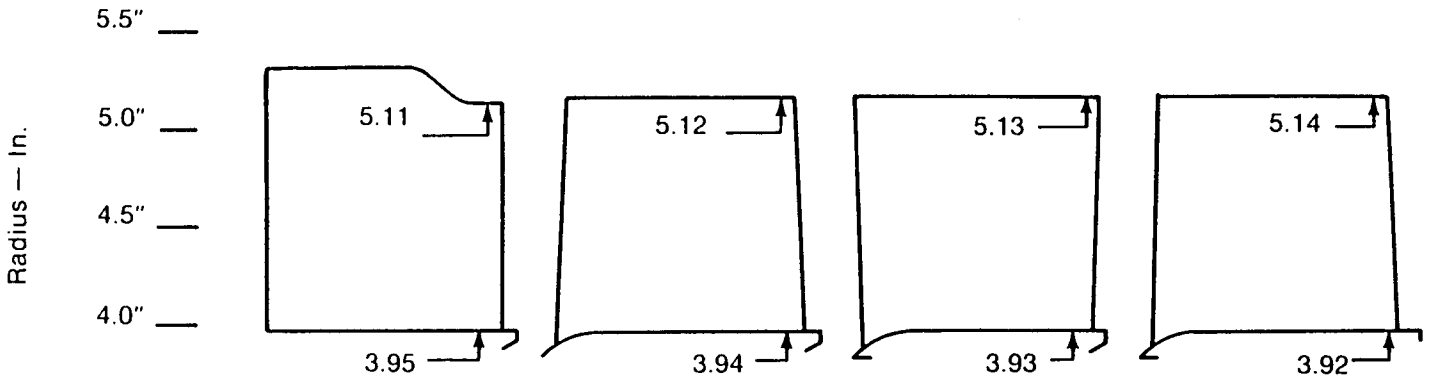

Turbine Data: (Overall)	Uncooled	Min Cooled Vane	Min Cooled Vane
$\eta_{T\text{-}T}$ %	82.5	80.9	80.9
$PR_{T\text{-}T}$	1.6	1.6	1.6
U/C_m	.49	.49	.49
$\dot{w}\sqrt{T}/P$ @ Inlet	.929	.863	.819
Speed — RPM	38000	38000	38000
C_x/U_m	.46	.43	.42

First Stage Data	Vane	Blade	Vane	Blade	Vane	Blade
# Foils	15	28	14	26	14	26
Aspect Ratio	.97	1.18	.97	1.18	.97	1.18
Turning — Degrees	77	136	78	137	78	138
Zweifel Coeff.	.69	.90	.70	.93	.70	.91
U_{rim} (Ft/Sec)	—	1300	—	1300	—	1300
AN^2 (IN^2/RPM^2)	—	500 X 10^8	—	500 X 10^8	—	500 X 10^8

FD236897
822903

Figure B.1A-1. Case No. 1A
Too = 1800°R, H_2/O_2

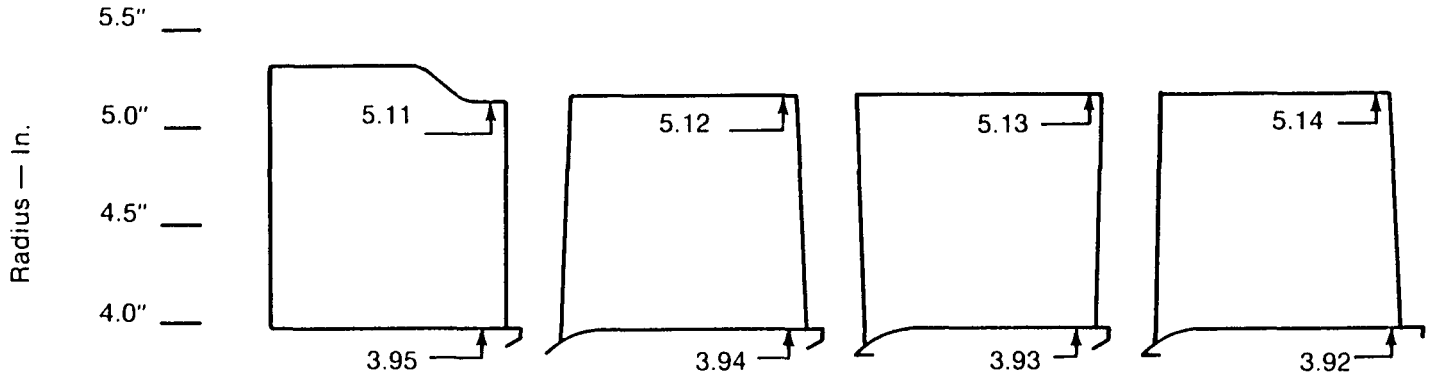

Turbine Data: (Overall)	Uncooled	Min Cooled Vane Min Cooled Blade	Max Cooled Vane Min Cooled Blade
η_{T-T} %	82.5	75.3	75.3
PR_{T-T}	1.6	1.6	1.6
U/C_m	.47	.48	.49
$\dot{w}\sqrt{T}/P$ @ Inlet	1.17	.90	.85
Speed — RPM	38000	38000	38000
C_x/U_m	.56	.47	.45

First Stage Data	Vane	Blade	Vane	Blade	Vane	Blade
# Foils	17	32	14	30	14	28
Aspect Ratio	.97	1.18	.97	1.18	.97	1.18
Turning — Degrees	75	130	78	136	78	138
Zweifel Coeff.	.70	.90	.70	.89	.68	.92
U_{rim} (Ft/Sec)	—	1300	—	1300	—	1300
AN^2 (IN^2/RPM^2)	—	500 X 10^8	—	500 X 10^8	—	500 X 10^8

FD236842
822903

Figure B.1A-2. Case No. 1A
Too = 2200°R, H_2/O_2

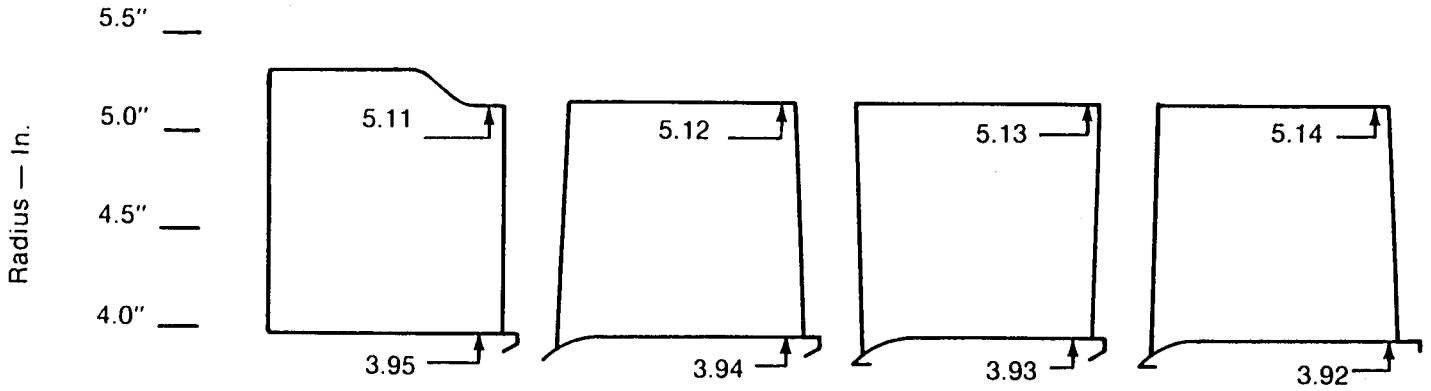

Turbine Data: (Overall)	Uncooled	Min Cooled Vane Min Cooled Blade	Max Cooled Vane Min Cooled Blade
$\eta_{T\text{-}T}$ %	82.5	75.3	74.8
$PR_{T\text{-}T}$	1.6	1.6	1.6
U/C_m	.46	.48	.48
$\dot{w}\sqrt{T}/P$ @ Inlet	1.44	1.08	1.00
Speed — RPM	38000	38000	38000
C_x/U_m	.67	.54	.51

First Stage Data	Vane	Blade	Vane	Blade	Vane	Blade
# Foils	19	36	16	32	15	32
Aspect Ratio	.97	1.18	.97	1.18	.97	1.18
Turning — Degrees	73	125	76	132	77	134
Zweifel Coeff.	.71	.90	.69	.92	.70	.89
U_{rim} (Ft/Sec)	—	1300	—	1300	—	1300
AN^2 (IN^2/RPM^2)	—	500 X 10^8	—	500 X 10^8	—	500 X 10^8

FD236843
822903

Figure B.1A-3. Case No. 1A

Too = 2600°R, H_2/O_2

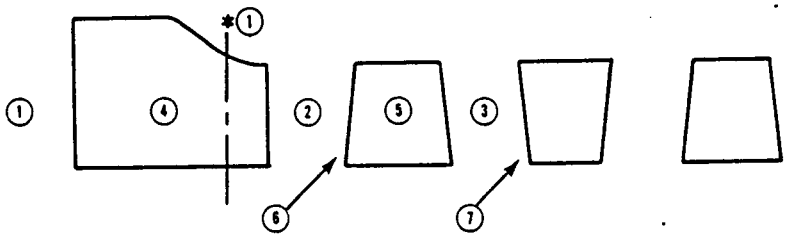

T_{00} = 1800°R O/F = 0.7	Uncooled		Min Cooled Vane		Max Cooled Vane	
	1st Stg	2nd Stg	1st Stg	2nd Stg	1st Stg	2nd Stg
① Turbine Inlet Flow ~ PPS	131.4	132.2	120.9	127.8	113.8	124.9
*① Vane Gaging Flow ~ PPS	131.4	132.8	127.1	127.8	124.2	124.9
② Blade Gaging Flow ~ PPS	131.6	133.2	127.2	128.8	124.3	125.9
③ Exit Flow ~ PPS	132.2	134.1	127.8	129.7	124.9	126.8
④ Vane & Platform C/A Flow ~ PPS	—	—	6.2	—	10.4	—
⑤ Blade & Platform C/A Flow ~ PPS	—	—	—	—	—	—
⑥ F. Disk C/A, Leakage Flow ~ PPS	.1	1.0	.1	1.0	.1	1.0
⑦ R. Disk C/A, Leakage Flow ~ PPS	.6	.9	.6	.9	.6	.9

$\dot{w}_{in} = 1 + O/F(\dot{w}_{H2} - \Sigma_{4\text{-}7})$
$\dot{w}_{H2} = 80$ PPS

FD236898
822903

Figure B.1A-4. Case No. 1A Flow Schematic

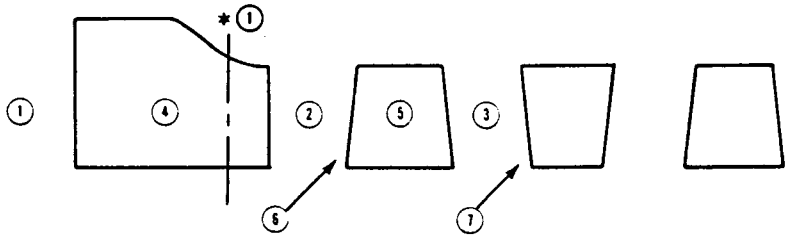

T_{00} = 2200°R O/F = 0.93	Uncooled 1st Stg	Uncooled 2nd Stg	Min Vane Min Blade 1st Stg	Min Vane Min Blade 2nd Stg	Max Vane Min Blade 1st Stg	Max Vane Min Blade 2nd Stg
① Turbine Inlet Flow ~ PPS	149.2	149.9	115.6	133.8	108.0	130.1
*① Vane Gaging Flow ~ PPS	149.2	149.9	121.5	133.8	117.8	130.1
② Blade Gaging Flow ~ PPS	149.3	150.9	133.2	134.8	129.5	131.1
③ Exit Flow ~ PPS	149.9	151.8	133.8	135.7	130.1	132.0
④ Vane & Platform C/A Flow ~ PPS	—	—	5.9	—	9.8	—
⑤ Blade & Platform C/A Flow ~ PPS	—	—	11.5	—	11.6	—
⑥ F. Disk C/A, Leakage Flow ~ PPS	.1	1.0	.1	1.0	.1	1.0
⑦ R. Disk C/A, Leakage Flow ~ PPS	.6	.9	.6	.9	.6	.9

$\dot{w}_{in} = 1 + O/F\,(W_{H2} - \Sigma_{4\text{-}7})$
$\dot{w}_{H2} = 80$ PPS

FD236844
822903

Figure B.1A-5. Case No. 1A Flow Schematic

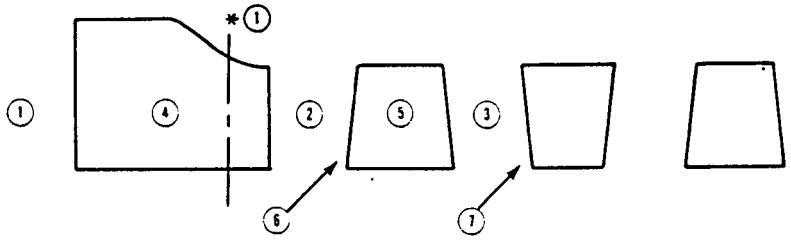

T_{00} = 2600°R O/F = 1.185	Uncooled		Min Vane Min Blade		Max Vane Min Blade	
	1st Stg	2nd Stg	1st Stg	2nd Stg	1st Stg	2nd Stg
① Turbine Inlet Flow ~ PPS	168.9	169.6	127.1	147.0	118.0	141.9
*① Vane Gaging Flow ~ PPS	168.9	169.6	133.6	147.0	128.7	141.9
② Blade Gaging Flow ~ PPS	169.0	170.6	146.4	148.0	141.3	142.9
③ Exit Flow ~ PPS	169.6	171.6	147.0	148.9	141.9	143.8
④ Vane & Platform C/A Flow ~ PPS	—	—	6.5	—	10.7	—
⑤ Blade & Platform C/A Flow ~ PPS	—	—	12.7	—	12.7	—
⑥ F. Disk C/A, Leakage Flow ~ PPS	.1	1.0	.1	1.0	.1	1.0
⑦ R. Disk C/A, Leakage Flow ~ PPS	.6	.9	.6	.9	.6	.9

$\dot{w}_{in} = 1 + O/F(\dot{w}_{H2} - \Sigma_{4\text{-}7})$
$\dot{w}_{H2} = 80$ PPS

FD236845
822903

Figure B.1A-6. Case No. 1A Flow Schematic

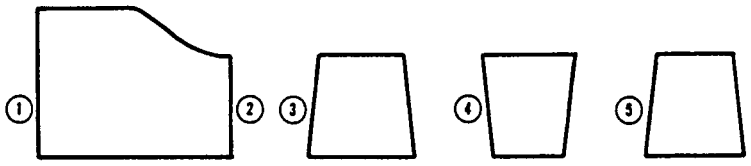

T_{00} = 1800°R	Uncooled	Min Cooled Vane	Max Cooled Vane
① Turbine Inlet ABS ~ °F	1340	1340	1340
② 1st Vane Exit ABS ~ °F	1340	1299	1275
③ 1st Blade Inlet REL ~ °F	1281	1240	1217
④ 2nd Vane Inlet ABS ~ °F	1251	1209	1189
⑤ 2nd Blade Inlet REL ~ °F	1192	1151	1132
T_{00} = 2200°R		Min Vane & Blade	Max Vane Min Blade
① Turbine Inlet ABS ~ °F	1740	1740	1740
② 1st Vane Exit ABS ~ °F	1740	1678	1635
③ 1st Blade Inlet REL ~ °F	1669	1609	1567
④ 2nd Vane Inlet ABS ~ °F	1635	1487	1447
⑤ 2nd Blade Inlet REL ~ °F	1564	1418	1379
T_{00} = 2600°R			
① Turbine Inlet ABS ~ °F	2140	2140	2140
② 1st Vane Exit ABS ~ °F	2140	2056	2001
③ 1st Blade Inlet REL ~ °F	2056	1975	1922
④ 2nd Vane Inlet ABS ~ °F	2021	1820	1770
⑤ 2nd Blade Inlet REL ~ °F	1937	1740	1691

FD236899
822903

Figure B.1A-7. Case No. 1A Gas Path Temperatures

T_{00} = 1800°R	Uncooled		Min Cooled Vane		Max Cooled Vane	
	Stg #1	Stg #2	Stg #1	Stg #2	Stg #1	Stg #2
$\eta_{T\text{-}T}$ Base ~ %	84.84	83.77	84.87	83.91	84.74	83.78
$\Delta\eta$ Disk C/A, Leakage, Windage	.16	.34	.31	.69	.33	.77
$\Delta\eta$ Vane & P/F C/A	—	—	2.33	—	2.70	—
$\Delta\eta$ Blade & P/F C/A	—	—	—	—	—	—
$\Delta\eta$ Blade Pumping	—	—	—	—	—	—
$\Delta\eta$ EGV	—	1.79	—	2.0	—	1.8
$\eta_{T\text{-}T}$ Cooled ~ %	84.72	81.64	82.23	81.22	81.71	81.21
$\eta_{T\text{-}T}$ Cooled Overall ~ %	82.5		80.9		80.9	

T_{00} = 2200°R			Min Cooled Vane Min Cooled Blade		Max Cooled Vane Min Cooled Blade	
$\eta_{T\text{-}T}$ Base ~ %	85.39	83.88	84.38	83.78	84.47	83.89
$\Delta\eta$ Disk C/A, Leakage, Windage	.15	.38	.27	.76	.33	.78
$\Delta\eta$ Vane & P/F C/A	—	—	2.28	—	2.66	—
$\Delta\eta$ Blade & P/F C/A	—	—	3.47	—	3.30	—
$\Delta\eta$ Blade Pumping	—	—	3.60	—	3.49	—
$\Delta\eta$ EGV	—	2.40	—	2.51	—	2.36
$\eta_{T\text{-}T}$ Cooled ~ %	85.24	81.10	74.76	80.51	74.69	80.75
$\eta_{T\text{-}T}$ Cooled Overall ~ %	82.5		75.3		75.3	

FD236846
822903

Figure B.1A-8. Case No. 1A Turbine Efficiency

T_{00} = 2600°R	Uncooled		Min Cooled Vane Min Cooled Blade		Max Cooled Vane Min Cooled Blade	
	Stg #1	Stg #2	Stg #1	Stg #2	Stg #1	Stg #2
η_{T-T} Base ~ %	85.65	84.15	84.48	84.16	84.21	84.05
$\Delta\eta$ Disk C/A, Leakage, Windage	.15	.34	.25	.71	.30	.73
$\Delta\eta$ Vane & P/F C/A	—	—	2.20	—	2.54	—
$\Delta\eta$ Blade & P/F C/A	—	—	3.27	—	3.49	—
$\Delta\eta$ Blade Pumping	—	—	3.48	—	3.70	—
$\Delta\eta$ EGV	—	3.2	—	3.0	—	2.71
η_{T-T} Cooled ~ %	85.50	80.61	75.28	80.45	74.18	80.61
η_{T-T} Cooled Overall ~ %	82.5		75.3		74.8	

FD236847
822903

Figure B.1A-9. Case No. 1A Turbine Efficiency

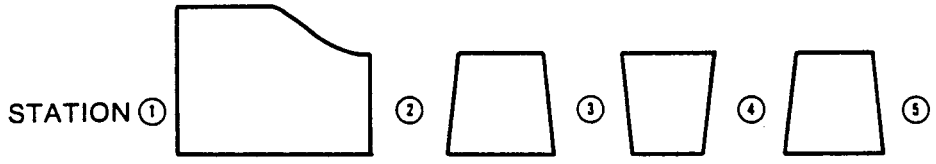

T_{00} = 2200°R, P_{00} = 6000 Psia, Min Cooled Vane & Blade

Station ① Static Pressure	5966 Psia
Station ② Static Pressure	5086 Psia
Station ③ Static Pressure	4737 Psia
Station ④ Static Pressure	3982 Psia
Station ⑤ Static Pressure	3678 Psia

1. Static Pressures are Mid-Span Values.
2. Although the Quoted Pressures are for a Specific Configuration, the Level is Typical Over the Horsepower Map.

FD236839
822903

Figure B.1A-10. Case No. 1A Gas Path Static Pressures

CASE 2

TURBINE EFFICIENCY DEFINITION AND AERODYNAMIC PARAMETERS

TURBINE EFFICIENCY DEFINITION AND AERODYNAMIC PARAMETERS

The definition of turbine efficiency quoted in this study is listed below:

$$\eta = \frac{W1B(\Delta HACT)}{WEX(\Delta HIDEAL)} = \frac{W1B(Cp(TOO - TEX)}{WEX(Cp \times TOO(1 - Pex/Poo^{\frac{\gamma-1}{\gamma}}))}$$

$$\text{or} \quad \frac{W1B(Cp\ (1 - Tex/Too)}{WEX(1 - Pex/Poo^{\frac{\gamma-1}{\gamma}})}$$

WIB — Blade flowrate available for work, which includes any coolant or leakage entering the mainstream flow upstream of the blade gaging (throat) - lbm/sec

WEX — Turbine exit flowrate including all coolant or leakage entering the turbine mainstream flow - lbm/sec.

HACT — Actual delivered turbine work - Btu/lbm

HIDEAL — Ideal turbine work - Btu/lbm

*Too — Turbine inlet temperature - °R

*Tex — Turbine exit temperature - °R

Poo — Turbine inlet total pressure - psia

Pex — Turbine exit total pressure - psia

γ — Ratio of specific heats at inlet conditions.

* For the case of the cooled turbines, the inlet temperature is based on a mixed temperature calculation which includes all the coolant flow entering upstream of the first vane gaging (throat). The exit temperature does not include mixing of the blade film coolant.

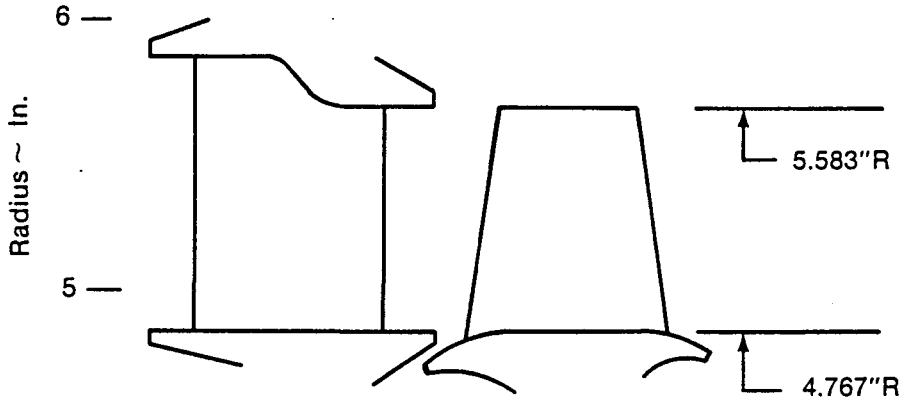

	Uncooled	Min Cooling	Max Cooling
$\eta_{T\text{-}T}$ ~ %	83.7	81.8	80.9
$PR_{T\text{-}T}$	1.6	1.6	1.6
U/C_m	.53	.55	.56
$\dot{w}\sqrt{T}/P$ @ Inlet	2.41	2.16	1.98
Speed ~ RPM	24000	24000	24000
C_x/U_m	.49	.46	.44

	Vane	Blade	Vane	Blade	Vane	Blade
# Foils	25	68	24	66	24	64
Aspect Ratio	.79	1.26	.79	1.26	.79	1.26
Turning ~ Degrees	74	117	74	118	75	119
Zweifel Coeff.	.7	.9	.7	.9	.7	.9
U_{rim} (Ft/Sec)	—	998	—	998	—	998
AN^2 (IN^2/RPM^2)	—	152 X 10^8	—	152 X 10^8	—	152 X 10^8

FD236900
822903

Figure B.2-1. Case No. 2
Too = 1800°R, O_2/CH_4

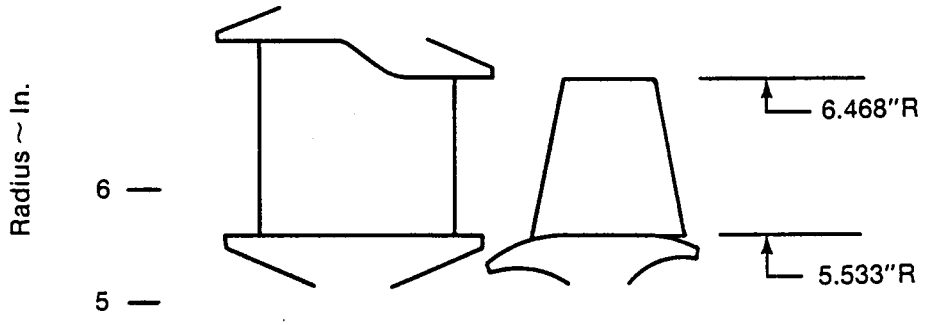

	Uncooled	Min Cooling	Max Cooling
$\eta_{T\text{-}T}$ %	84.5	81.9	80.8
$PR_{T\text{-}T}$	1.6	1.6	1.6
U/C_m	.53	.56	.57
$\dot{w}\sqrt{T}/P$ @ Inlet	3.11	2.74	2.48
Speed — RPM	24000	24000	24000
C_x/U_m	.49	.44	.43

	Vane	Blade	Vane	Blade	Vane	Blade
# Foils	29	74	27	70	27	68
Aspect Ratio	.92	1.34	.92	1.34	.92	1.34
Turning — Degrees	74	116	75	118	75	118
Zweifel ~ Coeff.	.7	.9	.7	.9	.7	.9
U_{rim} (Ft/Sec)	—	1159	—	1159	—	1159
AN^2 (IN^2/RPM^2)	—	208 X 10^8	—	208 X 10^8	—	208 X 10^8

FD229043
822903

Figure B.2-2. Case No. 2

Too = 2200°R, O_2/CH_4

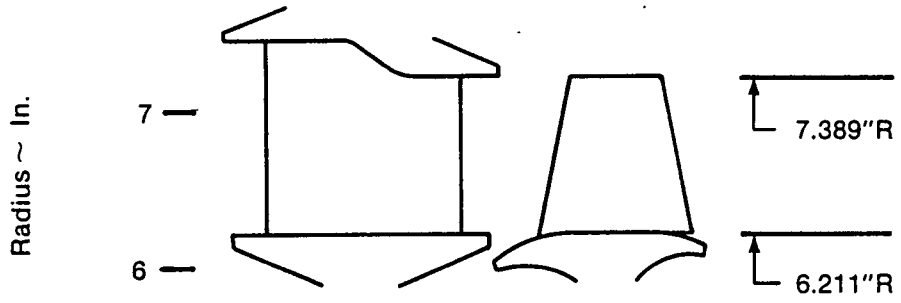

	Uncooled	Min Cooling	Max Cooling
$\eta_{T\text{-}T}$ ~ %	85.5	78.7	76.9
$PR_{T\text{-}T}$	1.6	1.6	1.6
U/C_m	.53	.56	.57
$\dot{w}\sqrt{T}/P$ @ Inlet	4.27	3.37	3.04
Speed ~ RPM	24000	24000	24000
C_x/U_m	.49	.39	.39

First Stage Data	Vane	Blade	Vane	Blade	Vane	Blade
# Foils	34	64	28	60	28	56
Aspect Ratio	1.16	1.31	1.16	1.31	1.16	1.31
Turning ~ Degrees	74	118	76	124	77	126
Zweifel Coeff.	.7	.9	.7	.9	.7	.9
U_{rim} (Ft/Sec)	—	1300	—	1300	—	1300
AN^2 (IN^2/RPM^2)	—	290 X 10^8	—	290 X 10^8	—	290 X 10^8

FD229044
822903

Figure B.2-3. Case No. 2
Too = 2600°R, O_2/CH_4

$\dot{W}_{in} = 1 + O/F\ (\dot{W}_{CH4} - \Sigma_{4-7})$
$\dot{W}_{CH4} = 280$ Lb/Sec

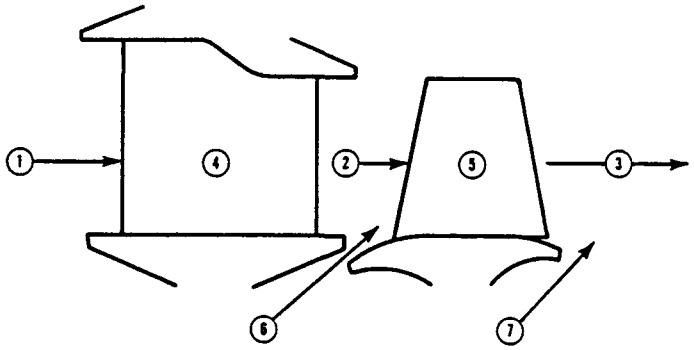

T_{00} = 1800°R O/F = 0.245	Uncooled	Min Cooling	Max Cooling
① Turbine Inlet Flow ~ Lb/Sec	340.42	304.28	280.96
② Blade Gaging Flow ~ Lb/Sec	341.76	334.65	330.06
③ Turbine Exit Flow ~ Lb/Sec	346.99	339.88	335.29
④ Vane & P/F Cooling Flow ~ Lb/Sec	0.00	29.03	47.76
⑤ Blade & P/F Cooling Flow ~ Lb/Sec	0.00	0.00	0.00
⑥ Front Disk Cooling/Lkg ~ Lb/Sec	1.34	1.34	1.34
⑦ Rear Disk Cooling/Lkg ~ Lb/Sec	5.23	5.23	5.23
T_{00} = 2200°R O/F = 0.46			
① Turbine Inlet Flow ~ Lb/Sec	397.97	349.32	318.86
② Blade Gaging Flow ~ Lb/Sec	399.72	384.39	374.79
③ Turbine Exit Flow ~ Lb/Sec	405.39	390.06	380.46
④ Vane & P/F Cooling Flow ~ Lb/Sec	0.00	33.32	54.18
⑤ Blade & P/F Cooling Flow ~ Lb/Sec	0.00	0.00	0.00
⑥ Front Disk Cooling/Lkg ~ Lb/Sec	1.75	1.75	1.75
⑦ Rear Disk Cooling/Lkg ~ Lb/Sec	5.67	5.67	5.67
T_{00} = 2600°R O/F = 0.85			
① Turbine Inlet Flow ~ Lb/Sec	502.15	396.31	357.72
② Blade Gaging Flow ~ Lb/Sec	504.52	453.18	435.45
③ Turbine Exit Flow ~ Lb/Sec	510.72	462.09	444.36
④ Vane & P/F Cooling Flow ~ Lb/Sec	0.00	37.69	58.54
⑤ Blade & P/F Cooling Flow ~ Lb/Sec	0.00	19.52	19.52
⑥ Front Disk Cooling/Lkg ~ Lb/Sec	2.37	2.37	2.37
⑦ Rear Disk Cooling/Lkg ~ Lb/Sec	6.20	6.20	6.20

FD229045
822903

Figure B.2-4. Case No. 2 Flow Schematic

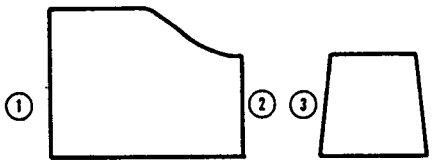

T_{00} = 1800°R	Uncooled	Min Cooled Vane	Max Cooled Vane
① Turbine Inlet ABS ~ °F	1340	1340	1340
② 1st Vane Exit ABS ~ °F	1340	1261	1209
③ 1st Blade Inlet REL ~ °F	1204	1130	1080
T_{00} = 2200°R			
① Turbine Inlet ABS ~ °F	1740	1740	1740
② 1st Vane Exit ABS ~ °F	1740	1618	1550
③ 1st Blade Inlet REL ~ °F	1572	1458	1393
T_{00} = 2600°R		Min Vane & Blade	Max Vane Min Blade
① Turbine Inlet ABS ~ °F	2140	2140	2140
② 1st Vane Exit ABS ~ °F	2140	1994	1941
③ 1st Blade Inlet REL ~ °F	1943	1805	1756

FD229046
822903

Figure B.2-5. Case No. 2 Gaspath Temperatures

T_{00} = 1800°R	Uncooled	Min Cooling	Max Cooling
① $\eta_{T\text{-}T}$ Base ~ %	86.6	86.4	86.4
$\Delta\eta$ Disk C/A, Leakage, Windage	-1.45	-1.6	-1.6
$\Delta\eta$ Vane & P/F Cooling	—	-1.9	-2.7
$\Delta\eta$ Blade & P/F Cooling	—	—	—
② $\eta_{T\text{-}T}$ Cooled x $\dot{w}_{1B}/\dot{w}_{ex}$ ~ %	83.7	81.8	80.9
T_{00} = 2200°R			
$\eta_{T\text{-}T}$ Base ~ %	87.5	87.3	87.4
$\Delta\eta$ Disk C/A, Leakage, Windage	-1.8	-2.1	-2.2
$\Delta\eta$ Vane & P/F Cooling	—	-2.2	-3.2
$\Delta\eta$ Blade & P/F Cooling	—	—	—
$\eta_{T\text{-}T}$ Cooled x $\dot{w}_{1B}/\dot{w}_{ex}$ ~ %	84.5	81.9	80.8
T_{00} = 2600°R			
$\eta_{T\text{-}T}$ Base ~ %	88.5	87.6	87.7
$\Delta\eta$ Disk C/A, Leakage, Windage	-1.9	-2.3	-2.5
$\Delta\eta$ Vane & P/F Cooling	—	-2.4	-3.8
$\Delta\eta$ Blade & P/F Cooling & Pumping	—	-2.7	-2.9
$\eta_{T\text{-}T}$ Cooled × $\dot{w}_{1B}/\dot{w}_{ex}$	85.5	78.7	76.9

① $\eta_{T\text{-}T}$ Base as Derived From Turbine Mean Line Design System (ΔH Actual/ΔH Ideal)

② $\eta_{T\text{-}T}$ Cooled = ($\eta_{T\text{-}T}$ Base - $\Delta\eta$ Cooling) × $\dot{w}$ 1st Blade Flow/$\dot{w}$ Turbine Exit Flow

FD236848
822903

Figure B.2-6. Case No. 2 Turbine Efficiency

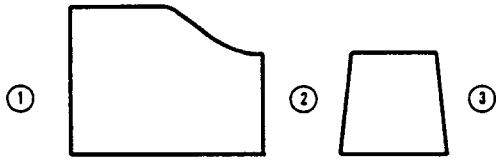

T_{00} = 2200°R, P_{00} = 6000 Psia, Min Cooled Vane & Blade

Station ① Static Pressure	5927 Psia
Station ② Static Pressure	4116 Psia
Station ③ Static Pressure	3650 Psia

1. Static Pressures are Mid-Span Values.
2. Although the Quoted Pressures are for a Specific Configuration, the Level is Typical Over the Horsepower Map.

FD229047
822903

Figure B.2-7. Case No. 2 Gas Path Static Temperatures

CASE 3

TURBINE EFFICIENCY DEFINITION AND AERODYNAMIC PARAMETERS

The definition of turbine efficiency quoted in this study is listed below:

$$\eta = \frac{W1B(\Delta \text{HACT 1 STG}) + W2B(\Delta h) + W3B(\Delta h) + W4B(\Delta \text{HACT 4 STG})}{WEX\ (\Delta \text{HIDEAL})}$$

$$= \frac{W1B(Cp(TO1-TX1) + W2B(Cp\Delta T) + W3B(Cp\Delta T) + W4B\ Cp(TO4-TX4)}{WEX\ (Cp \times TO1\ (1 - PX2/PO1^{\frac{\gamma-1}{\gamma}}))}$$

*TO1	Turbine inlet total temperature - °R
**TO2	2nd Stage inlet total temperature - °R
PO1	Turbine inlet total pressure - psia
PX2	Turbine exit total pressure - psia
***TX1	1st stage exit total temperature - °R
***TX2	2nd stage exit total temperature - °R
W1B	1st stage blade flowrate available for work which includes any coolant or leakage entering the mainstream flowpath upstream of the blade gaging (throat) - lbm/sec
W2B	2nd stage blade flowrate available for work which includes any coolant or leakage entering the mainstream flowpath upstream of the 2nd blade gaging (throat) - lbm/sec
WEX	Turbine exit flowrate including all coolant or leakage entering the mainstream flowpath - lbm/sec.
γ	Ratio of specific heats at inlet conditions.
Cp	Specific heat at constant pressure - Btu/lbm°F

* TO1 is based on a mixed temperature calculation which includes all coolant and leakage entering the mainstream flowpath stream of the 1st vane gaging (throat).

** TO2 is based on the 1st stage inlet mixed temperature (TO1) minus the ΔT due to 1st stage work plus a mixed temperature calculation including all coolant and leakage entering the mainstream aft of the 1st vane gaging and upstream of the 2nd vane gaging.

*** TX1 and TX2 are calculated from stage inlet temperatures minus stage work for their respective stages.

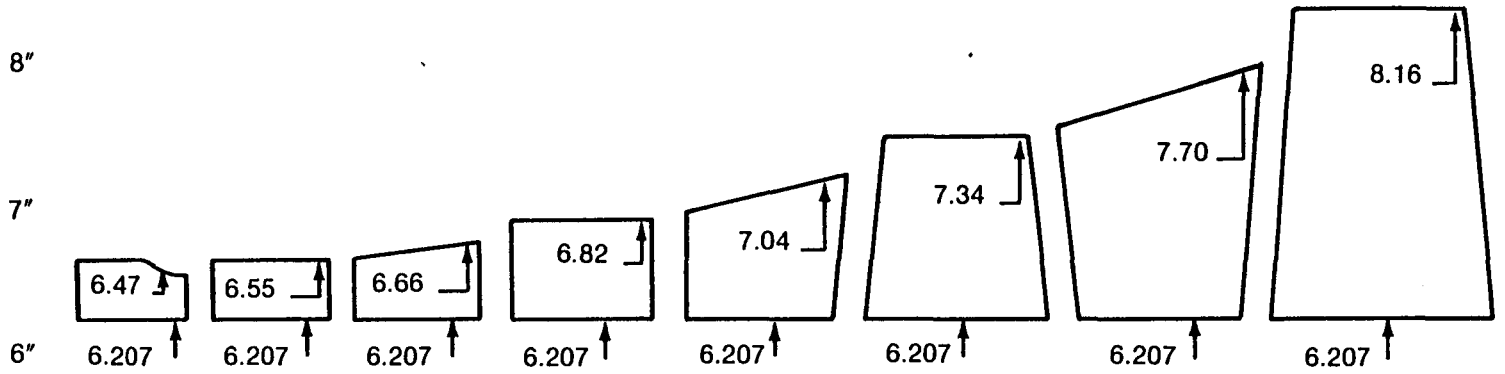

Turbine Data: (Overall)	Uncooled	Min Cooled Vane	Min Cooled Vane
Efficiency $_{T\text{-}T}$	76.6	75.4	75.1
$PR_{T\text{-}T}$	20.0	20.0	20.0
U/C_m	0.662	0.673	0.677
$\dot{w}\sqrt{T}/P$ @ Inlet	0.578	0.527	0.509
Speed — RPM	24000	24000	24000
C_x/U_m	0.222	0.213	0.209

First Stage Data	Vane	Blade	Vane	Blade	Vane	Blade
No. of Foils	25	38	24	38	23	38
Aspect Ratio	.385	.454	.385	.454	.385	.454
Turning — Degrees	81°	144°	81°	145°	81°	145°
Zweifel Coeff.	.735	.846	.741	.813	.763	.821
U_{rim} (Ft/Sec)	—	1300	—	1300	—	1300
AN^2 $(In^2/RPM^2) \times 10^9$	—	8.04	—	8.04	—	8.04

FD229048
822903

Figure B.3-1. Case No. 3
Too = 1800°R, CH_4/O_2

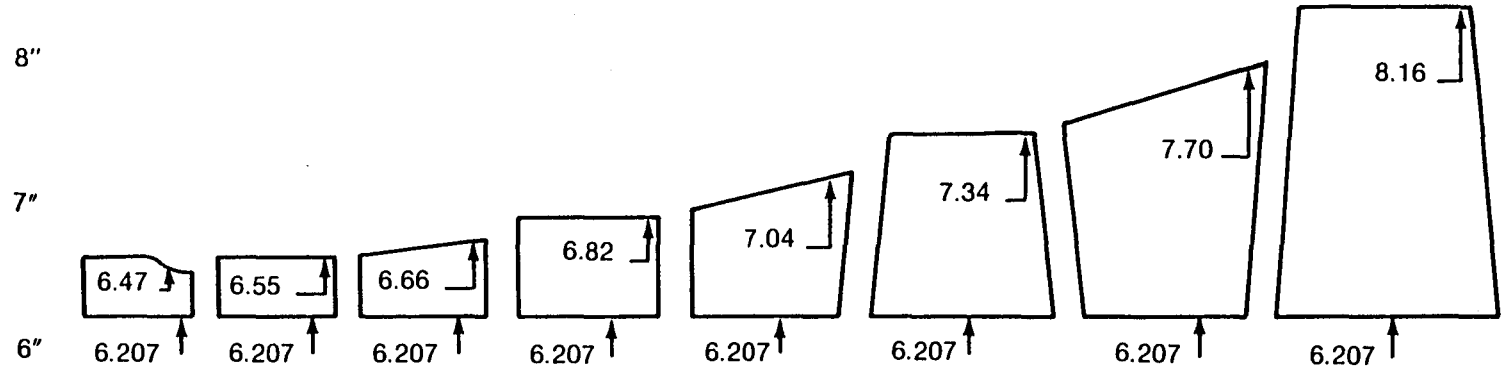

Turbine Data: (Overall)	Uncooled	Min Cooled Vane / Min Cooled Blade	Max Cooled Vane / Min Cooled Blade
Efficiency $_{T\text{-}T}$	78.6	76.4	74.9
$PR_{T\text{-}T}$	20.0	20.0	20.0
U/C_m	0.580	0.598	0.603
$\dot{w}\sqrt{T}/P$ @ Inlet	0.761	0.637	0.612
Speed — RPM	24000	24000	24000
C_x/U_m	0.341	0.309	0.302

First Stage Data	Vane	Blade	Vane	Blade	Vane	Blade
No. of Foils	33	54	29	51	29	50
Aspect Ratio	.385	.454	.385	.454	.385	.454
Turning — Degrees	77°	137°	79°	141°	79°	142°
Zweifel Coeff.	.752	.808	.758	.834	.744	.835
U_{rim} (Ft/Sec)	—	1300	—	1300	—	1300
AN^2 (In^2/RPM^2) $\times 10^9$	—	8.04	—	8.04	—	8.04

FD236849
822903

Figure B.3-2. Case No. 3

Too = 2200°R, CH_4/O_2

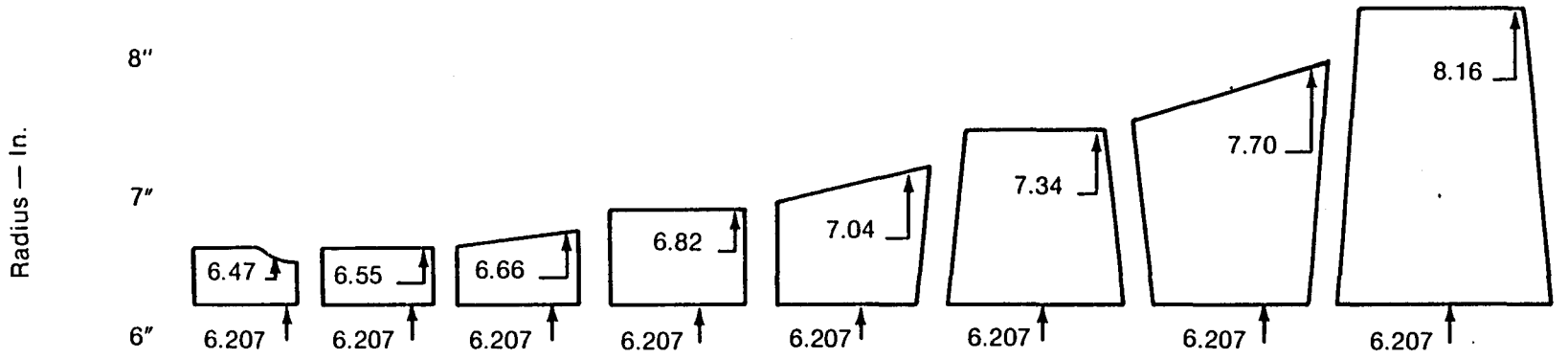

Turbine Data: (Overall)	Uncooled	Min Cooled Vane / Min Cooled Blade	Max Cooled Vane / Min Cooled Blade
Efficiency $_{T\text{-}T}$	80.8	77.0	76.8
$PR_{T\text{-}T}$	20.0	20.0	20.0
U/C_m	0.503	0.522	0.526
$\tilde{w}\sqrt{T}/P$ @ Inlet	1.085	0.864	0.825
Speed — RPM	24000	24000	24000
C_x/U_m	0.592	0.503	0.486

First Stage Data	Vane	Blade	Vane	Blade	Vane	Blade
No. of Foils	47	72	40	69	40	66
Aspect Ratio	.385	.454	.385	.454	.385	.454
Turning — Degrees	71°	124°	74°	131°	75°	132°
Zweifel Coeff.	.754	.841	.756	.834	.738	.852
U_{rim} (Ft/Sec)	—	1300	—	1300	—	1300
AN^2 (In^2/RPM^2) $\times 10^9$	—	8.04	—	8.04	—	8.04

FD236850
822903

Figure B.3-3. Case No. 3

Too = 2600°R, CH_4/O_2

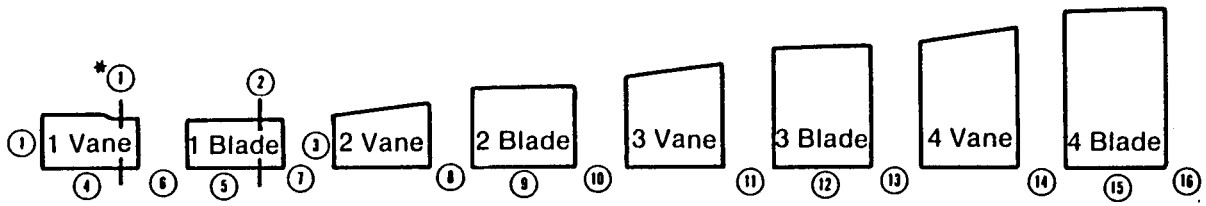

T_{00} = 1800°R O/F = 0.25	Uncooled	Min Vane	Max Vane
① Turbine Inlet Flow (All Flows in P.P.S.)	54.50	49.65	47.96
*① 1st Stg Vane Gaging Flow	54.50	53.52	53.19
② 1st Stg Blade Gaging Flow	57.16	56.18	55.85
③ 1st Stg Exit Flow	59.99	57.01	56.68
④ 1st Stg Vane & Platform C/A Flow	.00	3.87	5.23
⑤ 1st Stg Blade & Platform C/A Flow	.00	.00	.00
⑥ 1st Stg Front Disk Leakage & Attachment C/A Flow	2.66	2.66	2.66
⑦ 1st Stg Rear Disk Leakage Flow	.83	.83	.83
⑧ 2nd Stg Front Disk Leakage Flow	.58	.58	.58
⑨ 2nd Stg Attachment Cooling Flow	.82	.82	.82
⑩ 2nd Stg Rear Disk Leakage Flow	.41	.41	.41
⑪ 3rd Stg Front Disk Leakage Flow	.22	.22	.22
⑫ 3rd Stg Attachment Cooling Flow	.38	.38	.38
⑬ 3rd Stg Rear Disk Leakage Flow	.19	.19	.19
⑭ 4th Stg Front Disk Leakage Flow	.09	.09	.09
⑮ 4th Stg Attachment Cooling Flow	.14	.14	.14
⑯ 4th Stg Rear Disk Leakage Flow	.08	.08	.08

$\dot{W}_{in} = 1 + O/F\ (\dot{W}_{CH4} - \Sigma\ 4 \text{ to } 16)$
$\dot{W}_{CH4} = 50$ P.P.S.

FD229049
822903

Figure B.3-4. Case No. 3 Flow Schematic

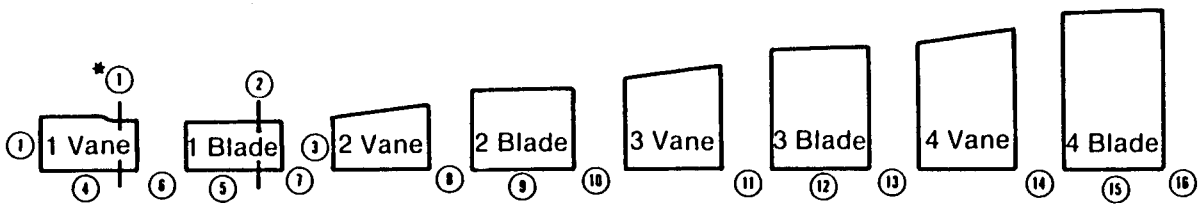

T_{00} = 2200°R 0/F = 0.483	Uncooled	Min Vane / Min Blade	Max Vane / Min Blade
① Turbine Inlet Flow (All Flows in P.P.S.)	64.88	54.36	52.19
*① 1st Stg Vane Gaging Flow	64.88	58.60	57.88
② 1st Stg Blade Gaging Flow	67.53	64.11	63.39
③ 1st Stg Exit Flow	68.36	64.94	64.22
④ 1st Stg Vane & Platform C/A Flow	.00	4.24	5.69
⑤ 1st Stg Blade & Platform C/A Flow	.00	2.86	2.86
⑥ 1st Stg Front Disk Leakage & Attachment C/A Flow	2.65	2.65	2.65
⑦ 1st Stg Rear Disk Leakage Flow	.83	.83	.83
⑧ 2nd Stg Front Disk Leakage Flow	.49	.49	.49
⑨ 2nd Stg Attachment Cooling Flow	.83	.83	.83
⑩ 2nd Stg Rear Disk Leakage Flow	.41	.41	.41
⑪ 3rd Stg Front Disk Leakage Flow	.22	.22	.22
⑫ 3rd Stg Attachment Cooling Flow	.38	.38	.38
⑬ 3rd Stg Rear Disk Leakage Flow	.19	.19	.19
⑭ 4th Stg Front Disk Leakage Flow	.09	.09	.09
⑮ 4th Stg Attachment Cooling Flow	.14	.14	.14
⑯ 4th Stg Rear Disk Leakage Flow	.08	.08	.08

$\dot{W}_{in} = 1 + O/F\ (\dot{W}_{CH4} - \Sigma\ 4 \text{ to } 16)$
$\dot{W}_{CH4} = 50$ P.P.S.

FD243401
822903

Figure B.3-5. Case No. 3 Flow Schematic

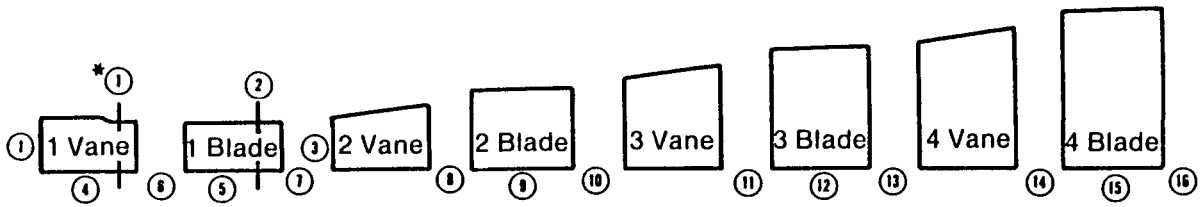

T_{00} = 2600°R O/F = 0.94	Uncooled	Min Vane Min Blade	Max Vane Min Blade
① Turbine Inlet Flow (All Flows in P.P.S.)	85.09	67.81	64.72
*① 1st Stg Vane Gaging Flow	85.09	73.10	71.78
② 1st Stg Blade Gaging Flow	87.69	79.25	77.93
③ 1st Stg Exit Flow	88.49	80.05	78.73
④ 1st Stg Vane & Platform C/A Flow	.00	5.29	7.06
⑤ 1st Stg Blade & Platform C/A Flow	.00	3.55	3.55
⑥ 1st Stg Front Disk Leakage & Attachment C/A Flow	2.60	2.60	2.60
⑦ 1st Stg Rear Disk Leakage Flow	.80	.80	.80
⑧ 2nd Stg Front Disk Leakage Flow	.47	.47	.47
⑨ 2nd Stg Attachment Cooling Flow	.80	.80	.80
⑩ 2nd Stg Rear Disk Leakage Flow	.40	.40	.40
⑪ 3rd Stg Front Disk Leakage Flow	.21	.21	.21
⑫ 3rd Stg Attachment Cooling Flow	.36	.36	.36
⑬ 3rd Stg Rear Disk Leakage Flow	.18	.18	.18
⑭ 4th Stg Front Disk Leakage Flow	.08	.08	.08
⑮ 4th Stg Attachment Cooling Flow	.17	.17	.17
⑯ 4th Stg Rear Disk Leakage Flow	.07	.07	.07

$\dot{w}_{in} = 1 + O/F\ (\dot{W}_{CH4} - \Sigma\ 4 \text{ to } 16)$
$\dot{w}_{CH4} = 50$ P.P.S.

FD243402
822903

Figure B.3-6. Case No. 3 Flow Schematic

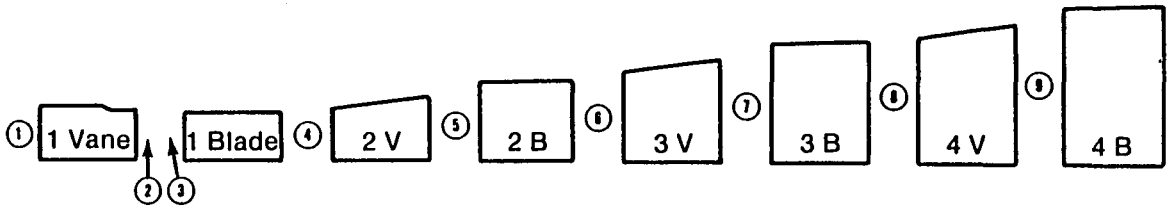

T_{00} = 1800°R	Uncooled	Min Vane	Max Vane
① Turbine Inlet — ABS °F	1340	1340	1340
② 1st Vane Exit — ABS °F	1340	1280	1257
③ 1st Blade Inlet — REL °F	1147	1090	1070
④ 2nd Vane Inlet — ABS °F	1028	977	959
⑤ 2nd Blade Inlet — REL °F	906	859	843
⑥ 3rd Vane Inlet — ABS °F	824	782	767
⑦ 3rd Blade Inlet — REL °F	687	648	634
⑧ 4th Vane Inlet — ABS °F	621	585	573
⑨ 4th Blade Inlet — ABS °F	477	445	434

FD236837
822903

Figure B.3-7a. Case No. 3 Gas Path Temperatures

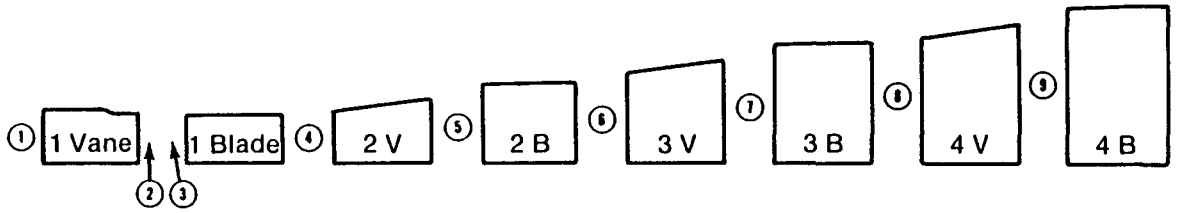

T_{00} = 2200°R	Uncooled	Min Vane Min Blade	Max Vane Min Blade
① Turbine Inlet — ABS °F	1740	1740	1740
② 1st Vane Exit — ABS °F	1740	1650	1618
③ 1st Blade Inlet — REL °F	1529	1437	1406
④ 2nd Vane Inlet — ABS °F	1373	1245	1679
⑤ 2nd Blade Inlet — REL °F	1224	1115	1091
⑥ 3rd Vane Inlet — ABS °F	1109	1011	989
⑦ 3rd Blade Inlet — REL °F	949	860	840
⑧ 4th Vane Inlet — ABS °F	852	774	756
⑨ 4th Blade Inlet — ABS °F	686	617	600

FD243403
822903

Figure B.3-7b. Case No. 3 Gas Path Temperatures

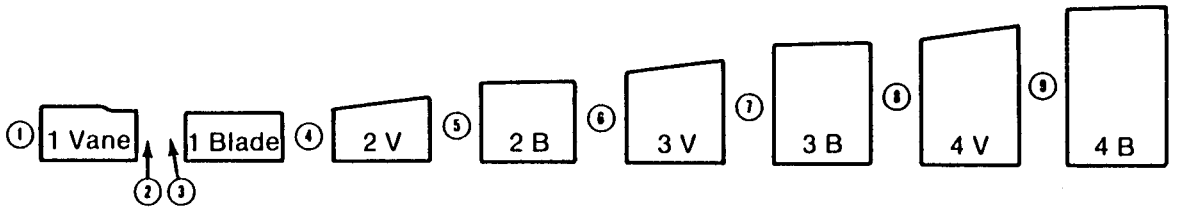

T_{00} = 2600°R	Uncooled	Min Vane Min Blade	Max Vane Min Blade
① Turbine Inlet — ABS °F	2140	2140	2140
② 1st Vane Exit — ABS °F	2140	2021	1979
③ 1st Blade Inlet — REL °F	1917	1797	1756
④ 2nd Vane Inlet — ABS °F	1732	1560	1524
⑤ 2nd Blade Inlet — REL °F	1560	1408	1375
⑥ 3rd Vane Inlet — ABS °F	1411	1273	1244
⑦ 3rd Blade Inlet — REL °F	1230	1105	1078
⑧ 4th Vane Inlet — ABS °F	1101	990	965
⑨ 4th Blade Inlet — ABS °F	915	816	794

FD243404
822903

Figure B.3-7c. Case No. 3 Gas Path Temperatures

T_{00} = 1800°R	Uncooled		Min Cooled Vane		Max Cooled Vane	
	Stg #1	Stg #2	Stg #1	Stg #2	Stg #1	Stg #2
η_{T-T} Base ~ %	69.1	78.5	68.7	78.5	68.4	78.5
$\Delta\eta$ Disk Coolant, Windage	4.6	3.8	5.8	4.7	5.9	4.9
$\Delta\eta$ Vane & Platform Coolant	—	—	1.7	—	2.6	—
η_{T-T} Cooled ~ %	64.5	74.7	61.2	73.8	59.9	73.6
	Stg #3	Stg #4	Stg #3	Stg #4	Stg #3	Stg #4
η_{T-T} Base ~ %	84.8	88.0	84.7	88.0	84.7	87.9
$\Delta\eta$ Disk Coolant, Windage	3.1	2.8	4.0	3.8	4.1	3.9
$\Delta\eta$ EGV	—	1.5	—	1.7	—	1.7
η_{T-T} Cooled ~ %	81.7	83.7	80.7	82.5	80.6	82.3
η_{T-T} Overall ~ %	76.6		75.4		75.1	

FD243405
822903

Figure B.3-8. Case No. 3 Turbine Efficiency

T_{00} = 2200°R	Uncooled		Min Cooled Vane Min Cooled Blade		Max Cooled Vane Min Cooled Blade	
	Stg #1	Stg #2	Stg #1	Stg #2	Stg #1	Stg #2
η_{T-T} Base ~ %	72.2	78.6	72.5	78.9	72.2	78.7
$\Delta\eta$ Disk Coolant, Windage	3.8	3.1	4.1	3.4	4.1	3.4
$\Delta\eta$ Vane & Platform Coolant	—	—	1.7	—	2.4	—
$\Delta\eta$ Blade & Platform Coolant	—	—	.9	—	.9	—
$\Delta\eta$ Blade Coolant Pumping	—	—	2.3	—	2.1	—
η_{T-T} Cooled ~ %	68.4	75.5	63.5	75.5	62.7	75.3
	Stg #3	Stg #4	Stg #3	Stg #4	Stg #3	Stg #4
η_{T-T} Base ~ %	85.1	88.3	85.3	88.3	85.2	88.3
$\Delta\eta$ Disk Coolant, Windage	2.6	2.2	2.9	2.4	2.8	2.6
$\Delta\eta$ EGV	—	.10	—	.60	—	.70
η_{T-T} Cooled ~ %	82.5	86.0	82.4	85.3	82.4	85.0
η_{T-T} Overall ~ %	78.6		76.4		74.9	

FD243406
822903

Figure B.3-9. Case No. 3 Turbine Efficiency

T_{00} = 2600°R	Uncooled		Min Cooled Vane Min Cooled Blade		Max Cooled Vane Min Cooled Blade	
	Stg #1	Stg #2	Stg #1	Stg #2	Stg #1	Stg #2
η_{T-T} Base ~ %	74.5	78.5	73.9	78.6	73.7	78.6
$\Delta\eta$ Disk Coolant, Windage	3.1	2.4	3.1	2.4	3.1	2.5
$\Delta\eta$ Vane & Platform Coolant	—	—	1.6	—	2.3	—
$\Delta\eta$ Blade & Platform Coolant	—	—	.8	—	.8	—
$\Delta\eta$ Blade Coolant Pumping	—	—	1.6	—	1.6	—
η_{T-T} Cooled ~ %	71.4	76.1	66.8	76.2	65.9	76.1
	Stg #3	Stg #4	Stg #3	Stg #4	Stg #3	Stg #4
η_{T-T} Base ~ %	84.8	87.8	84.9	87.7	84.9	87.8
$\Delta\eta$ Disk Coolant, Windage	1.9	1.5	2.0	1.6	2.0	1.8
$\Delta\eta$ EGV	—	.8	—	.2	—	.1
η_{T-T} Cooled ~ %	82.9	85.5	82.9	85.9	82.9	85.9
η_{T-T} Overall ~ %	80.8		77.0		76.8	

FD243407
822903

Figure B.3-10. Case No. 3 Turbine Efficiency

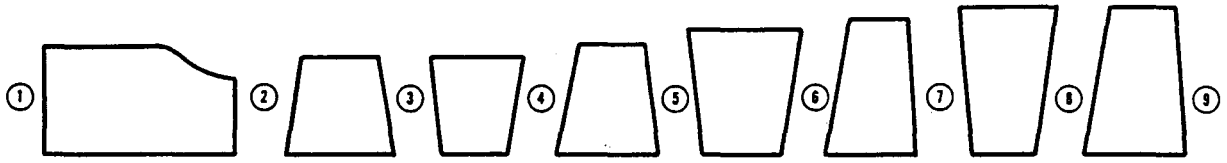

T_{00} = 2200°R, P_{00} = 4000 Psi, Min Cooled Vane & Blade

Station ① Static Pressure	3968 Psia
Station ② Static Pressure	2340 Psia
Station ③ Static Pressure	1882 Psia
Station ④ Static Pressure	1148 Psia
Station ⑤ Static Pressure	941 Psia
Station ⑥ Static Pressure	558 Psia
Station ⑦ Static Pressure	451 Psia
Station ⑧ Static Pressure	251 Psia
Station ⑨ Static Pressure	194 Psia

1. Static Pressures are Mid-Span Values.
2. Although the Quoted Pressures are for a Specific Configuration, the Level is Typical Over the Horsepower Map.

FD236838
822903

Figure B.3-11. Gas Path Static Pressures

End of Document